...

DISSERTATION

Brian Andrew Kish
Major, USAF

AFIT/DS/ENY/05-5

DEPARTMENT OF THE AIR FORCE
AIR UNIVERSITY

AIR FORCE INSTITUTE OF TECHNOLOGY

Wright-Patterson Air Force Base, Ohio

The views expressed in this dissertation are those of the author and do not reflect the official policy or position of the Department of Defense or the United States Government.

AFIT/DS/ENY/05-5

Establishment of a System Operating Characteristic for Autonomous Wide Area Search Vehicles

DISSERTATION

Presented to the Faculty

School of Engineering and Management

Air Force Institute of Technology

Air University

Air Education and Training Command

in Partial Fulfillment of the Requirements for the

Degree of Doctor of Philosophy

Brian Andrew Kish, B.S.A.E., M.S.A.E.
Major, USAF

September, 2005

AFIT/DS/ENY/05-5

Establishment of a System Operating Characteristic for Autonomous Wide Area Search Vehicles

Brian Andrew Kish, B.S.A.E., M.S.A.E.

Major, USAF

Approved:

Dr. David R. Jacques Commitee Chairman	Date
Dr. Meir Pachter Committee Member	Date
Maj Joerg D. Walter Committee Member	Date
Dr. Rusty O. Baldwin Dean's Representative	Date

Robert A. Calico, Jr
Dean

Acknowledgements

I would first like to thank my advisor, Dr. David Jacques, for developing my education plan, supplying the research topic, and teaching me about operational effectiveness for the search and destroy mission. Dr. Jacques was an outstanding advisor who was always available and talked at a level I could understand. I admire his systems engineering perspective and ability to get at the root of any problem. Next I would like to thank Dr. Meir Pachter for his detailed "To Do" handouts and editorial comments. His handouts were paramount in my research and helped me get over some tough hurdles. Like Dr. Jacques, he was always available and talked at a level I could understand. I would like to thank Maj Joerg Walter and Dr. Baldwin, the Dean's representative, for their participation in the process.

From the Math department, I would like to thank Dr. William Baker and Dr. Mark Oxley. During courses I took from them, I learned about math in ways I never would have dreamed about. In addition, they provided tremendous help after my courses. They would sometimes spend hours with me after showing up at their door without an appointment.

As for family, let me begin with my parents. They have always encouraged me without pressure my whole life. Though neither of them have a Bachelor's degree, their life experiences were more than enough to keep pace with my academic experiences. The saying "the older you get, the smarter your parents get" rings true everyday. Next I would like to thank my loving wife for her support and understanding. She never questioned the occasional night or weekend study session. I would also like to thank my son, who was born 10 months into the program, for changing my perspective on life. I see things now in ways only other parents understand.

Finally, I would like to thank Lt Col Mike Philips. He selected me among other applicants for the PhD pipeline program for instructing at Test Pilot School.

Brian Andrew Kish

Table of Contents

List of Figures

List of Tables

List of Symbols

Symbol Page

Symbol Page

List of Abbreviations

Abstract

The optimal employment of autonomous search and destroy vehicles is addressed. The results apply to air, land, or water vehicles with 1, k, or infinite warheads. The specific scenarios considered involve an air vehicle searching a battle space for stationary targets in the presence of false targets. Encounters are modelled with uniform, Poisson, and normal distributions. Linear and circular search patterns are examined. All relevant parameters are extracted from intelligence information, the sensor performance specification, and the air vehicle performance specification. Analytic system effectiveness measures are derived using applied probability theory. The effectiveness measures derived in this dissertation handle time-varying parameters which characterize the battle space environment and the performance of the system. This allows the formulation and solution of optimization problems that maximize the probability of target attacks while at the same time constraining the probability of false target attacks. Optimal schedules for controlling sensor threshold and area coverage rate during a mission are derived and compared to the constant-parameter results. These schedules establish a system operating characteristic. An increase in system effectiveness is demonstrated when parameters are dynamically controlled during a mission. Plots depicting sensitivity to the constraint on false target attacks and sensitivity to the number of warheads are generated to give decision makers the complete trade space for either designing new systems or operating existing systems.

Establishment of a System Operating Characteristic for Autonomous Wide Area Search Vehicles

I. Introduction

1.1 Motivation

Carl Von Clausewitz stated, "War is an extension of politics by other means" [10]. At the heart of wartime politics is blue-force casualties and collateral damage to non-combatant entities. Recent advances in autonomous target recognition and autonomous navigation have given political leaders the potential to prosecute targets in dangerous environments without having to worry about blue-force casualties. Collateral damage, however, still remains a concern. One can imagine the news headline when an autonomous search and destroy vehicle takes out a school bus filled with innocent children. Manned systems have relied on humans as additional checks to minimize collateral damage. In the case of autonomous systems, the human checks are, by definition, removed. Prior to employing any such system, one must determine how well the system can perform. System effectiveness is conditioned on the system operating characteristic, upon which the operating point is defined by area coverage rate and the sensor threshold used for target declaration. System effectiveness also depends on the battle space environment in terms of numbers and types of targets and false targets.

Determining or predicting system effectiveness can be done using mathematical analysis, computer simulation, experimentation, or operational flight test. **This research establishes a system operating characteristic for autonomous wide area search vehicles that can be used to analytically calculate system ef-**

fectiveness. The presence of false targets as well as a sensor's likelihood of misclassifying false targets is acknowledged up front. False targets can be non-combatant entities, decoys, or objects of little strategic value. Inputs to the mathematical "black box" in Figure 1.1 come from the order of battle intelligence, the sensor performance specification, and the air vehicle performance specification. The order of battle intelligence provides battle space dimensions, target distributions, and false target distributions. Sensor performance comes from Receiver Operating Characteristic (ROC) curves (determined experimentally), which relate true positive fraction to false positive fraction. Air vehicle performance involves airspeed limits and endurance values. Outputs from the black box are system effectiveness, a sensor threshold schedule, and an area coverage rate schedule. Any objects reported as targets (correctly or incorrectly) are attacked. The number of false target attacks during a mission is denoted m, and the number of target attacks is denoted n. System effectiveness can be quantified using the probability of at least $\hat{m}$ false target attacks, denoted $P(m \geq \hat{m})$, and the probability of at least $\hat{n}$ target attacks, denoted $P(n \geq \hat{n})$. The values for $\hat{m}$ and $\hat{n}$ are specified by the designer or mission planner. The contents of the black box will be revealed in Chapter II.

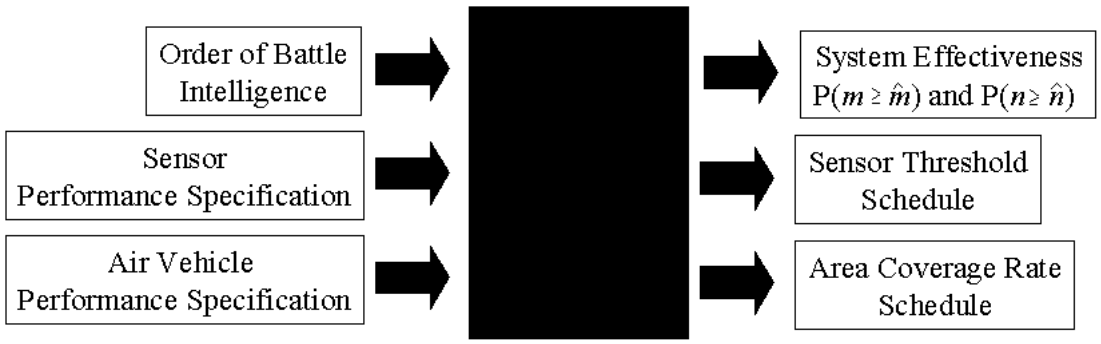

Figure 1.1 Input-Output Diagram.

Clearly one wants the expected number of target attacks to be high and the expected number of false target attacks to be low. Unfortunately, due to the ROC, adjusting the sensor threshold to increase the number of target attacks also increases

the number of false target attacks. For fixed mission durations, lower area coverage rates increase sensor performance, but decrease total area searched. These tradeoffs must be worked to find solutions. Once the internal definition of the black box in Figure 1.1 is known, optimization problems can be formulated and solved. The general optimal control problem will be of the form

$$\begin{aligned} \text{Max:} \quad & P\left(n \geq \hat{n}\right) \\ \text{subj to:} \quad & P\left(m \geq \hat{m}\right) \leq b \end{aligned}$$

where the upper bound b is set by the designer or mission planner. The control variables are area coverage rate and sensor threshold, which are further defined in the next section.

1.2 Search and Destroy Mission

The search and destroy mission involves searching, detecting, classifying, and attacking [1]. This can be done a number of ways. For example, a sensor craft can locate and classify objects, then pass the information to a separate bomber aircraft that performs the attacks. An Unmanned Combat Aerial Vehicle (UCAV) can locate, classify, and destroy objects on its own. An expendable autonomous wide area search munition locates, classifies, and destroys an object as well as itself in the process. All of the above concepts involve sensors with automatic target recognition (ATR) algorithms, and warheads. The mathematical foundation developed in this research handles systems with 1, k, or infinite warheads. Ironically, the infinite-warhead case can be used to mathematically evaluate the zero-warhead sensor craft case. The relation comes from the fact that a sensor craft broadcasts target coordinates assuming a shooter exists to destroy the targets. A sensor craft's mission does not terminate because it has no more warheads. It continues to search and classify until it is sent home or shot down. Thus a sensor craft is mathematically equivalent to a vehicle having an infinite number of warheads.

1.2.1 Searching. Searching requires a pattern and area coverage rate. Two search patterns are addressed in this research. The first pattern is the linear pattern depicted in Figure 1.2(a). Although Figure 1.2(a) shows a constant swath width, the linear pattern can can be used for any linear-symmetric battle space. Further, any randomly-shaped battle space can be broken up into piecewise linear-symmetric segments. The second pattern involves using concentric annuli emanating from the origin. Figure 1.2(b) shows one such annulus at radius r. Searching a disc of radius R using concentric annuli emanating from the origin approximates an outward spiral search pattern and is mathematically tractable.

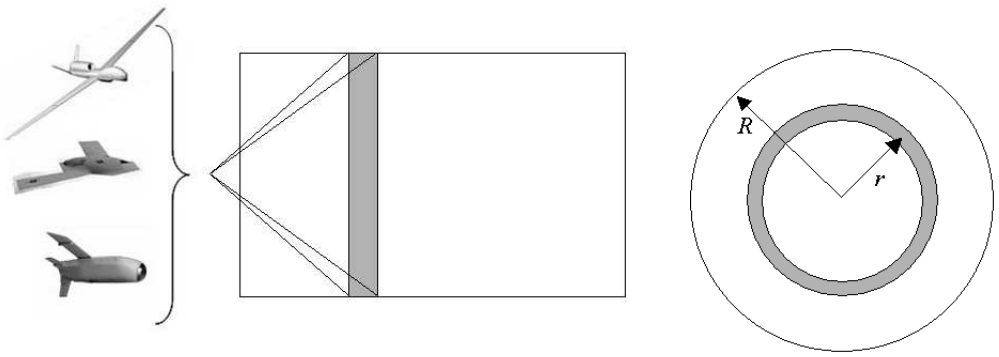

(a) Linear (b) Circular

Figure 1.2 Search Patterns

Area coverage rate can be varied a number of ways. For constant-altitude flight, area coverage rate is the product of velocity and swath width. Thus, changing either parameter changes the area coverage rate. Swath width is constrained by gimbal limits. For fixed degrees of azimuth and fixed velocity, changing altitude changes the area coverage rate. In this research, the flight condition in terms of altitude, velocity, and swath width will all be rolled up into area coverage rate, which will be one of the two control variables. Specific application of whether one varies altitude, velocity, or swath width is up to the designer or mission planner. An example of varying velocity to hold area coverage rate constant is given in Section 1.3.

1.2.2 Detecting. Detections will occur based on assumed target and false probability distributions. The seven battle space scenarios conceived by Jacques and Pachter [26] are examined in this research. Scenarios 1-4 use linear-symmetric battle spaces, and Scenarios 5-7 use circular battle spaces. The differences in the scenarios come from the target and false target probability distributions as well as the number of targets. For all scenarios, both targets and false targets are assumed fixed at unknown locations.

Scenario 1 consists of a single target uniformly distributed in a linear-symmetric battle space among a Poisson field of false targets.

Scenario 2 consists of a linear-symmetric battle space with a Poisson field of targets and a Poisson field of false targets.

Scenario 3 consists of N targets uniformly distributed in a linear-symmetric battle space among a Poisson field of false targets. Note: Scenario 1 is a special case of Scenario 3 with $N = 1$.

Scenario 4 consists of N targets and M false targets uniformly distributed in a linear-symmetric battle space.

Scenario 5 consists of N targets normally distributed in a circular battle space among a Poisson field of false targets. Normally distributed refers to a circular-normal distribution centered at the origin with a target standard deviation σ_y.

Scenario 6 consists of N targets and M false targets normally distributed in a circular battle space. Normally distributed refers to circular-normal distributions centered at the origin with a target standard deviation σ_y and a false target standard deviation σ_x.

Scenario 7 consists of a single target normally distributed in a circular battle space among a Poisson field of false targets. Note: Scenario 7 is a special case of Scenario 5 with $N = 1$.

Other combinations of target and false target distributions exist. Table 1.1 shows where the seven scenarios fall in a combination matrix for uniform, Poisson, and normal distributions. The techniques and results in this dissertation could easily be applied to the remaining combinations.

Table 1.1 Scenario Matrix

	uniform targets	Poisson targets	normal targets
uniform false targets	Scenario 4	—	—
Poisson false targets	Scenarios 1,3	Scenario 2	Scenarios 5,7
normal false targets	—	—	Scenario 6

1.2.3 Classifying. In practice, detected objects are classified to a certain level of discrimination. For example, one may classify on object as either air breathing or ballistic. A finer level of discrimination may be a specific type of air-breathing or ballistic object. Regardless of the level of discrimination, there is a point where the sensor reports a detected object as either a target thereby authorizing an attack, or a false target thereby commanding no attack. Sensor performance is judged by how often the sensor is correct. The probability of a target report is the probability the system correctly reports a *target* when a *target* is encountered. Selecting a sensor threshold is tantamount to selecting the probability of a target report. The sensor can also be wrong. By using a ROC curve to model sensor performance, the probability of attacking a *false* target can be written in terms of the probability of a target report. Therefore, the second control variable will be the probability of a target report.

1.2.4 Attacking. Any objects reported as targets (correctly or incorrectly) are authorized to be attacked. An autonomous munition would fly itself into the reported target, an autonomous UCAV would launch one of its warheads, or an autonomous sensor craft would broadcast target coordinates to shooters.

1.3 Hypothetical Operational Example

To help illustrate the relevance of this research, a hypothetical operational example is given. An intelligence source states that a strategic target is known to be in the area designated A_B in Figure 1.3, which is one of the most heavily defended areas in the region. It can be assumed the target is equally likely to appear anywhere in A_B. It is also known that some subareas of A_B have more false targets than others. The Battle Commander tasks his analysts to provide options involving an autonomous search and destroy vehicle. He would like the probability of attacking the target to be greater than 0.50. However, he would like the probability of attacking any false targets to be less than 0.30.

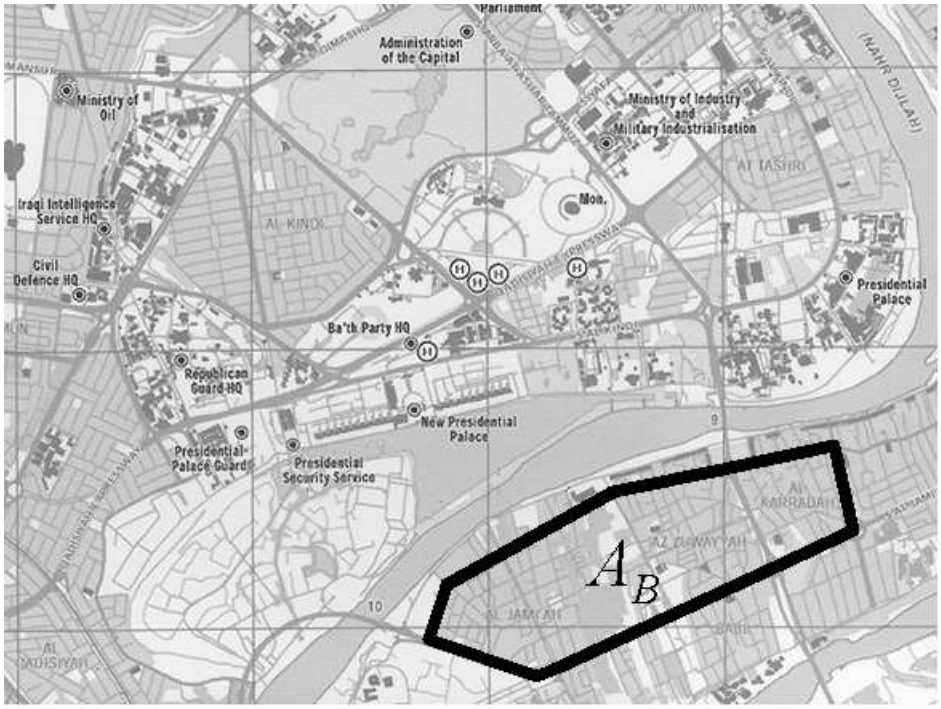

Figure 1.3 Hypothetical Operational Example. Map downloaded from [52].

Based on the order of battle intelligence given, the analysts use a uniform distribution to model the target encounter. Since false targets are often encountered at certain rates, they use a Poisson distribution based on the expected false target densities (denoted by α) shown in Figure 1.4 to model false target encounters.

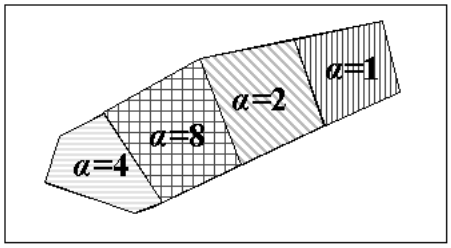

Figure 1.4 False Target Density Map.

Although A_B is not exactly a linear-symmetric battle space, the analysts assume the heading changes and additional area searched are small enough to make a linear-symmetric assumption valid. Hence, the operational example resembles Scenario 1. The sensor performance specification gives the ROC curve shown in Figure 1.5 for a constant area coverage rate of 5 $\frac{km^2}{min}$. The ROC curve was generated from experimental data using various signal-to-noise ratios. True positive fraction (TPF) is the probability of the sensor reporting a *target* when a *target* is encountered. False positive fraction (FPF) is the probability of the sensor reporting a *target* when a *false target* is encountered. The analysts use the curve fit in Figure 1.5 to mathematically relate TPF and FPF.

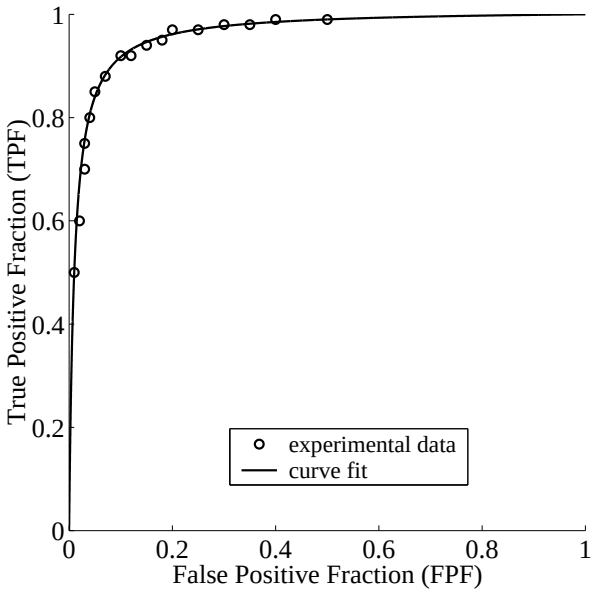

Figure 1.5 Receiver Operating Characteristic Curve.

It should be noted that TPF has the same definition as the probability of a target report. Thus scheduling TPF is the same as scheduling the probability of a target report. The sensor and ATR algorithm were designed for the constant area coverage rate of 5 $\frac{km^2}{min}$; therefore, the analysts decide to fix area coverage rate and use the single ROC curve provided. Adjusting sensor threshold over time moves the operating point along the ROC curve. This amounts to a schedule for TPF and a corresponding schedule for FPF. Assuming a constant area coverage rate of 5 $\frac{km^2}{min}$, the analysts must schedule airspeed and find the best schedule for either TPF. The assumed path is left to right; whereby, the vehicle starts in the area where $\alpha = 4$ $\frac{\text{encounters}}{km^2}$. Using differential equations, the analysts schedule airspeed to keep area coverage rate constant at 5 $\frac{km^2}{min}$. No optimization is required. The resulting schedule is shown in Figure 1.6. As one would expect, higher velocities are needed at the narrow portions of A_B, and lower velocities are needed at the wider portions. A velocity schedule like that shown in Figure 1.6 is plausible for an unmanned air vehicle.

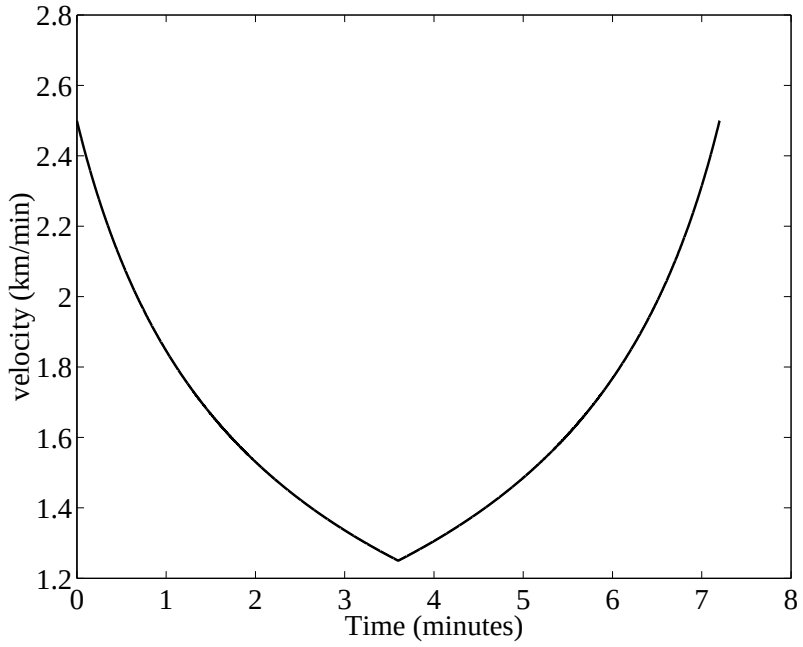

Figure 1.6 Velocity Schedule.

Using the results from this research, they calculate a number of schedules for TPF based on various b values. Three examples for an autonomous search and destroy vehicle with one warhead are shown in Figure 1.7. In areas where false target density is high, TPF is low and relatively flat. In areas where false target density is low, TPF is high and gradually increases as the time remaining decreases. The increase is more when the constraint on false target attacks is loose and less when it is tight.

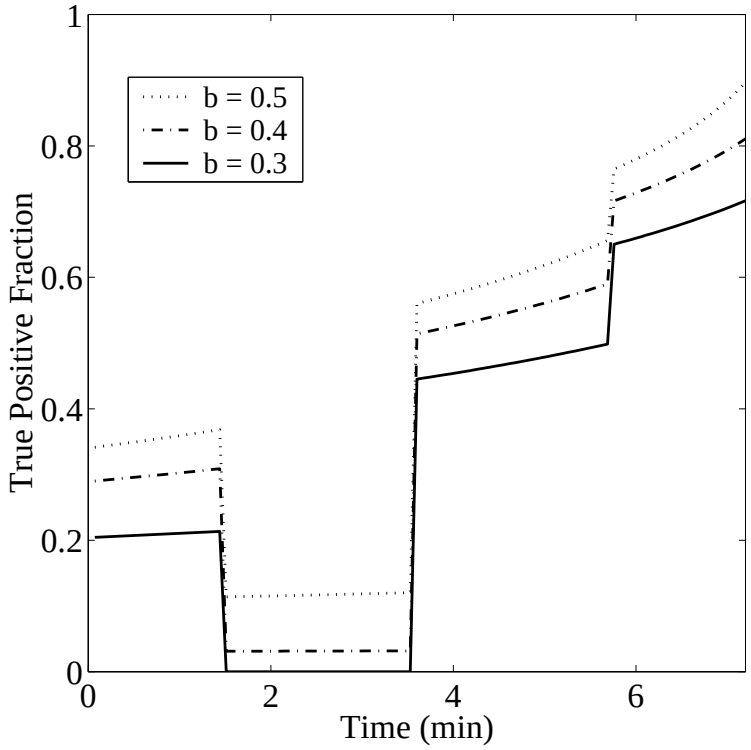

Figure 1.7 Probability of a Target Report (or True Positive Fraction) when One Warhead is Available.

The analysts repeat the calculations for 2, 3, and 5 warheads. The results for 5 warheads are approximately equal to the results for an infinite number of warheads; therefore, they conclude considering more than 5 warheads makes little sense. They generate a summary plot in Figure 1.8 of probability of attacking the target versus probability of attacking any false targets. In other words, they generate the system operating characteristic broken down by number of warheads and upper bound on false target attacks. Each point on the graph represents an optimal schedule for sensor threshold. Had area coverage rate been allowed to vary, each point would have represented the combined optimal schedules for area coverage rate and sensor threshold. Figure 1.8 shows the initial desire of getting the probability of attacking the target to be greater than 0.50 while keeping the probability of attacking any false targets less than 0.30 is not achievable. However, the Commander now has a complete depiction of the trade space. He or she can look at one figure and see the effects of changing constraint level or changing number of warheads.

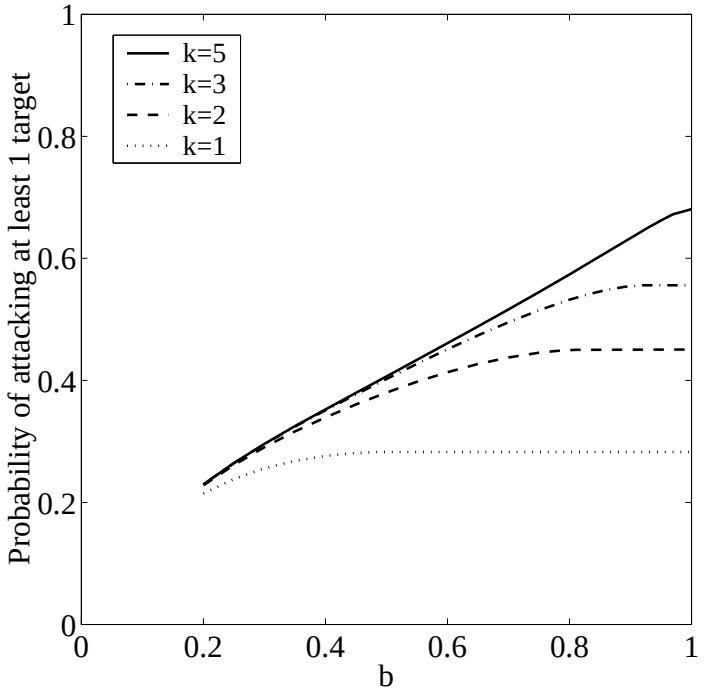

Figure 1.8 System Operating Characteristic.

1.4 Previous Work

The overarching problem of multi-vehicle cooperative control, which the present problem falls under, has a tremendous amount of literature. Programs such as DARPA's Taskable Agent Software Kit (TASK) are attempting to establish common infrastructure, mathematical foundations, and metrics for building, controlling, and understanding agent-based systems. Models range from biological [11] to physics-based control models [19]. Concepts like reactive behavior [18], game theory [29], and decision theory [21], [35] are being examined. In addition to military operations, applications include robot navigation [46], highway transportation [6], and drug interdiction [9]. Each research area has its own wealth of literature. The present research area involves analytic expressions for effectiveness of autonomous search and destroy vehicles. The literature related to this area falls into the following five categories:

- Single Target, No False Targets
- Single Target, False Targets
- Multiple Targets, No False Targets
- Multiple Targets, False Targets
- Moving Targets

In this dissertation, stationary targets and stationary false targets are examined. Since ATR performance is the focus, false targets are required. Thus, the category of multiple targets, multiple false targets is most relevant. For continuity, samples of literature found in each category as well as classic works and surveys are listed.

1.4.1 Classic Works. While many have contributed to search theory, Koopman, Stone, and Washburn seem to be the most influential. Koopman laid the foundation in the 1940s, when searching for U-boats in World War II motivated researchers to analyze the fundamental search problem. His work is summarized in [30]

and contains the much referenced exponential detection law. Stone wrote the first unified and comprehensive presentation of search theory results in 1975 [40]. More recently, he wrote a text book on Bayesian Multiple Target Tracking [42]. Washburn, currently a Professor of Operations Research at the Naval Postgraduate School, has written text books on both search theory [49] and game theory [51].

Two comprehensive review articles on search theory exist. Stone provides the historical perspective with his "What's Happened in Search Theory Since the 1975 Lanchester Prize?" article [41]. Benkoski, et al. provide the topic-by-topic perspective with their "A Survey of the Search Theory Literature" article [4]. Together, the articles give progress in search theory up through the 1980s, where the stationary target problem was thought to have "reached a mature state" [45].

The classic works of Koopman, Stone, and Washburn, as well as the literature listed in the surveys, provide an analytic foundation for basic search problems. However, the research does not address multiple-target, multiple-false-target problems nor the disposable-munition and multi-warhead-UCAV problems. In addition, the research does not allow sensor thresholds or operating conditions to vary with time.

1.4.2 Single Target, No False Targets. The single-target, no false-target problem is the simplest of the search and destroy problems. This does not mean the problem is trivial. Concepts such as target distribution, search effort, and timing need to be addressed.

Haoi and Leondes [22] tried to eliminate the need for knowing a target's *a priori* probability density function. Their goal was to maximize the probability of detecting the target using a single-try (non-redundant) search which was a function of search effort and target location. They used Dobbie's [16] extension of Koopman's exponential detection law, whereby search effort was a function of the searcher's location. They developed a search plan that traded off performance in terms of detection

probability for insensitivity to the target *a priori* probability density function. Their minimax solution guaranteed a non-zero detection probability, but not much more than that. This work is another example of how adding robustness decreases performance. In the present research, search plans are limited to linear and circular plans, and *a priori* probability density functions are assumed correct. That does not prohibit sensitivity studies to parameter changes in the probability distributions.

Iida, et al. [23] were able to relax the assumption of local effectiveness of searching effort, whereby only objects at a point (not objects in a neighborhood) are able to be detected. They assumed search effort was dependent on location and not time. Thus image and data processing time was assumed to be zero.

1.4.3 Single Target, False Targets. When two types of objects exist, detection alone no longer suffices. One must be able to classify an object as either a target or false target. Along with classification comes the chance to misclassify. Attacking a false target or not attacking a target can have grave consequences. For this dissertation, attacking false targets is the focus. Specifically, a maximum is set on the probability of at least $\hat{m}$ false target attacks. Detections are modelled based on target and false probability distributions. The detection process involves scanning an area for objects. Once an object is detected, a classification is made. Correct classification and misclassification are modelled with a Receiver Operating Characteristic curve.

The approach of scanning areas for objects, then classifying all detected objects was done by Stone and Stanshine [43], [44] in the early 1970s. They used a broad search density function to calculate search effort. They used Poisson distributions to model false target encounters. They also brought in the idea of optimization. Specifically they examined the problem of minimizing the mean time to find the target. However, the probability of classifying a false target as a target was assumed to be zero. Either an object was correctly classified after a certain amount of effort

or the searcher moved on. In addition, their search plan did not depend on the number of false targets found.

Dobbie [17] looked at allowing search plans to depend on the number of false targets found. He allowed for duplicative search, where the same spot could be searched more than once. His results, however, applied to a particular case where the number of false targets was bounded.

1.4.4 Multiple Targets, No False Targets. Multiple targets can be interpreted two ways. One can have multiple targets of the same type, or one can have multiple types of targets. In this dissertation, the focus is on multiple homogeneous targets. Cozzolino [12] examined multiple targets of different sizes. He used Poisson distributions for target encounters. Since he used a sensor craft, with no limits on the number of target declarations, he was not concerned with limiting the number of misclassifications. He simply classified an encounter, either correctly or incorrectly, then moved on with the search. A more realistic problem involves limiting the number of declarations (and warheads for subsequent attacks), thus conditioning success on the number of previous attacks. Special attention must be given to false target attack rate which, if too high, makes autonomous operation less attractive.

1.4.5 Multiple Targets, False Targets. Koopman, Stone, Washburn, and others cited thus far made great strides in developing analytic expressions, but they did not specifically address scenarios involving multiple targets, multiple false targets, and air vehicles with multiple warheads. Richardson [37] summarized assumptions made about measures of effectiveness, target motion, and ways in which search effort is characterized. According to Richardson, two of the most common measures of effectiveness are probability of detection and expected time to detection. While these are appropriate for certain problems, they do not address the real operational environment where false targets and decoys exist. In his remarks for future research,

Richardson addressed the need to examine scenarios with multiple targets and false targets.

Jacques, Pachter, Decker, Jeffcoat, and Slater have all recently published literature on analytic expressions for effectiveness of autonomous search and destroy vehicles. Jacques and Pachter [26] developed analytic expressions for autonomous wide area search and destroy munitions for the seven scenarios listed in Table 1.1. They offered a general approach for defining task benefits for cooperative behavior. However, their expressions assume the ATR probabilities, area coverage rate, target parameters, and false target parameters are all constant.

In 2004, Decker [15] extended the work of Jacques and Pachter to include multi-warhead autonomous search and destroy vehicles. He proved the munition, UCAV, and sensor craft problems could all be evaluated using a common mathematical framework. However, his expressions also assume the ATR probabilities, area coverage rate, target parameters, and false target parameters are all constant.

The recent expressions derived by Jacques, Pachter, and Decker [26], [15] were the starting point for this research. Many of the expressions were in closed form and ideal for parameter optimization problems. However, the battle space environment need not be constant. Moreover, the system operating point in terms of sensor threshold and area coverage rate need not be constant. A natural extension of their work involves deriving generalized expressions that can handle time-varying parameters.

Jeffcoat [27] examined the effect of cueing on the probability of target detection. He derived analytic expressions using Markov chains and established an upper bound on the benefits of cueing for two search munitions against stationary targets. His results, arrived at through a different approach, are similar to those of Jacques [25]. His method of using Markov chains was incorporated into Decker's work [15].

Slater [38] looked at task allocation where search munitions can either perform battle damage assessment or continue searching for new targets. If a search munition determines a target is still alive, it mounts a second attack. Otherwise it continues to search. His results show advantages to cooperative behavior are heavily dependent on the probabilities assumed for the initial discovery process, the effectiveness of the attack, and the value associated with striking real targets versus false targets. These results are in line with those produced by Jacques [25]. Slater derived analytic expressions for two search munitions. However, his expressions also assume the problem parameters are all constant throughout the mission.

1.4.6 Moving Targets. Although moving targets are not considered in this research, they exist in the battle space and will eventually need to be addressed. Moving-target problems are formidable. Assuming the initial target distribution is good for all time no longer works. Data association and tracking must be addressed. Time of information needs to be recorded. Models for target motion need to be derived. The most common way to handle moving targets is to assume the motion is Markov [3], [5], [50]. This makes the mathematics more tractable and allows use of common techniques such as Kalman filters [28], [34]. Recently, Dambreville [14] departed from the standard Markov assumption and considered the set of available target trajectories. He reasoned set trajectories were more realistic than simple probabilistic models. The problem resulted in games between the target and the searcher. The games were solved using approximation methods. Some proofs were provided for special cases such as convex evaluation functions. How Dambreville's results scale to more complex problems is unclear.

Mahler [20], [31], [33] presents a promising comprehensive approach to sensor management. He uses finite set statistics derived from point process theory [13], [47] and reformulates the multi-sensor, multi-target problem into a single-sensor, single-target problem. Specifically, all of the sensors are bundled into one giant meta-sensor, and all of the targets are bundled into one giant meta-target. All individual char-

acteristics are retained in the process. The mechanics to get solutions involves "set derivatives" and "set integrals". Practical solutions, however, involve approximation techniques. One example is the probability hypothesis density filter [32], [48] which is a 1st order approximation of the Bayes multi-target filter. While Mahler's approach seems to account for everything (moving targets, false targets, heterogeneous agents and targets popping in and out, etc.), Stone remarks "it is unnecessary and may even be counterproductive to use random sets to model the probability distribution of all the ways that contacts could have been produced but were not" [42].

1.4.7 System Operating Characteristic. The idea of establishing a *system* operating characteristic as opposed to a *receiver* operating characteristic is not new. In fact, a "receiver" in most applications is really a system of subcomponents. Papers by authors such as Bar-Shalom exist that describe a transition from receiver operating characteristic to system operating characteristic [2]. Regardless of the application, the "system" must be clearly defined. For the present research, the system is defined as the area coverage rate and automatic target recognition threshold. The combination of the sensor and the vehicle, whose motion together with the instantaneous sensor footprint, determines the area coverage rate. No literature was found using these definitions. Clearly one could define a different system and establish a different system operating characteristic.

1.5 Research Statement

The key element covered in this research *not* covered in the literature is time-varying parameters which leads to function optimization as opposed to parameter optimization. The result is a generalized mathematical framework that handles spatially different battle space environments and allows system operating points to vary with time. The mathematical framework applies to the munition, UCAV, and sensor craft problems. A schedule for sensor threshold and area coverage rate to maximum $P(n \geq \hat{n})$ for a given maximum allowable $P(m \geq \hat{m})$ is possible. These are tactical

solutions needed by the hands-on mission planner to maximize operational effectiveness. The generalized mathematical framework can handle the following three types of optimization problems:

- Fixed Area Coverage Rate, Fixed Threshold
- Fixed Area Coverage Rate, Variable Threshold
- Variable Area Coverage Rate, Variable Threshold

Up to now, only the first type was possible.

Expressions needed to calculate $P(n \geq \hat{n})$ and $P(m \geq \hat{m})$ for the seven scenarios listed in Table 1.1 are derived. To gain insight into the problem, analytic conclusions using the munition and sensor craft results for Scenarios 1, 2, and 7 are provided. Using these tractable instances, the problem can be bounded and numerical results can be verified. Numerical results from dynamic problems are also checked against analytic results from fixed problems.

1.6 Applicability

The results of this dissertation can be used in the design phase or operational phase of a system. The system can be manned, unmanned, airborne-based, land-based, or water-based. The sensor can be RADAR, SONAR, IR, LASER, or any other type of sensor whose performance can be modelled with a ROC curve. In the design phase, the results can be used to develop system requirements, compare competing designs, or verify simulation results. Parameter sensitivity studies can be done to determine the cost effectiveness of improving sensors, warheads, or vehicle performance. The mathematical framework enables sound systems engineering. In the operational phase, tactical decisions in the form of setting operating points and determining the number of warheads are possible using the results of this dissertation. The hypothetical operational example in Section 1.3 showed how summary plots of $P(n \geq \hat{n})$ versus upper bound on $P(m \geq \hat{m})$ give Commanders a complete picture

of the trade space. He or she can look at one figure and see the effects of changing constraint level or changing number of warheads.

1.7 Outline of Document

In Chapter II, the black box in Figure 1.1 is defined. The sequential events method used to calculate system effectiveness is explained. Everything needed to calculate $P(n \geq \hat{n})$ and $P(m \geq \hat{m})$ for the seven scenarios listed in Table 1.1 is provided. How a ROC curve relates ATR parameters and how to setup an optimal control problem are shown. Chapter II, together with AppendixA and Appendix B, contain the new analytic contributions to the field where the fundamental problem is generalized to handle time-varying parameters.

In Chapter III, analytic conclusions using the munition and sensor craft results for Scenarios 1, 2, and 7 are provided. The analytic conclusions are derived using well known methods from optimal control theory. The analytic conclusions are then used to verify the numerical results in Chapter IV, where various types of optimization problems listed in Section 1.5 are examined. Conclusions and recommendations for future research are given in Chapter V.

II. Problem Setup and Definitions

In this chapter, the black box in Figure 1.1 is defined. The sequential events method used to calculate system effectiveness is explained. Everything needed to calculate $P(n \geq \hat{n})$ and $P(m \geq \hat{m})$ for the seven scenarios listed in Table 1.1 is provided. How a ROC curve relates ATR parameters is shown. Finally, how to setup an optimal control problem is covered along with a sample formulation.

Thus far, notation for things like the battle space and the probability of at least $\hat{n}$ target attacks have been defined. To fill in the black box and setup optimal control problems, considerably more definitions are needed.

2.1 Sequential Events Method

The purpose of the sequential events method is to produce a probability density function that can be integrated to calculate an overall effectiveness or expected level of collateral damage. To model the search and destroy mission, the following area definitions which are illustrated in Figure 2.1 are needed:

$$\begin{aligned} A_B &\equiv \text{battle space} \\ A &\equiv \text{area covered through time } t \text{ or radius } r \\ A_s &\equiv \text{area covered through terminal time } T \text{ or terminal radius } R \\ dA &\equiv \text{area of sensor footprint at time } t \text{ or radius } r \\ A_f &\equiv A_s - (A + dA) \end{aligned}$$

Choosing to define the sensor footprint as the infinitesimal area dA allows for a physical interpretation of the mathematical operation of integration. One can think of dragging the sensor footprint over an area as an ordered search effort. For an event of interest (e.g. attacking a target) to occur in the sensor footprint at time t, certain events must occur prior to the event and certain events must occur after the event. For example, if all warheads were used prior to time t, there is no way an attack

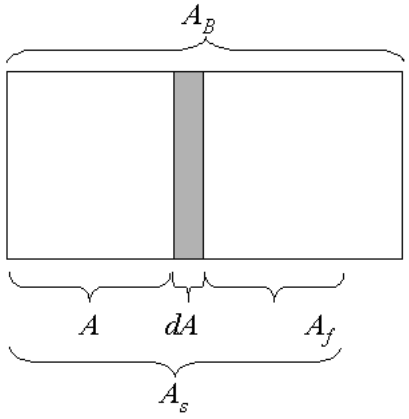

Figure 2.1 Area Definitions.

can occur at time t. Therefore, events must be sequenced based on conditions. The various events of interest and associated numbering scheme is defined below.

$i \equiv$ number of false target encounters in A

$j \equiv$ number of target encounters in A

$k \equiv$ number of warheads available at the beginning of a mission

$m \equiv$ number of false target attacks

$M \equiv$ number of false targets in A_B

$n \equiv$ number of target attacks

$N \equiv$ number of targets in A_B

$\mathcal{M} \equiv$ events involving false target encounters

$\mathcal{N} \equiv$ events involving target encounters

$\mathcal{T} \equiv$ events where targets are correctly classified and attacked

$\mathcal{F} \equiv$ events where false targets are misclassified and attacked

$\overline{\mathcal{T}} \equiv$ events where targets are misclassified and not attacked

$\overline{\mathcal{F}} \equiv$ events where false targets are correctly classified and not attacked

For notation, the number of events occurring in a given area is subscripted along with the applicable area. For example, $n-1$ target attacks in A is denoted $\mathcal{T}_{n-1,A}$. To calculate the probability of at least a certain number of attacks, one

needs to know the probability of an exact number of attacks. Decker showed one must distinguish between the case where all warheads are used and the case where warheads are left over [15]. The probability of exactly m false target attacks and n target attacks when $m+n=k$ is denoted $P_{m,n}^{(m+n=k)}$. The probability of exactly m false target attacks and n target attacks when $m+n<k$ is denoted $P_{m,n}^{(m+n<k)}$. Decker showed both cases are needed to calculate the overall probability of an exact number of target and false target attacks in A_s. In general terms, for distributions involving M false targets and N targets, he showed

$$\begin{aligned} P_{m,n}^{(m+n=k)}(A_s) &= \int_{A_s} \big[P\left(\mathcal{T}_{n-1,A} \cap \overline{\mathcal{T}}_{j-(n-1),A} \cap \mathcal{N}_{N-1-j,A_f} \cap \mathcal{T}_{1,dA}\right) \times \\ &\quad P\left(\mathcal{F}_{m,A} \cap \overline{\mathcal{F}}_{i-m,A} \cap \mathcal{M}_{M-i,A_f}\right) + \\ &\quad P\left(\mathcal{T}_{n,A} \cap \overline{\mathcal{T}}_{j-n,A} \cap \mathcal{N}_{N-j,A_f}\right) \times \\ &\quad P\left(\mathcal{F}_{m-1,A} \cap \overline{\mathcal{F}}_{i-(m-1),A} \cap \mathcal{M}_{M-1-i,A_f} \cap \mathcal{F}_{1,dA}\right)\big] \quad (2.1) \end{aligned}$$

and

$$\begin{aligned} P_{m,n}^{(m+n<k)}(A_s) &= \int_{A_s} \big[P\left(\mathcal{T}_{n-1,A} \cap \overline{\mathcal{T}}_{j-(n-1),A} \cap \overline{\mathcal{T}}_{N-1-j,A_f} \cap \mathcal{T}_{1,dA}\right) \times \\ &\quad P\left(\mathcal{F}_{m,A} \cap \overline{\mathcal{F}}_{i-m,A} \cap \overline{\mathcal{F}}_{M-i,A_f}\right) + \\ &\quad P\left(\mathcal{T}_{n,A} \cap \overline{\mathcal{T}}_{j-n,A} \cap \overline{\mathcal{T}}_{N-j,A_f}\right) \times \\ &\quad P\left(\mathcal{F}_{m-1,A} \cap \overline{\mathcal{F}}_{i-(m-1),A} \cap \overline{\mathcal{F}}_{M-1-i,A_f} \cap \mathcal{F}_{1,dA}\right)\big], \quad (2.2) \end{aligned}$$

where i is the number of false target encounters in A and j is the number of target encounters in A. The subtle difference between Eqs. (2.1) and (2.2) involves what must happen after time t or radius r in A_f. When $m+n=k$, once the final warhead is expended, one doesn't care if the vehicle comes across any more attack situations. An attack situation is one where an attack would occur if the vehicle had a limitless supply of warheads. Therefore, one only cares about the number of remaining encounters in A_f. When $m+n<k$, there can be no attacks in A_f.

Therefore, all subsequent target encounters must be misclassified, and all subsequent false target encounters must be correctly classified. In other words, $\mathcal{M}$'s and $\mathcal{N}$'s in Eq. (2.1) become $\overline{\mathcal{F}}$'s and $\overline{\mathcal{T}}$'s respectively in Eq. (2.2).

Calculating the probability of at least a certain number of attacks involves summing all the possible mutually exclusive probabilities. Thus,

$$P\left(m \geq \hat{m}\right) = \sum_{m=\hat{m}}^{\min\left(M,k-1\right)} \left[\sum_{n=0}^{\min\left(N,k-m-1\right)} P_{m,n}^{(m+n<k)} \right] + \sum_{m=\max\left(\hat{m},k-N\right)}^{k} P_{m,k-m}^{(m+n=k)} \tag{2.3}$$

and

$$P\left(n \geq \hat{n}\right) = \sum_{n=\hat{n}}^{\min\left(N,k-1\right)} \left[\sum_{m=0}^{\min\left(M,k-n-1\right)} P_{m,n}^{(m+n<k)} \right] + \sum_{n=\max\left(\hat{n},k-M\right)}^{k} P_{k-n,m}^{(m+n=k)}. \tag{2.4}$$

The cases when either $m = 0$ or $n = 0$ must be considered separately. Either case results in a negative subscript in Eqs. (2.1) and (2.2). If a subscript is negative, the corresponding probability is simply zero. When all warheads are used,

$$\begin{aligned} P_{m=0,n=k}^{(m+n=k)}\left(A_s\right) &= \int_{A_s} \left[P\left(\mathcal{T}_{k-1,A} \cap \overline{\mathcal{T}}_{j-(k-1),A} \cap \mathcal{N}_{N-1-j,A_f} \cap \mathcal{T}_{1,dA} \right) \times \right. \\ &\qquad \left. P\left(\overline{\mathcal{F}}_{i,A} \cap \mathcal{M}_{M-i,A_f} \right) \right] \end{aligned} \tag{2.5}$$

and

$$\begin{aligned} P_{m=k,n=0}^{(m+n=k)}\left(A_s\right) &= \int_{A_s} \left[P\left(\mathcal{F}_{k-1,A} \cap \overline{\mathcal{F}}_{i-(k-1),A} \cap \mathcal{M}_{M-1-i,A_f} \cap \mathcal{F}_{1,dA} \right) \times \right. \\ &\qquad \left. P\left(\overline{\mathcal{T}}_{j,A} \cap \mathcal{N}_{N-j,A_f} \right) \right] \end{aligned} \tag{2.6}$$

When warheads are left over,

$$P_{m=0,n<k}^{(m+n<k)}\left(A_s\right) = P\left(\mathcal{F}_{0,A_s}\right) \int_{A_s} P\left(\mathcal{T}_{n-1,A} \cap \overline{\mathcal{T}}_{j-(n-1),A} \cap \overline{\mathcal{T}}_{N-1-j,A_f} \cap \mathcal{T}_{1,dA} \right) \tag{2.7}$$

and

$$P^{(m+n<k)}_{m<k,n=0}\left(A_s\right) = P\left(\mathcal{T}_{0,A_s}\right)\int_{A_s} P\left(\mathcal{F}_{m-1,A}\cap\overline{\mathcal{F}}_{i-(m-1),A}\cap\overline{\mathcal{F}}_{M-1-i,A_f}\cap\mathcal{F}_{1,dA}\right) \quad (2.8)$$

An equivalent way to calculate $P\left(m \geq \hat{m}\right)$ is using

$$\begin{aligned} P\left(m \geq \hat{m}\right) &= 1 - P\left(m < \hat{m}\right) \\ &= 1 - \sum_{m=0}^{\min\left(M,\hat{m}-1\right)}\left[\sum_{n=0}^{\min\left(N,k-m-1\right)} P^{(m+n<k)}_{m,n}\right] - \sum_{m=\max\left(0,k-N\right)}^{\min\left(M,\hat{m}-1\right)} P^{(m+n=k)}_{m,k-m}, \end{aligned} \quad (2.9)$$

and an equivalent way to calculate $P\left(n \geq \hat{n}\right)$ is using

$$\begin{aligned} P\left(n \geq \hat{n}\right) &= 1 - P\left(n < \hat{n}\right) \\ &= 1 - \sum_{n=0}^{\min\left(N,\hat{n}-1\right)}\left[\sum_{m=0}^{\min\left(M,k-n-1\right)} P^{(m+n<k)}_{m,n}\right] - \sum_{n=\max\left(0,k-M\right)}^{\min\left(N,\hat{n}-1\right)} P^{(m+n=k)}_{k-n,n}, \end{aligned} \quad (2.10)$$

When using either Eqs. (2.9) or (2.10), the case when both $m = 0$ and $n = 0$ must also be considered separately. This can only occur when warheads are left over (assuming $k \geq 1$). The resulting probability is

$$P^{(m+n<k)}_{m=0,n=0}\left(A_s\right) = P\left(\mathcal{F}_{0,A_s}\right)P\left(\mathcal{T}_{0,A_s}\right) \quad (2.11)$$

Viewing Eqs. (2.1)-(2.11), 12 "elemental" probabilities emerge that need to be determined regardless of the probability distributions used. Table 2.1 lists the 12 elemental probabilities and the corresponding conditions.

2.2 Elemental Probabilities for Scenarios 1-7

One can now apply Eqs. (2.1)-(2.11) for Scenarios 1-7. Details for calculating the elemental probabilities for each scenario are given in Appendix B. Prior to

Table 2.1 Twelve Elemental Probabilities

Name	Elemental Probability	Condition
P_1	$P\left(\mathcal{T}_{n-1,A} \cap \overline{\mathcal{T}}_{j-(n-1),A} \cap \mathcal{N}_{N-1-j,A_f} \cap \mathcal{T}_{1,dA}\right)$	$P_{m,n}^{(m+n=k)}$
P_2	$P\left(\mathcal{F}_{m,A} \cap \overline{\mathcal{F}}_{i-m,A} \cap \mathcal{M}_{M-i,A_f}\right)$	$P_{m,n}^{(m+n=k)}$
P_3	$P\left(\mathcal{T}_{n,A} \cap \overline{\mathcal{T}}_{j-n,A} \cap \mathcal{N}_{N-j,A_f}\right)$	$P_{m,n}^{(m+n=k)}$
P_4	$P\left(\mathcal{F}_{m-1,A} \cap \overline{\mathcal{F}}_{i-(m-1),A} \cap \mathcal{M}_{M-1-i,A_f} \cap \mathcal{F}_{1,dA}\right)$	$P_{m,n}^{(m+n=k)}$
P_5	$P\left(\overline{\mathcal{F}}_{i,A} \cap \mathcal{M}_{M-i,A_f}\right)$	$P_{m=0,n=k}^{(m+n=k)}$
P_6	$P\left(\overline{\mathcal{T}}_{j,A} \cap \mathcal{N}_{N-j,A_f}\right)$	$P_{m=k,n=0}^{(m+n=k)}$
P_7	$P\left(\mathcal{T}_{n-1,A} \cap \overline{\mathcal{T}}_{j-(n-1),A} \cap \overline{\mathcal{T}}_{N-1-j,A_f} \cap \mathcal{T}_{1,dA}\right)$	$P_{m,n}^{(m+n<k)}$
P_8	$P\left(\mathcal{F}_{m,A} \cap \overline{\mathcal{F}}_{i-m,A} \cap \overline{\mathcal{F}}_{M-i,A_f}\right)$	$P_{m,n}^{(m+n<k)}$
P_9	$P\left(\mathcal{T}_{n,A} \cap \overline{\mathcal{T}}_{j-n,A} \cap \overline{\mathcal{T}}_{N-j,A_f}\right)$	$P_{m,n}^{(m+n<k)}$
P_{10}	$P\left(\mathcal{F}_{m-1,A} \cap \overline{\mathcal{F}}_{i-(m-1),A} \cap \overline{\mathcal{F}}_{M-1-i,A_f} \cap \mathcal{F}_{1,dA}\right)$	$P_{m,n}^{(m+n>k)}$
P_{11}	$P\left(\mathcal{F}_{0,A_s}\right)$	$P_{m=0,n<k}^{(m+n<k)}$
P_{12}	$P\left(\mathcal{T}_{0,A_s}\right)$	$P_{m<k,n=0}^{(m+n<k)}$

calculating an elemental probability, the probability of an exact number of classified encounters occurring up through a given time or radius for a given probability distribution is needed. These derivations are given in Appendix A.

When a sensor encounters an object, it compares the image to a stored template or pattern and either declares the object a target or a false target. In practice, detected objects are classified to a certain level of discrimination. For example, one may classify on object as either air breathing or ballistic. A finer level of discrimination may be a specific type of air-breathing or ballistic object. Regardless of the level of discrimination, there is a point where the sensor reports a detected object as either a target thereby authorizing an attack, or a false target thereby commanding no attack. Sensor performance is judged by how often the sensor is correct. The probability of a target report (P_{TR}) is the probability the sensor correctly reports a *target* when a *target* is encountered. The probability of a false target report (P_{FTR})

is the probability the sensor correctly reports a *false target* when a *false target* is encountered. Together, P_{TR} and P_{FTR} determine the entries of the binary "confusion matrix" shown in Table 2.2 which can be used to determine the outcome of a random draw each time an object is encountered in simulation.

Table 2.2 Simple Binary Confusion Matrix

	Encountered Object	
Declared Object	Target	False Target
Target	P_{TR}	$1 - P_{FTR}$
False Target	$1 - P_{TR}$	P_{FTR}

The expression $(1 - P_{TR})$ represents the probability the sensor reports a *false target* when a *target* is encountered. This type of error results in a target not being attacked. The expression $(1 - P_{FTR})$ represents the probability the sensor reports a *target* when a *false target* is encountered. This type of error results in a false target being attacked. For this binary confusion matrix, true positive fraction is P_{TR}, and false positive fraction is $(1 - P_{FTR})$. If multiple types of targets are involved, the dimension of the confusion matrix can be higher [24]. This research only considers the 2x2 confusion matrix in Table 2.2.

Allowing P_{TR} and $(1 - P_{FTR})$ to vary with time means integrals will appear in the expressions for the elemental probabilities. To ease the appearance of the equations and to help formulate optimal control problems, states are defined as the integrals. The state q represents the probability of encountering a single object. The state x represents either the unconditional probability of attacking a single false target (for Scenarios 4 and 6) or the Poisson parameter for false target attacks (for Scenarios 1, 2, 3, 5, and 7). The state y represents either the unconditional probability of attacking a single target (for Scenarios 1, 3, 4, 5, 6, and 7) or the Poisson parameter for target attacks (for Scenario 2).

In the remainder of this section, a two-part table is provided for each scenario containing the 12 elemental probabilities and corresponding state definitions. *Temporal* variables are used for Scenarios 1-4 assuming the mission ends at time T. One can readily re-derive expressions assuming *spatial* variables; however, area coverage rate would no longer appear in the expressions. Search paths for Scenarios 1-4 are linear as depicted in Figure 2.2(a). *Spatial* variables are used for Scenarios 5-7 assuming the mission ends at radius R. One can readily re-derive expressions for Scenarios 5-7 assuming *temporal* variables. Area coverage rate would enter into the expressions in the form of $Q = 2\pi r\dot{r}$. A state for radius r would need to be added. Bounding Q would result in state-dependent inequality constraints that are undefined at $r = 0$. For this reason, *spatial* variables are used for Scenarios 5-7. Search paths for Scenarios 5-7 rely on concentric annuli as depicted in Figure 2.2(b).

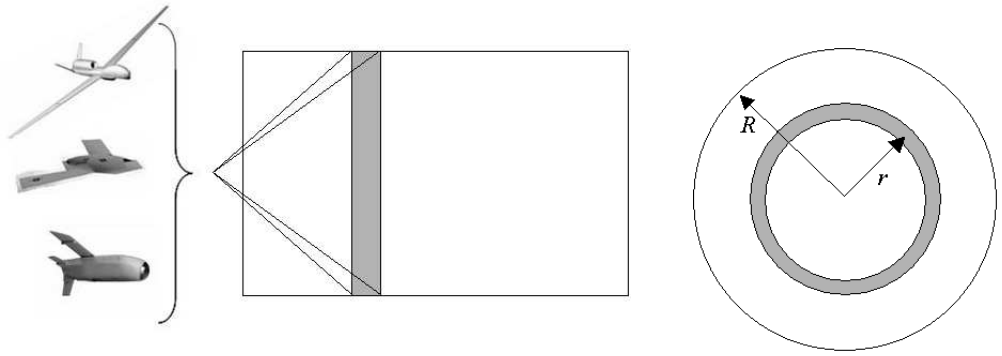

(a) Linear (b) Circular

Figure 2.2 Search Patterns

Table 2.3 Scenario 1 Elemental Probabilities and State Definitions

P_1	$=$	$\frac{1}{A_B} P_{TR}(t)\, Q(t)\, dt$
P_2	$=$	$e^{-x(t)} \frac{[x(t)]^m}{m!}$
P_3	$=$	$[1 - y(t)]$
P_4	$=$	$e^{-x(t)} \frac{[x(t)]^{(m-1)}}{(m-1)!} [1 - P_{FTR}(t)]\, Q(t)\, \alpha(t)\, dt$
P_5	$=$	$e^{-x(t)}$
P_6	$=$	$[1 - y(t)]$
P_7	$=$	$\frac{1}{A_B} P_{TR}(t)\, Q(t)\, dt$
P_8	$=$	$e^{-x(T)} \frac{[x(t)]^m}{m!}$
P_9	$=$	$[1 - y(T)]$
P_{10}	$=$	$e^{-x(T)} \frac{[x(t)]^{(m-1)}}{(m-1)!} [1 - P_{FTR}(t)]\, Q(t)\, \alpha(t)\, dt$
P_{11}	$=$	$e^{-x(T)}$
P_{12}	$=$	$[1 - y(T)]$
$x(t)$	$\equiv$	$\int_0^t [1 - P_{FTR}(\tau)]\, Q(\tau)\, \alpha(\tau)\, d\tau$
$y(t)$	$\equiv$	$\int_0^t \frac{1}{A_B} P_{TR}(\tau)\, Q(\tau)\, d\tau$

2.2.1 Scenario 1. For this scenario, one target is uniformly distributed among a Poisson field of false targets with density $\alpha(t)$. The air vehicle flies along a straight path with area coverage rate $Q(t)$. Table 2.3 lists the 12 elemental probabilities and the corresponding state definitions.

Table 2.4 Scenario 2 Elemental Probabilities and State Definitions

P_1	=	$e^{-y(t)}\frac{[y(t)]^{(n-1)}}{(n-1)!}P_{TR}(t)\,Q(t)\,\beta(t)\,dt$
P_2	=	$e^{-x(t)}\frac{[x(t)]^m}{m!}$
P_3	=	$e^{-y(t)}\frac{[y(t)]^n}{n!}$
P_4	=	$e^{-x(t)}\frac{[x(t)]^{(m-1)}}{(m-1)!}\left[1-P_{FTR}(t)\right]Q(t)\,\alpha(t)\,dt$
P_5	=	$e^{-x(t)}$
P_6	=	$e^{-y(t)}$
P_7	=	$e^{-y(T)}\frac{[y(t)]^{(n-1)}}{(n-1)!}P_{TR}(t)\,Q(t)\,\beta(t)\,dt$
P_8	=	$e^{-x(T)}\frac{[x(t)]^m}{m!}$
P_9	=	$e^{-y(T)}\frac{[y(t)]^n}{n!}$
P_{10}	=	$e^{-x(T)}\frac{[x(t)]^{(m-1)}}{(m-1)!}\left[1-P_{FTR}(t)\right]Q(t)\,\alpha(t)\,dt$
P_{11}	=	$e^{-x(T)}$
P_{12}	=	$e^{-y(T)}$
$x(t)$	$\equiv$	$\int_0^t\left[1-P_{FTR}(\tau)\right]Q(\tau)\,\alpha(\tau)\,d\tau$
$y(t)$	$\equiv$	$\int_0^t P_{TR}(\tau)\,Q(\tau)\,\beta(\tau)\,d\tau$

2.2.2 Scenario 2. For this scenario, there is a Poisson field of false targets with density $\alpha(t)$ and a Poisson field of targets with density $\beta(t)$. The air vehicle flies along a straight path with area coverage rate $Q(t)$. Table 2.4 lists the 12 elemental probabilities and the corresponding state definitions.

Table 2.5 Scenario 3 Elemental Probabilities and State Definitions

P_1	=	$\sum_{j=n-1}^{N-1} \left\{ \binom{N-1}{j} \binom{j}{n-1} [y(t)]^{n-1} [q(t) - y(t)]^{j-(n-1)} [1 - q(t)]^{N-1-j} \right\} \times$ $\frac{N}{A_B} P_{TR}(t) Q(t) dt$
P_2	=	$e^{-x(t)} \frac{[x(t)]^m}{m!}$
P_3	=	$\sum_{j=n}^{N} \left\{ \binom{N}{j} \binom{j}{n} [y(t)]^n [q(t) - y(t)]^{j-n} [1 - q(t)]^{N-j} \right\}$
P_4	=	$e^{-x(t)} \frac{[x(t)]^{(m-1)}}{(m-1)!} [1 - P_{FTR}(t)] Q(t) \alpha(t) dt$
P_5	=	$e^{-x(t)}$
P_6	=	$[1 - y(t)]^N$
P_7	=	$\sum_{j=n-1}^{N-1} \left\{ \binom{N-1}{j} \binom{j}{n-1} [y(t)]^{n-1} [q(t) - y(t)]^{j-(n-1)} \times [1 - q(t) - y(T) + y(t)]^{N-1-j} \right\} \frac{N}{A_B} P_{TR}(t) Q(t) dt$
P_8	=	$e^{-x(T)} \frac{[x(t)]^m}{m!}$
P_9	=	$\sum_{j=n}^{N} \left\{ \binom{N}{j} \binom{j}{n} [y(t)]^n [q(t) - y(t)]^{j-n} [1 - q(t) - y(T) + y(t)]^{N-j} \right\}$
P_{10}	=	$e^{-x(T)} \frac{[x(t)]^{(m-1)}}{(m-1)!} [1 - P_{FTR}(t)] Q(t) \alpha(t) dt$
P_{11}	=	$e^{-x(T)}$
P_{12}	=	$[1 - y(T)]^N$
$q(t)$	$\equiv$	$\int_0^t \frac{1}{A_B} Q(\tau) d\tau$
$x(t)$	$\equiv$	$\int_0^t [1 - P_{FTR}(\tau)] Q(\tau) \alpha(\tau) d\tau$
$y(t)$	$\equiv$	$\int_0^t \frac{1}{A_B} P_{TR}(\tau) Q(\tau) d\tau$

2.2.3 Scenario 3. For this scenario, N targets are uniformly distributed among a Poisson field of false targets with density $\alpha(t)$. The air vehicle flies along a straight path with area coverage rate $Q(t)$. Table 2.5 lists the 12 elemental probabilities and the corresponding state definitions. As stated previously, Scenario 1 is a special case of Scenario 3 with $N = 1$.

Table 2.6 Scenario 4 Elemental Probabilities and State Definitions

P_1	$=$	$\sum_{j=n-1}^{N-1} \left\{ \binom{N-1}{j} \binom{j}{n-1} [y(t)]^{n-1} [q(t)-y(t)]^{j-(n-1)} [1-q(t)]^{N-1-j} \right\} \times$ $\frac{N}{A_B} P_{TR}(t) Q(t) dt$
P_2	$=$	$\sum_{i=m}^{M} \left\{ \binom{M}{i} \binom{i}{m} [x(t)]^m [q(t)-x(t)]^{i-m} [1-q(t)]^{M-i} \right\}$
P_3	$=$	$\sum_{j=n}^{N} \left\{ \binom{N}{j} \binom{j}{n} [y(t)]^n [q(t)-y(t)]^{j-n} [1-q(t)]^{N-j} \right\}$
P_4	$=$	$\sum_{i=m-1}^{M-1} \left\{ \binom{M-1}{i} \binom{i}{m-1} [x(t)]^{m-1} [q(t)-x(t)]^{i-(m-1)} [1-q(t)]^{M-1-i} \right\} \times$ $\frac{M}{A_B} [1-P_{FTR}(t)] Q(t) dt$
P_5	$=$	$[1-x(t)]^M$
P_6	$=$	$[1-y(t)]^N$
P_7	$=$	$\sum_{j=n-1}^{N-1} \left\{ \binom{N-1}{j} \binom{j}{n-1} [y(t)]^{n-1} [q(t)-y(t)]^{j-(n-1)} \times [1-q(t)-y(T)+y(t)]^{N-1-j} \right\} \frac{N}{A_B} P_{TR}(t) Q(t) dt$
P_8	$=$	$\sum_{i=m}^{M} \left\{ \binom{M}{i} \binom{i}{m} [x(t)]^m [q(t)-x(t)]^{i-m} [1-q(t)-x(T)+x(t)]^{M-i} \right\}$
P_9	$=$	$\sum_{j=n}^{N} \left\{ \binom{N}{j} \binom{j}{n} [y(t)]^n [q(t)-y(t)]^{j-n} [1-q(t)-y(T)+y(t)]^{N-j} \right\}$
P_{10}	$=$	$\sum_{i=m-1}^{M-1} \left\{ \binom{M-1}{i} \binom{i}{m-1} [x(t)]^{m-1} [q(t)-x(t)]^{i-(m-1)} \times [1-q(t)-x(T)+x(t)]^{M-1-i} \right\} \frac{M}{A_B} [1-P_{FTR}(t)] Q(t) dt$
P_{11}	$=$	$[1-x(T)]^M$
P_{12}	$=$	$[1-y(T)]^N$
$q(t)$	$\equiv$	$\int_0^t \frac{1}{A_B} Q(\tau) d\tau$
$x(t)$	$\equiv$	$\int_0^t \frac{1}{A_B} [1-P_{FTR}(\tau)] Q(\tau) d\tau$
$y(t)$	$\equiv$	$\int_0^t \frac{1}{A_B} P_{TR}(\tau) Q(\tau) d\tau$

2.2.4 Scenario 4. For this scenario, N targets and M false targets are uniformly distributed in the battle space. The air vehicle flies along a straight path with area coverage rate $Q(t)$. Table 2.6 lists the 12 elemental probabilities and the corresponding state definitions.

Table 2.7 Scenario 5 Elemental Probabilities and State Definitions

P_1	=	$\sum_{j=n-1}^{N-1} \left\{ \binom{N-1}{j} \binom{j}{n-1} [y(r)]^{n-1} [q_y(r) - y(r)]^{j-(n-1)} [1 - q_y(r)]^{N-1-j} \right\}$
		$\times N P_{TR}(r) \frac{r}{\sigma_y^2} e^{-\frac{r^2}{2\sigma_y^2}} dr$
P_2	=	$e^{-x(r)} \frac{[x(r)]^m}{m!}$
P_3	=	$\sum_{j=n}^{N} \left\{ \binom{N}{j} \binom{j}{n} [y(r)]^n [q_y(r) - y(r)]^{j-n} [1 - q_y(r)]^{N-j} \right\}$
P_4	=	$e^{-x(r)} \frac{[x(r)]^{(m-1)}}{(m-1)!} [1 - P_{FTR}(r)] 2\pi r \alpha(r) dr$
P_5	=	$e^{-x(r)}$
P_6	=	$[1 - y(r)]^N$
P_7	=	$\sum_{j=n-1}^{N-1} \left\{ \binom{N-1}{j} \binom{j}{n-1} [y(r)]^{n-1} [q_y(r) - y(r)]^{j-(n-1)} \times \right.$
		$\left. [1 - q_y(r) - y(R) + y(r)]^{N-1-j} \right\} N P_{TR}(r) \frac{r}{\sigma_y^2} e^{-\frac{r^2}{2\sigma_y^2}} dr$
P_8	=	$e^{-x(R)} \frac{[x(r)]^m}{m!}$
P_9	=	$\sum_{j=n}^{N} \left\{ \binom{N}{j} \binom{j}{n} [y(r)]^n [q_y(r) - y(r)]^{j-n} [1 - q_y(r) - y(R) + y(r)]^{N-j} \right\}$
P_{10}	=	$e^{-x(R)} \frac{[x(r)]^{(m-1)}}{(m-1)!} [1 - P_{FTR}(r)] 2\pi r \alpha(r) dr$
P_{11}	=	$e^{-x(R)}$
P_{12}	=	$[1 - y(R)]^N$
$q_y(r)$	≡	$\int_0^r \frac{\rho}{\sigma_y^2} e^{-\frac{\rho^2}{2\sigma_y^2}} d\rho$
$x(r)$	≡	$\int_0^r [1 - P_{FTR}(\rho)] 2\pi\rho\alpha(\rho) d\rho$
$y(r)$	≡	$\int_0^r P_{TR}(\rho) \frac{\rho}{\sigma_y^2} e^{-\frac{\rho^2}{2\sigma_y^2}} d\rho$

2.2.5 Scenario 5. For this scenario, N targets are normally distributed among a Poisson field of false targets with density $\alpha(\rho)$. Normally-distributed refers to a circular normal distribution with standard deviation σ_y. The search area A_s is a circular disc of radius R. The air vehicle searches the disc using concentric annuli of radius r and thickness dr. The search begins at the origin of the disc and progresses outward. Table 2.7 lists the 12 elemental probabilities and the corresponding state definitions.

Table 2.8 Scenario 6 Elemental Probabilities and State Definitions

P_1	=	$\sum_{j=n-1}^{N-1} \binom{N-1}{j} \binom{j}{n-1} [y(r)]^{n-1} [q_y(r) - y(r)]^{j-(n-1)} [1 - q_y(r)]^{N-1-j}$
		$\times N P_{TR}(r) \frac{r}{\sigma_y^2} e^{-\frac{r^2}{2\sigma_y^2}} dr$
P_2	=	$\sum_{i=m}^{M} \binom{M}{i} \binom{i}{m} [x(r)]^m [q_x(r) - x(r)]^{j-n} [1 - q_x(r)]^{M-i}$
P_3	=	$\sum_{j=n}^{N} \binom{N}{j} \binom{j}{n} [y(r)]^n [q_y(r) - y(r)]^{j-n} [1 - q_y(r)]^{N-j}$
P_4	=	$\sum_{i=m-1}^{M-1} \binom{M-1}{i} \binom{i}{m-1} [x(r)]^{m-1} [q_x(r) - x(r)]^{i-(m-1)} [1 - q_x(r)]^{M-1-i}$
		$\times M [1 - P_{FTR}(r)] \frac{r}{\sigma_x^2} e^{-\frac{r^2}{2\sigma_x^2}} dr$
P_5	=	$[1 - x(r)]^M$
P_6	=	$[1 - y(r)]^N$
P_7	=	$\sum_{j=n-1}^{N-1} \binom{N-1}{j} \binom{j}{n-1} [y(r)]^{n-1} [q_y(r) - y(r)]^{j-(n-1)} \times$
		$[1 - q_y(r) - y(R) + y(r)]^{N-1-j} N P_{TR}(r) \frac{r}{\sigma_y^2} e^{-\frac{r^2}{2\sigma_y^2}} dr$
P_8	=	$\sum_{i=m}^{M} \binom{M}{i} \binom{i}{m} [x(r)]^m [q_x(r) - x(r)]^{i-m} [1 - q_x(r) - x(R) + x(r)]^{M-i}$
P_9	=	$\sum_{j=n}^{N} \binom{N}{j} \binom{j}{n} [y(r)]^n [q_y(r) - y(r)]^{j-n} [1 - q_y(r) - y(R) + y(r)]^{N-j}$
P_{10}	=	$\sum_{i=m-1}^{M-1} \binom{M-1}{i} \binom{i}{m-1} [x(r)]^{m-1} [q_x(r) - x(r)]^{i-(m-1)} \times$
		$[1 - q_x(r) - x(R) + x(r)]^{M-1-i} M [1 - P_{FTR}(r)] \frac{r}{\sigma_x^2} e^{-\frac{r^2}{2\sigma_x^2}} dr$
P_{11}	=	$[1 - x(R)]^M$
P_{12}	=	$[1 - y(R)]^N$
$q_x(r)$	$\equiv$	$\int_0^r \frac{\rho}{\sigma_x^2} e^{-\frac{\rho^2}{2\sigma_x^2}} d\rho$ $\qquad$ $q_y(r) \equiv \int_0^r \frac{\rho}{\sigma_y^2} e^{-\frac{\rho^2}{2\sigma_y^2}} d\rho$
$x(r)$	$\equiv$	$\int_0^r [1 - P_{FTR}(\rho)] \frac{\rho}{\sigma_x^2} e^{-\frac{\rho^2}{2\sigma_x^2}} d\rho$
$y(r)$	$\equiv$	$\int_0^r P_{TR}(\rho) \frac{\rho}{\sigma_y^2} e^{-\frac{\rho^2}{2\sigma_y^2}} d\rho$

2.2.6 Scenario 6. For this scenario, N targets and M false targets are normally distributed (circular) with standard deviations σ_y and σ_x respectively. Table 2.8 lists the 12 elemental probabilities and the corresponding state definitions.

Table 2.9 Scenario 7 Elemental Probabilities and State Definitions

P_1	$=$	$P_{TR}(r)\,\frac{r}{\sigma_y^2}e^{-\frac{r^2}{2\sigma_y^2}}dr$
P_2	$=$	$e^{-x(r)}\frac{[x(r)]^m}{m!}$
P_3	$=$	$[1-y(r)]$
P_4	$=$	$e^{-x(r)}\frac{[x(r)]^{(m-1)}}{(m-1)!}[1-P_{FTR}(r)]\,2\pi r\alpha(r)\,dr$
P_5	$=$	$e^{-x(r)}$
P_6	$=$	$[1-y(r)]$
P_7	$=$	$P_{TR}(r)\,\frac{r}{\sigma_y^2}e^{-\frac{r^2}{2\sigma_y^2}}dr$
P_8	$=$	$e^{-x(R)}\frac{[x(r)]^m}{m!}$
P_9	$=$	$[1-y(R)]$
P_{10}	$=$	$e^{-x(R)}\frac{[x(r)]^{(m-1)}}{(m-1)!}[1-P_{FTR}(r)]\,2\pi r\alpha(r)\,dr$
P_{11}	$=$	$e^{-x(R)}$
P_{12}	$=$	$[1-y(R)]$
$x(r)$	$\equiv$	$\int_0^r[1-P_{FTR}(\rho)]\,2\pi\rho\alpha(\rho)\,d\rho$
$y(r)$	$\equiv$	$\int_0^r P_{TR}(\rho)\,\frac{\rho}{\sigma_y^2}e^{-\frac{\rho^2}{2\sigma_y^2}}d\rho$

2.2.7 Scenario 7. This scenario is the specific case of Scenario 5 when $N = 1$. Table 2.9 lists the 12 elemental probabilities and the corresponding state definitions.

2.3 System Operating Characteristic

Everything needed to calculate $P(m \geq \hat{m})$ and $P(n \geq \hat{n})$ has been provided. How the ATR parameters are related is now examined. The parameters P_{TR} and P_{FTR} characterize the sensor's performance and are not independent. They are often linked by a Receiver Operating Characteristic (ROC) curve. A mathematical representation of the ROC curve produces a graph of true positive fraction (P_{TR}) versus false positive fraction ($1 - P_{FTR}$) that starts at $(0, 0)$, then monotonically increases to $(1, 1)$. The ROC curve model adapted from Ref. [36] is used in this reasearch:

$$(1 - P_{FTR}) = \frac{P_{TR}}{(1 - c) P_{TR} + c} \tag{2.12}$$

where the parameter, $c \in [1, \infty)$, will depend on the sensor and data processing algorithm. It will also depend on the vehicle speed (dwell time), and engagement geometry, which includes flight altitude and look angle. A family of ROC curves

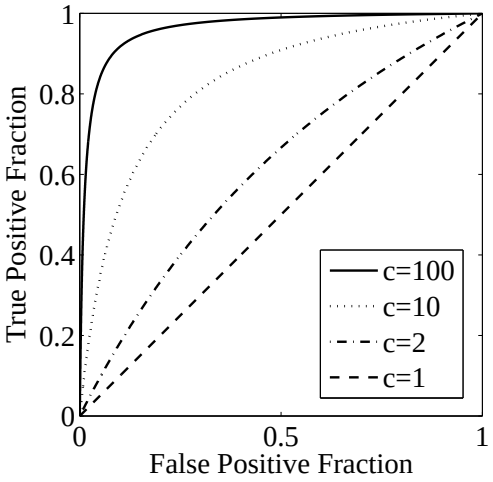

Figure 2.3 Family of ROC Curves.

parameterized by c is shown in Figure 2.3. As c increases, the ROC improves. As $c \to \infty$, the area under the curve approaches unity indicating perfect classification.

For a given sensor and algorithm with a constant area coverage rate, the operating point on a ROC curve is determined by the sensor's threshold for declaring

target. Although typically it must be determined from experimentation, it will be assumed the relation between P_{TR} and $(1 - P_{FTR})$ is known, and can be approximated using Eq. (2.12). Thus, our goal is finding the optimal probability of a target report (P^*_{TR}) – either constant, or as a function of elapsed time or space covered. Optimal solutions will be denoted with $*$.

If area coverage rate is allowed to vary, the operating point in essence moves from ROC curve to ROC curve. Better performance is expected at slower area coverage rates, since longer dwell times allow for more sensing and data processing. Conversely, worse performance is expected at higher area coverage rates. One way to model this effect is having the parameter c be inversely proportional to area coverage rate Q. It is assumed experimental results will yield a scaled nominal area coverage rate, Q_n, such that when Q_n is divided by Q, the ROC curve is approximated using the ROC parameter

$$c = \frac{Q_n}{Q} \tag{2.13}$$

in Eq. (2.12). There is still the requirement of $c > 1$, thus $Q < Q_n$. The goal is to find the optimal combination of P_{TR} and Q – either constant, or as a function of elapsed time or space covered. The combination of P_{TR} and Q establishes a system operating characteristic.

2.4 Optimal Control Formulation

An operator wants the expected number of target attacks to be high and the expected number of false target attacks to be low. One is interested in *a priori* predictions of effectiveness and thus use $P(n \geq \hat{n})$ and $P(m \geq \hat{m})$. Unfortunately due to the ROC, adjusting the sensor threshold to increase the number of target attacks also increases the number of false target attacks. Thus, the operator's objectives are competing, and a trade-off situation arises. To ensure $P(m \geq \hat{m})$ stays low, a constraint is imposed on it. The general optimization problem statement is then

$$\begin{aligned} \text{Max:} \quad & P\left(n \geq \hat{n}\right) \\ \text{subj to:} \quad & P\left(m \geq \hat{m}\right) \leq b \end{aligned}$$

where the upper bound b, threshold for target attacks $\hat{n}$, threshold for false target attacks $\hat{m}$, and mission duration T are set by the designer or mission planner. The decision variables are P_{TR} and Q.

Everything needed to calculate $P\left(n \geq \hat{n}\right)$ and $P\left(m \geq \hat{m}\right)$ has been provided as well as a way to relate P_{TR} and $(1 - P_{FTR})$. The problem can now be formulated as an optimal control problem whose solution method is given in various text books. The notation used by Bryson and Ho [8] is used and the problem is posed in their standard form which is

$$\begin{aligned} \text{Min:} \quad & J\left[\mathbf{s}\left(t\right), \mathbf{u}\left(t\right)\right] = \phi\left[\mathbf{s}\left(T\right)\right] + \int_0^T L\left[\mathbf{s}\left(t\right), \mathbf{u}\left(t\right), t\right] dt \\ \text{Subj to:} \quad & \dot{\mathbf{s}} = \mathbf{f}\left[\mathbf{s}\left(t\right), \mathbf{u}\left(t\right), t\right], \, \mathbf{s}\left(0\right) = 0 \end{aligned}$$

Since their standard form involves minimizing a cost functional J, the objective function (maximizing $P\left(n \geq \hat{n}\right)$) is multiplied by minus one. The integrand L then becomes the negative of the probability density function for $P\left(n \geq \hat{n}\right)$. The state vector $\mathbf{s}(t)$ consists of the states defined for calculating elemental probabilities ($q\left(t\right)$, $x\left(t\right)$, and $y\left(t\right)$) augmented with a state representing $P\left(m \geq \hat{m}\right)$, which is denoted $z(t)$ for brevity. Initial conditions on the states are zero. The terminal conditions on q, x, and y are free, whereas $z\left(T\right) \leq b$. The vector $\mathbf{f}[\mathbf{s}\left(t\right), \mathbf{u}\left(t\right), t]$ specifies the dynamics. The control vector $\mathbf{u}(t)$ consists of the decision variables P_{TR} and Q. The performance objective ϕ is a function of the the final states.

The Pontryagin Maximum Principle [8] is invoked, which involves forming the Hamiltonian, H, given by

$$H\left[\mathbf{s}\left(t\right), \mathbf{u}\left(t\right), t\right] = L\left[\mathbf{s}\left(t\right), \mathbf{u}\left(t\right), t\right] + \lambda^{\mathrm{T}}\left(t\right) \mathbf{f}\left[\mathbf{s}\left(t\right), \mathbf{u}\left(t\right), t\right] \tag{2.14}$$

where λ is the vector of costates. Note: T is mission duration and T is the transpose operator. The costate differential equations are

$$\dot{\lambda}^{\mathrm{T}} = -\frac{\partial H}{\partial \mathbf{s}} = -\frac{\partial L}{\partial \mathbf{s}} - \lambda^{\mathrm{T}} \frac{\partial \mathbf{f}}{\partial \mathbf{s}}. \tag{2.15}$$

The constraint involving z amounts to a "path constraint", which results in λ_z being constant for all time [8]. Since $q(T)$, $x(T)$, and $y(T)$ are free, $\lambda_q(T) = \lambda_x(T) = \lambda_y(T) = 0$. Finally, the optimal control is derived using the first-order necessary condition

$$\frac{\partial H}{\partial \mathbf{u}} = \mathbf{0}. \tag{2.16}$$

The differential equations from this formulation are coupled, so closed-form solutions do not exist. Instead, the state and costate equations must be numerically integrated. Two-point-boundary-value problems of this form can be solved using a "shooting method" [7] or a discrete-time, gradient-based solver such as Matlab's® fmincon routine.

2.5 Sample Formulation

To make sense of everything covered in Sections 2.1-2.4, a sample formulation is provided. But first, here is a recap of where the various parameters come from.

Designer or Mission Planner: $\hat{m}$, $\hat{n}$, b, k, T, R

Order of Battle Intelligence: α, β, N, M, σ_x, σ_y, A_B

Performance Specifications: c, Q_n, Q_{min}, Q_{max}

Let $\hat{m} = \hat{n} = 1$, and assume T and b are designated. In addition, assume both the number of targets N and the number of false targets M are both greater than the number of warheads k. At this point, the actual values for T, b, N, M, and k are not needed and can remain parameters. The optimization problem becomes

$$\begin{aligned} \text{Max:} \quad & P(n \geq 1) \\ \text{subj to:} \quad & P(m \geq 1) \leq b \end{aligned}$$

Using Eqs. 2.10 and 2.9 gives

$$\begin{aligned} P(n \geq 1) &= 1 - P(n = 0) \\ &= 1 - \sum_{m=0}^{k-1} P_{m,0}^{(m+n<k)} - P_{k,0}^{(m+n=k)} \end{aligned} \tag{2.17}$$

and

$$\begin{aligned} P(m \geq 1) &= 1 - P(m = 0) \\ &= 1 - \sum_{n=0}^{k-1} P_{0,n}^{(m+n<k)} - P_{0,k}^{(m+n=k)}. \end{aligned} \tag{2.18}$$

Substituting elemental probabilities gives

$$P(n \geq 1) = 1 - P_{11}P_{12} - \sum_{m=1}^{k-1} \int_0^T P_{10}P_{12} - \int_0^T P_4 P_6 \tag{2.19}$$

and

$$P(m \geq 1) = 1 - P_{11}P_{12} - \sum_{n=1}^{k-1} \int_0^T P_7 P_{11} - \int_0^T P_1 P_5. \tag{2.20}$$

Bryson and Ho [8] notation becomes

$$\phi[\mathbf{s}(T)] = P_{11}P_{12} \tag{2.21}$$

$$L[\mathbf{s}(t), \mathbf{u}(t)]\, dt = P_4 P_6 + \sum_{m=1}^{k-1} P_{10}P_{12} \tag{2.22}$$

$$\mathbf{u}(t) = [P_{TR}(t) \;\; Q(t)]^{\mathrm{T}} \tag{2.23}$$

$$\mathbf{s}(t) = [q(t) \;\; x(t) \;\; y(t) \;\; z(t)]^{\mathrm{T}} \tag{2.24}$$

where $q(t)$, $x(t)$, and $y(t)$ are defined once a scenario is selected, and

$$z(t) = 1 - P_{11}P_{12} - \int_0^T \left(P_1 P_5 + \sum_{n=1}^{k-1} P_7 P_{11} \right) \tag{2.25}$$

For example, if Scenario 2 elemental probabilities are used, then

$$x(t) = \int_0^t \left[1 - P_{FTR}(\tau)\right] Q(\tau)\, \alpha(\tau)\, d\tau \tag{2.26}$$

$$y(t) = \int_0^t P_{TR}(\tau)\, Q(\tau)\, \beta(\tau)\, d\tau \tag{2.27}$$

$$\phi\left[\mathbf{s}(T)\right] = e^{-x(T)} e^{-y(T)} \tag{2.28}$$

$$\begin{aligned} L\left[\mathbf{s}(t), \mathbf{u}(t)\right] = {} & e^{-x(t)} \frac{\left[x(t)\right]^{(m-1)}}{(m-1)!} \left[1 - P_{FTR}(t)\right] Q(t)\, \alpha(t)\, e^{-y(t)} + \\ & \sum_{m=1}^{k-1} e^{-x(T)} \frac{\left[x(t)\right]^{(m-1)}}{(m-1)!} \left[1 - P_{FTR}(t)\right] Q(t)\, \alpha(t)\, e^{-y(T)} \end{aligned} \tag{2.29}$$

$$\begin{aligned} z(t) = 1 - e^{-x(t)} e^{-y(t)} - \int_0^t \Bigg\{ & e^{-y(\tau)} \frac{\left[y(\tau)\right]^{(n-1)}}{(n-1)!} P_{TR}(\tau)\, Q(\tau)\, \beta(\tau)\, e^{-x(\tau)} + \\ & \sum_{n=1}^{k-1} e^{-y(t)} \frac{\left[y(\tau)\right]^{(n-1)}}{(n-1)!} P_{TR}(\tau)\, Q(\tau)\, \beta(\tau)\, e^{-x(t)} \Bigg\} d\tau \end{aligned} \tag{2.30}$$

Everything thus far was accomplished without specifying a ROC model. If constant area coverage rate is assumed constant and Eq. (2.12) is used for ROC model, then

$$x(t) = \int_0^t \left[\frac{P_{TR}(\tau)}{(1-c) P_{TR}(\tau) + c} \right] wv\alpha(\tau)\, d\tau \tag{2.31}$$

$$y(t) = \int_0^t P_{TR}(\tau)\, wv\beta(\tau)\, d\tau \tag{2.32}$$

$$\phi\left[\mathbf{s}(T)\right] = e^{-x(T)} e^{-y(T)} \tag{2.33}$$

$$L\left[\mathbf{s}\left(t\right),\mathbf{u}\left(t\right)\right]=e^{-x(t)}\frac{\left[x\left(t\right)\right]^{(m-1)}}{(m-1)!}\left[\frac{P_{TR}\left(t\right)}{\left(1-c\right)P_{TR}\left(t\right)+c}\right]wv\alpha\left(t\right)e^{-y(t)}+$$
$$\sum_{m=1}^{k-1}e^{-x(T)}\frac{\left[x\left(t\right)\right]^{(m-1)}}{(m-1)!}\left[\frac{P_{TR}\left(t\right)}{\left(1-c\right)P_{TR}\left(t\right)+c}\right]wv\alpha\left(t\right)e^{-y(T)} \quad (2.34)$$

$$z\left(t\right)=1-e^{-x(t)}e^{-y(t)}-\int_{0}^{t}\left\{e^{-y(\tau)}\frac{\left[y\left(\tau\right)\right]^{(n-1)}}{(n-1)!}P_{TR}\left(\tau\right)wv\beta\left(\tau\right)e^{-x(\tau)}+\right.$$
$$\left.\sum_{n=1}^{k-1}e^{-y(t)}\frac{\left[y\left(\tau\right)\right]^{(n-1)}}{(n-1)!}P_{TR}\left(\tau\right)wv\beta\left(\tau\right)e^{-x(t)}\right\}d\tau \quad (2.35)$$

In this case, the only control variable is P_{TR}. The densities $\alpha\left(t\right)$ and $\beta\left(t\right)$ would be specified from the order of battle intelligence. The ROC parameter c would be taken from the sensor performance specification for the given area coverage rate. This completes the sample formulation. The solution can be found using a shooting method or a discrete-time, gradient-based solver. The system effectiveness would be known along with the schedule for sensor threshold. While jumping straight to a numerical solver may be tempting, insight would be lost into the how the solution should behave. Thus in Chapter III, the optimal control is analytically calculated using $\frac{\partial H}{\partial \mathbf{u}}=\mathbf{0}$ for tractable instances of Scenarios 1, 2, and 7.

III. Analysis

In this chapter, analytic conclusions are provided for the munition and sensor craft problems for Scenarios 1, 2, and 7. Using these tractable instances, the problem can be bounded and insight can be gained prior to calculating numerical solutions. Ten theorems are presented from which the following conclusions are drawn:

1. For Scenarios 1 and 2 with $k = 1$ and no constraint on $P(m \geq \hat{m})$, if T, Q, α, and β are constant, the unbounded P_{TR}^* is monotonically increasing with time.

2. For Scenarios 1, 2, and 7 with $k = \infty$, $\hat{n} = 1$, and no constraint on $P(m \geq \hat{m})$, if T (or R), Q, α, and β are constant, the bounded $P_{TR}^* = P_{TR_{max}}^* = 1$.

3. For Scenarios 1 and 2 with $k = \infty$ and $P(m \geq \hat{m}) = b$, if T, Q, α, and β are constant, then P_{TR}^* is constant for all time.

4. For Scenarios 1 and 2 with $k = 1$ or $k = \infty$, if T, α, and β are constant and $Q(t)$ is unbounded, then the unbounded P_{TR}^* is given by

$$P_{TR}^*(t) = \frac{Q_n}{2Q_n - Q^*(t)} \tag{3.1}$$

5. For Scenario 7 with $k = \infty$ and $P(m \geq \hat{m}) = b$, if R and α are constant, then P_{TR}^* is monotonically decreasing with radius.

The remainder of this chapter contains detailed calculations required for the 10 theorems. The general approach involves forming a Hamiltonian for each problem, then solving $\frac{\partial H}{\partial \mathbf{u}} = \mathbf{0}$ to determine the form of the optimal control. Next the derivative of the optimal control with respect to time or radius is taken to determine any trends (e.g. increasing, decreasing, or constant). The reader can skip to Chapter IV for applications that demonstrate the conclusions above.

3.1 Scenario 1: Fixed T, Fixed Q, Variable P_{TR}

For Scenario 1, one target is uniformly distributed among a Poisson field of false targets with density α, which is assumed constant. The air vehicle flies along a straight path with area coverage rate $Q(t)$. For now Q is constant and specified. Therefore, the only decision variable is P_{TR}. Constant Q implies the ROC parameter c is constant.

3.1.1 Munition Problem. To start, in addition to assuming T, Q, and α are constant, there is no constraint on $P(m \geq \hat{m})$.

Theorem 1 (Scenario 1 with $k = 1$ and no constraint on $P(m \geq \hat{m})$) *If T, Q, and α are constant, the unbounded P_{TR}^* is monotonically increasing.*

Proof: Let the state x be

$$x(t) = \int_0^t \alpha Q \left[1 - P_{FTR}(\tau)\right] d\tau. \tag{3.2}$$

The corresponding L is

$$L = -\frac{Q}{A_B} P_{TR}(t)\, e^{-x(t)}. \tag{3.3}$$

The derivative of the state is

$$\dot{x}(t) = \alpha Q \left[1 - P_{FTR}(t)\right]. \tag{3.4}$$

After applying Eq. (2.12) for the ROC model, the Hamiltonian becomes

$$H = -\frac{Q}{A_B} P_{TR} e^{-x} + \lambda_x \alpha Q \frac{P_{TR}}{(1-c)\, P_{TR} + c} \tag{3.5}$$

and the costate differential equation becomes

$$\dot{\lambda}_x(t) = -\frac{Q}{A_B} P_{TR}(t)\, e^{-x(t)}. \tag{3.6}$$

Taking the partial derivative of H with respect to the decision variable P_{TR} gives

$$\frac{\partial H}{\partial P_{TR}} = -\frac{Q}{A_B}e^{-x} + \frac{\lambda_x \alpha Q c}{\left[(1-c)\,P_{TR} + c\right]^2} \tag{3.7}$$

Solving $\frac{\partial H}{\partial P_{TR}} = 0$, the optimal control is

$$P^*_{TR}(t) = \frac{c \pm \sqrt{\lambda_x(t)\,\alpha c A_B e^{x(t)}}}{c-1}. \tag{3.8}$$

Only the "minus" root is of interest, since the "plus" root puts P_{TR} outside of $[0,1]$ for all time. Taking the derivative of Eq. (3.8) with respect to t gives

$$\dot{P}^*_{TR}(t) = \frac{-1}{2(c-1)}\sqrt{\frac{\alpha c A_B}{\lambda_x(t)\,e^{x(t)}}}\left[\lambda_x(t)\,\dot{x}(t) + \dot{\lambda}_x(t)\right]e^{x(t)}. \tag{3.9}$$

Using Eqs. (3.4) and (3.6) for $\dot{x}(t)$ and $\dot{\lambda}_x(t)$ yields

$$\dot{P}^*_{TR}(t) = Q\sqrt{\frac{\alpha e^{-x(t)}}{4cA_B\lambda_x(t)}}\left[P^*_{TR}(t)\right]^2 > 0. \tag{3.10}$$

□

At the terminal point where $\lambda_x(T) = 0$, $P^*_{TR}(T) = \frac{c}{c-1} > 1$. Thus, the constraint $P_{TR} \leq 1$ becomes active prior to the end and remains active until time T. See Appendix D for further analysis on when the constraint becomes active. This represents a "go for broke" tactic in the end game. This strategy of starting conservative then gradually increasing aggressiveness until the end, where an all out effort is tried, is common in game theory. Without a constraint on false target attacks, the system has nothing to lose by declaring all objects as targets near the end.

Next, the effects of adding a constraint on false target attacks is examined. With a constraint on $P(m \geq \hat{m})$, the following states are needed:

$$x(t) = \int_0^t \alpha Q \left[1 - P_{FTR}(\tau)\right] d\tau \tag{3.11}$$

$$y(t) = \int_0^t \frac{Q}{A_B} P_{TR}(\tau)\, d\tau \tag{3.12}$$

$$z(t) = \int_0^t \alpha Q \left[1 - P_{FTR}(\tau)\right] \left[1 - y(\tau)\right] e^{-x(\tau)} d\tau. \tag{3.13}$$

The corresponding L is still

$$L = -\frac{Q}{A_B} P_{TR}(t)\, e^{-x(t)}. \tag{3.14}$$

The derivatives of the states are

$$\dot{x}(t) = \alpha Q \left[1 - P_{FTR}(t)\right] \tag{3.15}$$

$$\dot{y}(t) = \frac{Q}{A_B} P_{TR}(t) \tag{3.16}$$

$$\dot{z}(t) = \alpha Q \left[1 - P_{FTR}(t)\right] \left[1 - y(t)\right] e^{-x(t)} \tag{3.17}$$

After applying Eq. (2.12) for the ROC model, the Hamiltonian becomes

$$H = \left(\lambda_y - e^{-x}\right) \frac{Q}{A_B} P_{TR} + \alpha Q \frac{P_{TR}}{(1-c) P_{TR} + c} \left[\lambda_x + \lambda_z (1 - y) e^{-x}\right] \tag{3.18}$$

and the costate differential equations become

$$\dot{\lambda}_x(t) = \lambda_z \alpha Q \frac{P_{TR}(t)}{(1-c) P_{TR}(t) + c} \left[1 - y(t)\right] e^{-x(t)} - \frac{Q}{A_B} P_{TR}(t)\, e^{-x(t)} \tag{3.19}$$

$$\dot{\lambda}_y(t) = \lambda_z \alpha Q \frac{P_{TR}(t)}{(1-c) P_{TR}(t) + c} e^{-x(t)} \tag{3.20}$$

$$\dot{\lambda}_z(t) = 0 \tag{3.21}$$

Taking the partial derivative of H with respect to the decision variable P_{TR} gives

$$\frac{\partial H}{\partial P_{TR}} = \left(\lambda_y - e^{-x}\right) \frac{Q}{A_B} + \frac{\left[\lambda_x + \lambda_z \left(1 - y\right) e^{-x}\right] \alpha Q c}{\left[\left(1 - c\right) P_{TR} + c\right]^2} \tag{3.22}$$

Solving $\frac{\partial H}{\partial P_{TR}} = 0$, the optimal control is

$$P^*_{TR}(t) = \frac{c \pm \sqrt{\frac{\left\{\lambda_x(t) + \lambda_z[1 - y(t)]e^{-x(t)}\right\} \alpha c A_B}{\left[e^{-x(t)} - \lambda_y(t)\right]}}}{c - 1}. \tag{3.23}$$

Only the "minus" root is of interest, since the "plus" root puts P_{TR} outside of $[0, 1]$ for all time. While taking the derivative of Eq. (3.23) with respect to t is possible, there are too many terms involved to discern any trends. Nonetheless, Eq. (3.23) shows the form of the optimal control.

3.1.2 Sensor Craft Problem. The sensor craft problem does not condition $P\left(n \geq \hat{n}\right)$ on the number of previous attacks. For Scenario 1,

$$P\left(n = 1\right) = \int_0^T \frac{Q}{A_B} P_{TR}\left(t\right) dt. \tag{3.24}$$

Theorem 2 (Scenario 1 with $k = \infty$ and no constraint on $P\left(m \geq \hat{m}\right)$) *If T, Q, and α are constant, the optimal constrained solution is $P^*_{TR} = P^*_{TR_{max}} = 1$.*

Proof: With no constraint on $P\left(m \geq \hat{m}\right)$, the optimal control is clearly $P^*_{TR} = P^*_{TR_{max}} = 1$ for all time.

□

This is not a practical solution, since all false targets would be declared targets and attacked. With an infinite amount of warheads and no constraint on false target attacks, there is no reason not to attack every object encountered.

Next, the effect of adding a constraint on false target attacks is examined. The sensor craft problem does not condition $P(m \geq \hat{m})$ on the number of previous attacks.

Theorem 3 (Scenario 1 with $k = \infty$, $\hat{m} = 1$, and $P(m \geq 1) = b$) *If T, Q, and α are constant, $P_{TR}^{*}(t) = \frac{-c \ln[1-b]}{(1-c)\ln[1-b]+\alpha QT}$.*

Proof: With a constraint on $P(m \geq \hat{m})$, the states become

$$x(t) = \int_0^t \alpha Q \left[1 - P_{FTR}(\tau)\right] d\tau \tag{3.25}$$

$$z(t) = 1 - \sum_{m=0}^{\hat{m}-1} \frac{[x(t)]^m}{m!} e^{-x(t)} \tag{3.26}$$

The corresponding L is

$$L = -\frac{Q}{A_B} P_{TR}(t). \tag{3.27}$$

The derivatives of the states are

$$\dot{x}(t) = \alpha Q \left[1 - P_{FTR}(t)\right] \tag{3.28}$$

$$\dot{z}(t) = \alpha Q \left[1 - P_{FTR}(t)\right] \left\{ \frac{[x(t)]^{(\hat{m}-1)}}{(\hat{m}-1)!} \right\} e^{-x(t)} \tag{3.29}$$

After applying Eq. (2.12) for the ROC model, the Hamiltonian becomes

$$H = -\frac{Q}{A_B} P_{TR} + \alpha Q \frac{P_{TR}}{(1-c)P_{TR} + c} \left\{ \lambda_x + \lambda_z \left[\frac{x^{(\hat{m}-1)}}{(\hat{m}-1)!} \right] e^{-x} \right\} \tag{3.30}$$

and the costate differential equations become

$$\dot{\lambda}_x(t) = -\lambda_z \alpha Q \frac{P_{TR}(t)}{(1-c)P_{TR}(t) + c} \left[\frac{(\hat{m}-1)}{x(t)} - 1 \right] \left\{ \frac{[x(t)]^{(\hat{m}-1)}}{(\hat{m}-1)!} \right\} e^{-x(t)} \tag{3.31}$$

$$\dot{\lambda}_z(t) = 0 \tag{3.32}$$

Taking the partial derivative of H with respect to the decision variable P_{TR} gives

$$\frac{\partial H}{\partial P_{TR}} = -\frac{Q}{A_B} + \frac{\alpha Q c \left\{ \lambda_x + \lambda_z \left[\frac{x^{(\hat{m}-1)}}{(\hat{m}-1)!} \right] e^{-x} \right\}}{\left[(1-c) P_{TR} + c \right]^2} \tag{3.33}$$

Solving $\frac{\partial H}{\partial P_{TR}} = 0$, the optimal control is

$$P_{TR}^{*}(t) = \frac{c \pm \sqrt{\left\{ \lambda_x(t) + \lambda_z \left[\frac{[x(t)]^{(\hat{m}-1)}}{(\hat{m}-1)!} \right] e^{-x(t)} \right\} \alpha c A_B}}{c-1}. \tag{3.34}$$

Only the "minus" root is of interest, since the "plus" root puts P_{TR} outside of $[0,1]$ for all time. Taking the derivative of Eq. (3.34) with respect to t gives

$$\dot{P}_{TR}^{*}(t) = \frac{-1}{2(c-1)} \sqrt{\frac{\alpha c A_B}{\left\{ \lambda_x(t) + \lambda_z \left[\frac{[x(t)]^{(\hat{m}-1)}}{(\hat{m}-1)!} \right] e^{-x(t)} \right\}}} \times \left\{ \dot{\lambda}_x(t) + \lambda_z \dot{x}(t) \left[\frac{(\hat{m}-1)}{x(t)} - 1 \right] \left\{ \frac{[x(t)]^{(\hat{m}-1)}}{(\hat{m}-1)!} \right\} e^{-x(t)} \right\}. \tag{3.35}$$

Using Eq. (3.28) for $\dot{x}(t)$ with Eq. (2.12) for the ROC model yields

$$\dot{P}_{TR}^{*}(t) = 0 \tag{3.36}$$

implying P_{TR}^{*} is constant for all time. When target and false target densities remain fixed throughout the search effort and the amount of warheads is infinite, the problem becomes an infinite horizon problem, where optimal solutions are constant. Consider the case when $\hat{m} = 1$. For constant T, Q, α, and P_{TR},

$$P(m \geq 1) = 1 - e^{-\alpha Q T (1 - P_{FTR})} \leq b. \tag{3.37}$$

Applying Eq. (2.12) for the ROC model and assuming the constraint is active, the optimal control is

$$P_{TR}^{*}(t) = \frac{-c \ln[1-b]}{(1-c)\ln[1-b] + \alpha Q T}. \tag{3.38}$$

□

3.2 Scenario 1: Fixed T, Variable Q, Variable P_{TR}

The assumption that Q is constant is now relaxed. Therefore, the ROC parameter c is no longer constant. Equation (2.13), where $c(t) \equiv \frac{Q_n}{Q(t)}$ is used. Recall Q_n is a constant. The decision variables are Q and P_{TR}.

Theorem 4 (Scenario 1 with $k = 1$ or $k = \infty$) *If T and α are constant and Q is unbounded, the unbounded $P_{TR}^{*}(t) = \frac{Q_n}{2Q_n - Q^{*}(t)}$.*

Proof: Consider both the munition and sensor craft problems.

3.2.1 Munition Problem. For $k = 1$, dynamic Q, and dynamic P_{TR}, the states becomes

$$x(t) = \int_0^t \alpha Q(\tau)\left[1 - P_{FTR}(\tau)\right] d\tau \tag{3.39}$$

$$y(t) = \int_0^t \frac{1}{A_B} Q(\tau) P_{TR}(\tau)\, d\tau \tag{3.40}$$

$$z(t) = \int_0^t \alpha Q(\tau)\left[1 - P_{FTR}(\tau)\right]\left[1 - y(\tau)\right] e^{-x(\tau)} d\tau. \tag{3.41}$$

The corresponding L is

$$L = -\frac{1}{A_B} Q(t) P_{TR}(t)\, e^{-x(t)}. \tag{3.42}$$

The derivatives of the states are

$$\begin{aligned}
\dot{x}(t) &= \alpha Q(t)\left[1 - P_{FTR}(t)\right] && (3.43)\\
\dot{y}(t) &= \frac{1}{A_B} Q(t) P_{TR}(t) && (3.44)\\
\dot{z}(t) &= \alpha Q(t)\left[1 - P_{FTR}(t)\right]\left[1 - y(t)\right] e^{-x(t)} && (3.45)
\end{aligned}$$

Equation (2.12) becomes

$$\left[1 - P_{FTR}(t)\right] = \frac{Q(t) P_{TR}(t)}{Q(t) P_{TR}(t) + Q_n\left[1 - P_{TR}(t)\right]}. \quad (3.46)$$

Using Eq. (3.46), the Hamiltonian becomes

$$H = \left(\lambda_y - e^{-x}\right)\frac{1}{A_B} Q P_{TR} + \alpha \frac{Q^2 P_{TR}}{Q P_{TR} + Q_n\left(1 - P_{TR}\right)}\left[\lambda_x + \lambda_z (1 - y) e^{-x}\right] \quad (3.47)$$

and the costate differential equations become

$$\begin{aligned}
\dot{\lambda}_x &= \lambda_z \alpha \frac{Q^2(t) P_{TR}(t)}{Q(t) P_{TR}(t) + Q_n\left[1 - P_{TR}(t)\right]}\left[1 - y(t)\right] e^{-x(t)}\\
&\quad - \frac{1}{A_B} Q(t) P_{TR}(t) e^{-x(t)} && (3.48)\\
\dot{\lambda}_y &= \lambda_z \alpha \frac{Q^2(t) P_{TR}(t)}{Q(t) P_{TR}(t) + Q_n\left[1 - P_{TR}(t)\right]} e^{-x(t)} && (3.49)\\
\dot{\lambda}_z &= 0 && (3.50)
\end{aligned}$$

Taking the partial derivative of H with respect to the decision variable P_{TR} gives

$$\frac{\partial H}{\partial P_{TR}} = Q\left\{\left(\lambda_y - e^{-x}\right)\frac{1}{A_B} + \frac{\left[\lambda_x + \lambda_z (1 - y) e^{-x}\right] Q_n \alpha Q}{\left[Q P_{TR} + Q_n\left(1 - P_{TR}\right)\right]^2}\right\} \quad (3.51)$$

Taking the partial derivative of H with respect to the decision variable Q gives

$$\frac{\partial H}{\partial Q} = P_{TR}\left\{\left(\lambda_y - e^{-x}\right)\frac{1}{A_B} + \alpha\left[\lambda_x + \lambda_z (1 - y) e^{-x}\right]\frac{Q^2 P_{TR} + 2 Q_n Q\left(1 - P_{TR}\right)}{\left[Q P_{TR} + Q_n\left(1 - P_{TR}\right)\right]^2}\right\} \quad (3.52)$$

Ignoring the trivial solutions $P_{TR} = 0$ and $Q = 0$, the necessary conditions become

$$\left\{ \left(\lambda_y - e^{-x}\right) \frac{1}{A_B} + \frac{\left[\lambda_x + \lambda_z \left(1 - y\right) e^{-x}\right] Q_n \alpha Q}{\left[QP_{TR} + Q_n \left(1 - P_{TR}\right)\right]^2} \right\} = 0 \tag{3.53}$$

and

$$\left\{ \left(\lambda_y - e^{-x}\right) \frac{1}{A_B} + \alpha \left[\lambda_x + \lambda_z \left(1 - y\right) e^{-x}\right] \frac{Q^2 P_{TR} + 2Q_n Q \left(1 - P_{TR}\right)}{\left[QP_{TR} + Q_n \left(1 - P_{TR}\right)\right]^2} \right\} = 0 \tag{3.54}$$

Subtracting Eq. (3.53) from Eq. (3.54) gives

$$\alpha \left[\lambda_x + \lambda_z \left(1 - y\right) e^{-x}\right] \frac{Q^2 P_{TR} + 2Q_n Q \left(1 - P_{TR}\right)}{\left[QP_{TR} + Q_n \left(1 - P_{TR}\right)\right]^2} - \frac{\left[\lambda_x + \lambda_z \left(1 - y\right) e^{-x}\right] Q_n \alpha Q}{\left[QP_{TR} + Q_n \left(1 - P_{TR}\right)\right]^2} = 0 \tag{3.55}$$

Grouping like terms yields

$$\alpha Q \left[\lambda_x + \lambda_z \left(1 - y\right) e^{-x}\right] \frac{QP_{TR} - 2Q_n P_{TR} + Q_n}{\left[QP_{TR} + Q_n \left(1 - P_{TR}\right)\right]^2} = 0 \tag{3.56}$$

resulting in the necessary condition

$$\left[\lambda_x + \lambda_z \left(1 - y\right) e^{-x}\right] \left[QP_{TR} - 2Q_n P_{TR} + Q_n\right] = 0. \tag{3.57}$$

Thus, either

$$P_{TR}^{*}\left(t\right) = \frac{Q_n}{2Q_n - Q^{*}\left(t\right)} \tag{3.58}$$

or

$$\lambda_x \left(t\right) = -\lambda_z \left[1 - y\left(t\right)\right] e^{-x(t)}. \tag{3.59}$$

In the case where $P_{TR}^{*}\left(t\right) = \frac{Q_n}{2Q_n - Q^{*}(t)}$, insight can be gained looking to the relations between the parameters. From the requirement that $c > 1$, $Q^{*}\left(t\right) < Q_n$. So as Q^{*}

increases, P_{TR}^{*} increases. Further, for $Q^{*} \in (0, Q_n)$, $P_{TR}^{*} \in \left(\frac{1}{2}, 1\right)$. In other words,

$$P_{TR}^{*}(t) > 0.5 \tag{3.60}$$

For $Q_n >> Q^{*}$ (which is the case when $c = 100$), $P_{TR}^{*} \approx 0.5$ for all time. In addition, the relation between P_{TR}^{*} and Q^{*} does not depend on α or the value of b.

The case where $\lambda_x(t) = -\lambda_z [1 - y(t)] e^{-x(t)}$ never occurred in practice. In addition, the case where $P_{TR}^{*}(t) = \frac{Q_n}{2Q_n - Q^{*}(t)}$ shows up again and again in this Chapter and in practice. Therefore, it will be the focus.

3.2.2 Sensor Craft Problem. For $k = \infty$, dynamic Q, and dynamic P_{TR}, the states become

$$x(t) = \int_0^t \alpha Q(\tau) [1 - P_{FTR}(\tau)] d\tau \tag{3.61}$$

$$z(t) = 1 - \sum_{m=0}^{\hat{m}-1} \frac{[x(t)]^m}{m!} e^{-x(t)} \tag{3.62}$$

The corresponding L is

$$L = -\frac{1}{A_B} Q(t) P_{TR}(t). \tag{3.63}$$

The derivatives of the states are

$$\dot{x}(t) = \alpha Q(t) [1 - P_{FTR}(t)] \tag{3.64}$$

$$\dot{z}(t) = \alpha Q(t) [1 - P_{FTR}(t)] \left(\frac{[x(t)]^{(\hat{m}-1)}}{(\hat{m}-1)!} \right) e^{-x(t)} \tag{3.65}$$

After applying Eq. (3.46), the Hamiltonian becomes

$$H = -\frac{1}{A_B} Q P_{TR} + \alpha \frac{Q^2 P_{TR}}{Q P_{TR} + Q_n (1 - P_{TR})} \left[\lambda_x + \lambda_z \left(\frac{[x(t)]^{(\hat{m}-1)}}{(\hat{m}-1)!} \right) e^{-x} \right] \tag{3.66}$$

and the costate differential equations become

$$\begin{aligned}\dot{\lambda}_x(t) &= -\lambda_z\alpha\frac{Q^2(t)P_{TR}(t)}{Q(t)P_{TR}(t)+Q_n[1-P_{TR}(t)]}\left[\frac{(\hat{m}-1)}{x(t)}-1\right]\left(\frac{[x(t)]^{(\hat{m}-1)}}{(\hat{m}-1)!}\right)e^{-x(t)} \\ &\quad -\frac{1}{A_B}Q(t)P_{TR}(t) \qquad (3.67)\\ \dot{\lambda}_z(t) &= 0 \qquad (3.68)\end{aligned}$$

Taking the partial derivative of H with respect to the decision variable P_{TR} gives

$$\frac{\partial H}{\partial P_{TR}} = Q\left\{-\frac{1}{A_B}+\frac{\left[\lambda_x+\lambda_z\left(\frac{[x(t)]^{(\hat{m}-1)}}{(\hat{m}-1)!}\right)e^{-x}\right]Q_n\alpha Q}{[QP_{TR}+Q_n(1-P_{TR})]^2}\right\} \qquad (3.69)$$

Taking the partial derivative of H with respect to the decision variable Q gives

$$\frac{\partial H}{\partial Q} = P_{TR}\left\{-\frac{1}{A_B}+\alpha\left[\lambda_x+\lambda_z\left(\frac{[x(t)]^{(\hat{m}-1)}}{(\hat{m}-1)!}\right)e^{-x}\right]\frac{Q^2P_{TR}+2Q_nQ(1-P_{TR})}{[QP_{TR}+Q_n(1-P_{TR})]^2}\right\} \qquad (3.70)$$

Ignoring the trivial solutions $P_{TR}=0$ and $Q=0$, the necessary conditions become

$$\left\{-\frac{1}{A_B}+\frac{\left[\lambda_x+\lambda_z\left(\frac{[x(t)]^{(\hat{m}-1)}}{(\hat{m}-1)!}\right)e^{-x}\right]Q_n\alpha Q}{[QP_{TR}+Q_n(1-P_{TR})]^2}\right\}=0 \qquad (3.71)$$

and

$$\left\{-\frac{1}{A_B}+\alpha\left[\lambda_x+\lambda_z\left(\frac{[x(t)]^{(\hat{m}-1)}}{(\hat{m}-1)!}\right)e^{-x}\right]\frac{Q^2P_{TR}+2Q_nQ(1-P_{TR})}{[QP_{TR}+Q_n(1-P_{TR})]^2}\right\}=0 \qquad (3.72)$$

Subtracting Eq. (3.71) from Eq. (3.72) gives

$$\begin{aligned}&\alpha\left[\lambda_x+\lambda_z\left(\frac{[x(t)]^{(\hat{m}-1)}}{(\hat{m}-1)!}\right)e^{-x}\right]\frac{Q^2P_{TR}+2Q_nQ(1-P_{TR})}{[QP_{TR}+Q_n(1-P_{TR})]^2} \\ &\qquad -\frac{\left[\lambda_x+\lambda_z\left(\frac{[x(t)]^{(\hat{m}-1)}}{(\hat{m}-1)!}\right)e^{-x}\right]Q_n\alpha Q}{[QP_{TR}+Q_n(1-P_{TR})]^2}=0 \qquad (3.73)\end{aligned}$$

Grouping like terms yields

$$\alpha Q\left[\lambda_x+\lambda_z\left(\frac{\left[x\left(t\right)\right]^{(\hat{m}-1)}}{(\hat{m}-1)!}\right)e^{-x}\right]\frac{QP_{TR}-2Q_nP_{TR}+Q_n}{\left[QP_{TR}+Q_n\left(1-P_{TR}\right)\right]^2}=0 \tag{3.74}$$

resulting in the necessary condition

$$\left[\lambda_x+\lambda_z\left(\frac{\left[x\left(t\right)\right]^{(\hat{m}-1)}}{(\hat{m}-1)!}\right)e^{-x}\right]\left[QP_{TR}-2Q_nP_{TR}+Q_n\right]=0. \tag{3.75}$$

Thus, either

$$P_{TR}^{*}\left(t\right)=\frac{Q_n}{2Q_n-Q^{*}\left(t\right)} \tag{3.76}$$

or

$$\lambda_x\left(t\right)=-\lambda_z\left(\frac{\left[x\left(t\right)\right]^{(\hat{m}-1)}}{(\hat{m}-1)!}\right)e^{-x(t)} \tag{3.77}$$

Equation (3.76) is the same necessary condition as the single warhead case.

□

Thus, it appears the necessary condition in Eq. (3.76) holds regardless of the number of warheads, false target density, or maximum allowable $P\left(m\geq\hat{m}\right)$. This, of course, assumes unbounded design variables. If Q saturates at an upper or lower bound, the fixed-Q necessary conditions are used. Numerical examples in Chapter IV will address the bounded-Q case.

3.3 Scenario 2: Fixed T, Fixed Q, Variable P_{TR}

For Scenario 2, there is a Poisson field of targets with density β and a Poisson field of false targets with density α. Both β and α are assumed constant. The air vehicle flies along a straight path with area coverage rate $Q(t)$. For now Q is assumed constant and specified. Therefore, the only decision variable is P_{TR}. Constant Q implies the ROC parameter c is constant.

3.3.1 Munition Problem. To start, in addition to assuming T, Q, β, and α are constant, there is no constraint on $P(m \geq \hat{m})$.

Theorem 5 (Scenario 2 with $k = 1$ and no constraint on $P(m \geq \hat{m})$) *If T, Q, β, and α are constant, the unbounded P_{TR}^{*} is monotonically increasing.*

Proof: The only state needed is

$$x(t) = \int_0^t \left\{ \left[1 - P_{FTR}(\tau) \right] \alpha + P_{TR}(\tau) \beta \right\} Q d\tau \tag{3.78}$$

which is the combined Poisson parameter for both target attacks and false target attacks. The corresponding L is

$$L = -P_{TR}(t) \beta Q e^{-x(t)}. \tag{3.79}$$

The derivative of the state is

$$\dot{x}(t) = \left\{ \left[1 - P_{FTR}(t) \right] \alpha + P_{TR}(t) \beta \right\} Q. \tag{3.80}$$

After applying Eq. (2.12) for the ROC model, the Hamiltonian becomes

$$H = -P_{TR} \beta Q e^{-x} + \lambda_x \left[\frac{P_{TR} \alpha}{(1-c) P_{TR} + c} + P_{TR} \beta \right] Q \tag{3.81}$$

and the costate differential equation becomes

$$\dot{\lambda}_x(t) = -P_{TR}(t)\,\beta Q e^{-x(t)}. \tag{3.82}$$

Taking the partial derivative of H with respect to the decision variable P_{TR} gives

$$\frac{\partial H}{\partial P_{TR}} = -\beta Q e^{-x} + \lambda_x Q \left\{ \frac{\alpha c}{\left[(1-c)\,P_{TR} + c\right]^2} + \beta \right\} \tag{3.83}$$

Solving $\frac{\partial H}{\partial P_{TR}} = 0$, the optimal control is

$$P^*_{TR}(t) = \frac{c \pm \sqrt{\frac{\alpha c \lambda_x(t)}{\beta\left[e^{-x(t)} - \lambda_x(t)\right]}}}{c-1}. \tag{3.84}$$

Only the "minus" root is of interest, since the "plus" root puts P_{TR} outside of $[0,1]$ for all time. Taking the derivative of Eq. (3.84) with respect to t gives

$$\dot{P}^*_{TR}(t) = \frac{-1}{2(c-1)} \sqrt{\frac{\alpha c\left[e^{-x(t)} - \lambda_x(t)\right]}{\beta \lambda_x(t)}} \left\{ \frac{e^{-x(t)}\left[\lambda_x(t)\,\dot{x}(t) + \dot{\lambda}_x(t)\right]}{\left[e^{-x(t)} - \lambda_x(t)\right]^2} \right\}. \tag{3.85}$$

Using Eqs. (3.80) and (3.82) for $\dot{x}(t)$ and $\dot{\lambda}_x(t)$ yields

$$\dot{P}^*_{TR}(t) = Q \sqrt{\frac{\alpha\beta e^{-2x(t)}}{4c\lambda_x(t)\left[e^{-x(t)} - \lambda_x(t)\right]}}\left[P^*_{TR}(t)\right]^2 > 0. \tag{3.86}$$

□

At the terminal point where $\lambda_x(T) = 0$, $P^*_{TR}(T) = \frac{c}{c-1} > 1$. Thus, the constraint $P_{TR} \leq 1$ becomes active prior to the end and remains active until time T. This represents the same "go for broke" tactic seen in Scenario 1.

Next, the effect of adding a constraint on false target attacks is examined. With a constraint on $P(m \geq \hat{m})$, the following states are needed:

$$x(t) = \int_0^t \{[1 - P_{FTR}(\tau)]\alpha + P_{TR}(\tau)\beta\} Q d\tau \tag{3.87}$$

$$z(t) = \int_0^t \alpha Q [1 - P_{FTR}(\tau)] e^{-x(\tau)} d\tau. \tag{3.88}$$

The corresponding L is still

$$L = -P_{TR}(t)\beta Q e^{-x(t)}. \tag{3.89}$$

The derivatives of the states are

$$\dot{x}(t) = \{[1 - P_{FTR}(t)]\alpha + P_{TR}(t)\beta\} Q \tag{3.90}$$

$$\dot{z}(t) = \alpha Q [1 - P_{FTR}(t)] e^{-x(t)} \tag{3.91}$$

After applying Eq. (2.12) for the ROC model, the Hamiltonian becomes

$$H = \left(\lambda_x - e^{-x}\right) P_{TR}\beta Q + \frac{P_{TR}\alpha Q}{(1-c)P_{TR} + c}\left[\lambda_x + \lambda_z e^{-x}\right] \tag{3.92}$$

and the costate differential equations become

$$\dot{\lambda}_x(t) = \lambda_z \alpha Q \frac{P_{TR}(t)}{(1-c)P_{TR}(t) + c} e^{-x(t)} - P_{TR}(t)\beta Q e^{-x(t)} \tag{3.93}$$

$$\dot{\lambda}_z(t) = 0 \tag{3.94}$$

Taking the partial derivative of H with respect to the decision variable P_{TR} gives

$$\frac{\partial H}{\partial P_{TR}} = \left(\lambda_x - e^{-x}\right)\beta Q + \frac{[\lambda_x + \lambda_z e^{-x}]\alpha Q c}{[(1-c)P_{TR} + c]^2} \tag{3.95}$$

Solving $\frac{\partial H}{\partial P_{TR}} = 0$, the optimal control is

$$P^*_{TR}(t) = \frac{c \pm \sqrt{\frac{\alpha c\left[\lambda_x(t)+\lambda_z e^{-x(t)}\right]}{\beta\left[e^{-x(t)}-\lambda_x(t)\right]}}}{c-1}. \tag{3.96}$$

Only the "minus" root is of interest, since the "plus" root puts P_{TR} outside of $[0,1]$ for all time. While taking the derivative of Eq. (3.96) with respect to t is possible, there are too many terms involved to discern any trends. Nonetheless, Eq. (3.96) shows the form of the optimal control.

3.3.2 Sensor Craft Problem. The sensor craft problem does not condition $P(n \geq \hat{n})$ on the number of previous attacks. For Scenario 2,

$$P(n \geq \hat{n}) = 1 - \sum_{n=0}^{\hat{n}-1} \frac{\left[\int_0^T P_{TR}(t)\,\beta Q dt\right]^n}{n!} e^{-\int_0^T P_{TR}(t)\beta Q dt}. \tag{3.97}$$

Theorem 6 (Scenario 2 with $k = \infty$, $\hat{n} = 1$, and no constraint on $P(m \geq \hat{m})$) *If T, Q, and β are constant, the optimal constrained solution is $P^*_{TR} = P^*_{TR_{max}} = 1$.*

Proof: In the case of $\hat{n} = 1$,

$$P(n \geq 1) = 1 - e^{-\int_0^T P_{TR}(t)\beta Q dt}, \tag{3.98}$$

and with no constraint on $P(m \geq \hat{m})$, the optimal control is clearly $P^*_{TR} = P^*_{TR_{max}} = 1$ for all time.

□

This is not a practical solution, since all false targets would be declared targets and attacked. With an infinite amount of warheads and no constraint on false target attacks, there is no reason not to attack every object encountered.

Next, the effect of adding a constraint on false target attacks is examined. The sensor craft problem does not condition $P(m \geq \hat{m})$ on the number of previous attacks.

Theorem 7 (Scenario 2 with $k = \infty$, $\hat{m} = 1$, and $P(m \geq 1) = b$) *If T, Q, and α are constant, $P_{TR}^{*}(t) = \frac{-c \ln[1-b]}{(1-c)\ln[1-b]+\alpha QT}$.*

Proof: With a constraint on $P(m \geq \hat{m})$, the states become

$$x(t) = \int_0^t \alpha Q \left[1 - P_{FTR}(\tau)\right] d\tau \tag{3.99}$$

$$y(t) = \int_0^t \beta Q P_{TR}(\tau)\, d\tau \tag{3.100}$$

$$z(t) = 1 - \sum_{m=0}^{\hat{m}-1} \frac{[x(t)]^m}{m!} e^{-x(t)} \tag{3.101}$$

In this formulation, ϕ is used and $L = 0$. The corresponding ϕ is

$$\phi = -\left\{1 - \sum_{n=0}^{\hat{n}-1} \frac{[y(T)]^n}{n!} e^{-y(T)}\right\}. \tag{3.102}$$

The derivatives of the states are

$$\dot{x}(t) = \alpha Q \left[1 - P_{FTR}(t)\right] \tag{3.103}$$

$$\dot{y}(t) = \beta Q P_{TR}(t) \tag{3.104}$$

$$\dot{z}(t) = \alpha Q \left[1 - P_{FTR}(t)\right] \left\{\frac{[x(t)]^{(\hat{m}-1)}}{(\hat{m}-1)!}\right\} e^{-x(t)} \tag{3.105}$$

After applying Eq. (2.12) for the ROC model, the Hamiltonian becomes

$$H = \alpha Q \frac{P_{TR}}{(1-c)P_{TR} + c} \left\{\lambda_x + \lambda_z \left[\frac{x^{(\hat{m}-1)}}{(\hat{m}-1)!}\right] e^{-x}\right\} + \lambda_y \beta Q P_{TR} \tag{3.106}$$

and the costate differential equations become

$$\dot{\lambda}_x(t) = \frac{-\lambda_z \alpha Q P_{TR}(t)}{(1-c) P_{TR}(t) + c} \left[\frac{(\hat{m}-1)}{x(t)} - 1 \right] \left\{ \frac{[x(t)]^{(\hat{m}-1)}}{(\hat{m}-1)!} \right\} e^{-x(t)} \quad (3.107)$$

$$\dot{\lambda}_y(t) = 0 \quad (3.108)$$

$$\dot{\lambda}_z(t) = 0 \quad (3.109)$$

with

$$\lambda_y = \sum_{n=0}^{\hat{n}-1} \left[\frac{n}{y(T)} - 1 \right] \frac{[y(T)]^n}{n!} e^{-y(T)} \quad (3.110)$$

Taking the partial derivative of H with respect to the decision variable P_{TR} gives

$$\frac{\partial H}{\partial P_{TR}} = \frac{\alpha Q c \left\{ \lambda_x + \lambda_z \left[\frac{x^{(\hat{m}-1)}}{(\hat{m}-1)!} \right] e^{-x} \right\}}{\left[(1-c) P_{TR} + c \right]^2} + \lambda_y \beta Q \quad (3.111)$$

Solving $\frac{\partial H}{\partial P_{TR}} = 0$, the optimal control is

$$P^*_{TR}(t) = \frac{c \pm \sqrt{\left\{ \lambda_x(t) + \lambda_z \left[\frac{[x(t)]^{(\hat{m}-1)}}{(\hat{m}-1)!} \right] e^{-x(t)} \right\} \frac{-\alpha c}{\beta \lambda_y}}}{c-1}. \quad (3.112)$$

Only the "minus" root is of interest, since the "plus" root puts P_{TR} outside of $[0,1]$ for all time. Taking the derivative of Eq. (3.112) with respect to t gives

$$\dot{P}^*_{TR}(t) = \frac{-1}{2(c-1)} \sqrt{\frac{-\alpha c}{\beta \lambda_y \left\{ \lambda_x(t) + \lambda_z \left[\frac{[x(t)]^{(\hat{m}-1)}}{(\hat{m}-1)!} \right] e^{-x(t)} \right\}}} \times \left\{ \dot{\lambda}_x(t) + \lambda_z \dot{x}(t) \left[\frac{(\hat{m}-1)}{x(t)} - 1 \right] \left\{ \frac{[x(t)]^{(\hat{m}-1)}}{(\hat{m}-1)!} \right\} e^{-x(t)} \right\}. \quad (3.113)$$

Using Eq. (3.103) for $\dot{x}(t)$ with Eq. (2.12) for the ROC model and Eq. (3.107) for $\dot{\lambda}_x(t)$ yields

$$\dot{P}^*_{TR}(t) = 0 \quad (3.114)$$

implying P_{TR}^{*} is constant for all time. When target and false target densities remain fixed throughout the search effort and the amount of warheads is infinite, the problem becomes an infinite horizon problem, where optimal solutions are constant. Consider the case when $\hat{m} = 1$. For constant T, Q, α, and P_{TR},

$$P\left(m \geq 1\right) = 1 - e^{-\alpha QT(1-P_{FTR})} \leq b. \tag{3.115}$$

Applying Eq. (2.12) for the ROC model and assuming the constraint is active, the optimal control is

$$P_{TR}^{*}\left(t\right) = \frac{-c\ln\left[1-b\right]}{\left(1-c\right)\ln\left[1-b\right] + \alpha QT}. \tag{3.116}$$

□

Both Scenario 1 and Scenario 2 have the same Poisson field of false targets with density α. With infinite warheads, the constraint on false target attacks will produce the same optimal solution regardless of the target distribution. Thus, Eq. (3.116) matches Eq. (3.38).

3.4 Scenario 2: Fixed T, Variable Q, Variable P_{TR}

The assumption that Q is constant is now relaxed. Therefore, the ROC parameter c is no longer constant. Equation (2.13), where $c\left(t\right) \equiv \frac{Q_n}{Q(t)}$ is used. Recall Q_n is a constant. The decision variables are Q and P_{TR}.

Theorem 8 (Scenario 2 with $k = 1$ or $k = \infty$) *If T, β, and α are constant and Q is unbounded, the unbounded $P_{TR}^{*}\left(t\right) = \frac{Q_n}{2Q_n - Q^{*}(t)}$.*

Proof: Consider the munition and sensor craft problems.

3.4.1 Munition Problem. For $k = 1$, dynamic Q, and dynamic P_{TR}, the states becomes

$$x(t) = \int_0^t \{[1 - P_{FTR}(\tau)]\alpha + P_{TR}(\tau)\beta\} Q(\tau) d\tau \quad (3.117)$$

$$z(t) = \int_0^t \alpha Q(\tau)[1 - P_{FTR}(\tau)] e^{-x(\tau)} d\tau. \quad (3.118)$$

The corresponding L is

$$L = -P_{TR}(t)\beta Q(t) e^{-x(t)}. \quad (3.119)$$

The derivatives of the states are

$$\dot{x}(t) = \{[1 - P_{FTR}(t)]\alpha + P_{TR}(t)\beta\} Q(t) \quad (3.120)$$

$$\dot{z}(t) = \alpha Q(t)[1 - P_{FTR}(t)] e^{-x(t)} \quad (3.121)$$

Equation (2.12) becomes

$$[1 - P_{FTR}(t)] = \frac{Q(t) P_{TR}(t)}{Q(t) P_{TR}(t) + Q_n [1 - P_{TR}(t)]}. \quad (3.122)$$

Using Eq. (3.122), the Hamiltonian becomes

$$H = \left(\lambda_x - e^{-x}\right) Q P_{TR}\beta + \alpha \frac{Q^2 P_{TR}}{Q P_{TR} + Q_n (1 - P_{TR})} \left[\lambda_x + \lambda_z e^{-x}\right] \quad (3.123)$$

and the costate differential equations become

$$\dot{\lambda}_x = \lambda_z \alpha \frac{Q^2(t) P_{TR}(t)}{Q(t) P_{TR}(t) + Q_n [1 - P_{TR}(t)]} e^{-x(t)} - Q(t) P_{TR}(t)\beta e^{-x(t)} \quad (3.124)$$

$$\dot{\lambda}_z = 0 \quad (3.125)$$

Taking the partial derivative of H with respect to the decision variable P_{TR} gives

$$\frac{\partial H}{\partial P_{TR}} = Q\left\{\left(\lambda_x - e^{-x}\right)\beta + \frac{\left[\lambda_x + \lambda_z e^{-x}\right] Q_n \alpha Q}{\left[QP_{TR} + Q_n\left(1 - P_{TR}\right)\right]^2}\right\} \tag{3.126}$$

Taking the partial derivative of H with respect to the decision variable Q gives

$$\frac{\partial H}{\partial Q} = P_{TR}\left\{\left(\lambda_x - e^{-x}\right)\beta + \alpha\left[\lambda_x + \lambda_z e^{-x}\right]\frac{Q^2 P_{TR} + 2Q_n Q\left(1 - P_{TR}\right)}{\left[QP_{TR} + Q_n\left(1 - P_{TR}\right)\right]^2}\right\} \tag{3.127}$$

Ignoring the trivial solutions $P_{TR} = 0$ and $Q = 0$, the necessary conditions become

$$\left\{\left(\lambda_x - e^{-x}\right)\beta + \frac{\left[\lambda_x + \lambda_z e^{-x}\right] Q_n \alpha Q}{\left[QP_{TR} + Q_n\left(1 - P_{TR}\right)\right]^2}\right\} = 0 \tag{3.128}$$

and

$$\left\{\left(\lambda_x - e^{-x}\right)\beta + \alpha\left[\lambda_x + \lambda_z e^{-x}\right]\frac{Q^2 P_{TR} + 2Q_n Q\left(1 - P_{TR}\right)}{\left[QP_{TR} + Q_n\left(1 - P_{TR}\right)\right]^2}\right\} = 0 \tag{3.129}$$

Subtracting Eq. (3.128) from Eq. (3.129) gives

$$\alpha\left[\lambda_x + \lambda_z e^{-x}\right]\frac{Q^2 P_{TR} + 2Q_n Q\left(1 - P_{TR}\right)}{\left[QP_{TR} + Q_n\left(1 - P_{TR}\right)\right]^2} - \frac{\left[\lambda_x + \lambda_z e^{-x}\right] Q_n \alpha Q}{\left[QP_{TR} + Q_n\left(1 - P_{TR}\right)\right]^2} = 0 \tag{3.130}$$

Grouping like terms, yields

$$\alpha Q\left[\lambda_x + \lambda_z e^{-x}\right]\frac{QP_{TR} - 2Q_n P_{TR} + Q_n}{\left[QP_{TR} + Q_n\left(1 - P_{TR}\right)\right]^2} = 0 \tag{3.131}$$

resulting in the necessary condition

$$\left[\lambda_x + \lambda_z e^{-x}\right]\left[QP_{TR} - 2Q_n P_{TR} + Q_n\right] = 0. \tag{3.132}$$

Thus, either

$$P_{TR}^*(t) = \frac{Q_n}{2Q_n - Q^*(t)} \tag{3.133}$$

or

$$\lambda_x(t) = -\lambda_z e^{-x(t)} \tag{3.134}$$

$P^*_{TR}(t) = \frac{Q_n}{2Q_n - Q^*(t)}$ is the same necessary condition as the single warhead case for Scenario 1. Both Scenario 1 and Scenario 2 have the same Poisson field of false targets with density α. Thus, it makes intuitive sense the same necessary condition should hold.

3.4.2 Sensor Craft Problem. For $k = \infty$, dynamic Q, and dynamic P_{TR}, the states become

$$x(t) = \int_0^t \alpha Q(\tau)\left[1 - P_{FTR}(\tau)\right] d\tau \tag{3.135}$$

$$y(t) = \int_0^t \beta Q(\tau) P_{TR}(\tau)\, d\tau \tag{3.136}$$

$$z(t) = 1 - \sum_{m=0}^{\hat{m}-1} \frac{[x(t)]^m}{m!} e^{-x(t)} \tag{3.137}$$

In this formulation, ϕ is used and $L = 0$. The corresponding ϕ is

$$\phi = -\left\{1 - \sum_{n=0}^{\hat{n}-1} \frac{[y(T)]^n}{n!} e^{-x(T)}\right\}. \tag{3.138}$$

The derivatives of the states are

$$\dot{x}(t) = \alpha Q(t)\left[1 - P_{FTR}(t)\right] \tag{3.139}$$

$$\dot{y}(t) = \beta Q(t) P_{TR}(t) \tag{3.140}$$

$$\dot{z}(t) = \alpha Q(t)\left[1 - P_{FTR}(t)\right]\left\{\frac{[x(t)]^{(\hat{m}-1)}}{(\hat{m}-1)!}\right\} e^{-x(t)} \tag{3.141}$$

After applying Eq. (3.122), the Hamiltonian becomes

$$H = \alpha \frac{Q^2 P_{TR}}{QP_{TR} + Q_n(1 - P_{TR})}\left\{\lambda_x + \lambda_z\left[\frac{x^{(\hat{m}-1)}}{(\hat{m}-1)!}\right] e^{-x}\right\} + \lambda_y \beta Q P_{TR} \tag{3.142}$$

and the costate differential equations become

$$\begin{aligned}
\dot{\lambda}_x(t) &= \frac{-\lambda_z \alpha Q^2(t) P_{TR}(t)}{Q(t) P_{TR}(t) + Q_n [1 - P_{TR}(t)]} \times \\
&\quad \left[\frac{(\hat{m}-1)}{x(t)} - 1\right] \left\{\frac{[x(t)]^{(\hat{m}-1)}}{(\hat{m}-1)!}\right\} e^{-x(t)} \qquad (3.143) \\
\dot{\lambda}_y(t) &= 0 \qquad (3.144) \\
\dot{\lambda}_z(t) &= 0 \qquad (3.145)
\end{aligned}$$

Taking the partial derivative of H with respect to the decision variable P_{TR} gives

$$\frac{\partial H}{\partial P_{TR}} = Q \left\{ \frac{\left[\lambda_x + \lambda_z \left(\frac{[x(t)]^{(\hat{m}-1)}}{(\hat{m}-1)!}\right) e^{-x}\right] Q_n \alpha Q}{\left[Q P_{TR} + Q_n (1 - P_{TR})\right]^2} + \lambda_y \beta \right\} \qquad (3.146)$$

Taking the partial derivative of H with respect to the decision variable Q gives

$$\frac{\partial H}{\partial Q} = P_{TR} \left\{ \alpha \left[\lambda_x + \lambda_z \left(\frac{[x(t)]^{(\hat{m}-1)}}{(\hat{m}-1)!}\right) e^{-x}\right] \frac{Q^2 P_{TR} + 2 Q_n Q (1 - P_{TR})}{\left[Q P_{TR} + Q_n (1 - P_{TR})\right]^2} + \lambda_y \beta \right\} \qquad (3.147)$$

Ignoring the trivial solutions $P_{TR} = 0$ and $Q = 0$, the necessary conditions become

$$\left\{ \frac{\left[\lambda_x + \lambda_z \left(\frac{[x(t)]^{(\hat{m}-1)}}{(\hat{m}-1)!}\right) e^{-x}\right] Q_n \alpha Q}{\left[Q P_{TR} + Q_n (1 - P_{TR})\right]^2} + \lambda_y \beta \right\} = 0 \qquad (3.148)$$

and

$$\left\{ \alpha \left[\lambda_x + \lambda_z \left(\frac{[x(t)]^{(\hat{m}-1)}}{(\hat{m}-1)!}\right) e^{-x}\right] \frac{Q^2 P_{TR} + 2 Q_n Q (1 - P_{TR})}{\left[Q P_{TR} + Q_n (1 - P_{TR})\right]^2} + \lambda_y \beta \right\} = 0 \qquad (3.149)$$

Subtracting Eq. (3.148) from Eq. (3.149) gives

$$\alpha\left[\lambda_x+\lambda_z\left(\frac{[x(t)]^{(\hat{m}-1)}}{(\hat{m}-1)!}\right)e^{-x}\right]\frac{Q^2P_{TR}+2Q_nQ\left(1-P_{TR}\right)}{\left[QP_{TR}+Q_n\left(1-P_{TR}\right)\right]^2} - \frac{\left[\lambda_x+\lambda_z\left(\frac{[x(t)]^{(\hat{m}-1)}}{(\hat{m}-1)!}\right)e^{-x}\right]Q_n\alpha Q}{\left[QP_{TR}+Q_n\left(1-P_{TR}\right)\right]^2}=0 \quad (3.150)$$

Grouping like terms gives

$$\alpha Q\left[\lambda_x+\lambda_z\left(\frac{[x(t)]^{(\hat{m}-1)}}{(\hat{m}-1)!}\right)e^{-x}\right]\frac{QP_{TR}-2Q_nP_{TR}+Q_n}{\left[QP_{TR}+Q_n\left(1-P_{TR}\right)\right]^2}=0 \quad (3.151)$$

resulting in the necessary condition

$$\left[\lambda_x+\lambda_z\left(\frac{[x(t)]^{(\hat{m}-1)}}{(\hat{m}-1)!}\right)e^{-x}\right]\left[QP_{TR}-2Q_nP_{TR}+Q_n\right]=0. \quad (3.152)$$

Thus, either

$$P_{TR}^{*}(t)=\frac{Q_n}{2Q_n-Q^{*}(t)} \quad (3.153)$$

or

$$\lambda_x(t)=-\lambda_z\left(\frac{[x(t)]^{(\hat{m}-1)}}{(\hat{m}-1)!}\right)e^{-x(t)} \quad (3.154)$$

$P_{TR}^{*}(t)=\frac{Q_n}{2Q_n-Q^{*}(t)}$ is the same necessary condition as the single warhead case.

Thus, it appears the necessary condition in Eq. (3.153) holds regardless of the number of warheads, false target density, or maximum allowable $P(m\geq\hat{m})$. This, of course, assumes unbounded design variables. If Q saturates at an upper or lower bound, the fixed-Q necessary conditions are used.

3.5 Scenario 7: Fixed R, Fixed Q, Variable P_{TR}

For Scenario 7, one target is normally distributed among a Poisson field of false targets with density α, which is assumed constant. Normally-distributed refers to a circular normal distribution with standard deviation σ_y. The search area A_s is a circular disc of radius R, which is prescribed. The air vehicle searches the disc using concentric annuli of radius r and thickness dr. Each annulus is covered using a constant Q; therefore, the ROC parameter c is constant. As r increases, the time it takes to cover the corresponding annulus also increases. The search begins at the origin of the disc and progresses outward. The only decision variable is P_{TR}.

3.5.1 Munition Problem. In additional to assuming R, Q, and α are constant, the constraint on $P(m \geq \hat{m})$ is initially removed. In doing so, only the following state is needed:

$$x(r) = \int_0^r 2\pi\alpha\rho \left[1 - P_{FTR}(\rho)\right] d\rho. \tag{3.155}$$

The corresponding L is

$$L = -P_{TR}(r) \frac{r}{\sigma_y^2} e^{-\frac{r^2}{2\sigma_y^2}} e^{-x(r)}. \tag{3.156}$$

The derivative of the state is

$$\dot{x}(r) = 2\pi\alpha r \left[1 - P_{FTR}(r)\right]. \tag{3.157}$$

After applying Eq. (2.12) for the ROC model, the Hamiltonian becomes

$$H = -P_{TR} \frac{r}{\sigma_y^2} e^{-\frac{r^2}{2\sigma_y^2}} e^{-x} + \lambda_x 2\pi\alpha r \frac{P_{TR}}{(1-c) P_{TR} + c} \tag{3.158}$$

and the costate differential equation becomes

$$\dot{\lambda}_x(r) = -P_{TR}(r)\frac{r}{\sigma_y^2}e^{-\frac{r^2}{2\sigma_y^2}}e^{-x(r)}. \tag{3.159}$$

Taking the partial derivative of H with respect to the decision variable P_{TR} gives

$$\frac{\partial H}{\partial P_{TR}} = -\frac{r}{\sigma_y^2}e^{-\frac{r^2}{2\sigma_y^2}}e^{-x} + \frac{\lambda_x 2\pi\alpha r c}{\left[(1-c)P_{TR}+c\right]^2} \tag{3.160}$$

Solving $\frac{\partial H}{\partial P_{TR}} = 0$, the optimal control is

$$P_{TR}^*(r) = \frac{c \pm \sqrt{\lambda_x(r)\,2\pi\alpha c\sigma_y^2 e^{\left[x(r)+\frac{r^2}{2\sigma_y^2}\right]}}}{c-1}. \tag{3.161}$$

Only the "minus" root is of interest, since the "plus" root puts P_{TR} outside of $[0,1]$. Taking the derivative of Eq. (3.161) with respect to r gives

$$\dot{P}_{TR}^*(r) = \frac{-1}{2(c-1)}\sqrt{\frac{2\pi\alpha c\sigma_y^2}{\lambda_x(r)\,e^{\left[x(r)+\frac{r^2}{2\sigma_y^2}\right]}}} \times e^{\left[x(r)+\frac{r^2}{2\sigma_y^2}\right]}\left[\lambda_x(r)\,\dot{x}(r) + \lambda_x(r)\frac{r}{\sigma_y^2} + \dot{\lambda}_x(r)\right]. \tag{3.162}$$

Using Eqs. (3.157) and (3.159) for $\dot{x}(r)$ and $\dot{\lambda}_x(r)$ yields

$$\dot{P}_{TR}^*(r) = \sqrt{\frac{\pi\alpha r^2}{2c\lambda_x(r)\,\sigma_y^2 e^{\left[x(r)+\frac{r^2}{2\sigma_y^2}\right]}}}\left\{[P_{TR}^*(r)]^2 - \frac{c}{(c-1)}\lambda_x(r)\,e^{\left[x(r)+\frac{r^2}{2\sigma_y^2}\right]}\right\}. \tag{3.163}$$

Unlike Scenarios 1 and 2, there is no discernable trend. Nonetheless, Eq. (3.161) shows the form of the optimal control.

Next, the effect of adding a constraint on false target attacks is examined. With a constraint on $P(m \geq \hat{m})$, the states are

$$x(r) = \int_0^r 2\pi\alpha\rho\left[1 - P_{FTR}(\rho)\right] d\rho \tag{3.164}$$

$$y(r) = \int_0^r P_{TR}(\rho) \frac{\rho}{\sigma_y^2} e^{-\frac{\rho^2}{2\sigma_y^2}} d\rho \tag{3.165}$$

$$z(r) = \int_0^r 2\pi\alpha\rho\left[1 - P_{FTR}(\rho)\right]\left[1 - y(\rho)\right] e^{-x(\rho)} d\rho. \tag{3.166}$$

The corresponding L is still

$$L = -P_{TR}(r) \frac{r}{\sigma_y^2} e^{-\frac{r^2}{2\sigma_y^2}} e^{-x(r)}. \tag{3.167}$$

The derivatives of the states are

$$\dot{x}(r) = 2\pi\alpha r\left[1 - P_{FTR}(r)\right] \tag{3.168}$$

$$\dot{y}(r) = P_{TR}(r) \frac{r}{\sigma_y^2} e^{-\frac{r^2}{2\sigma_y^2}} \tag{3.169}$$

$$\dot{z}(r) = 2\pi\alpha r\left[1 - P_{FTR}(r)\right]\left[1 - y(r)\right] e^{-x(r)} \tag{3.170}$$

After applying Eq. (2.12) for the ROC model, the Hamiltonian becomes

$$H = \left(\lambda_y - e^{-x}\right) P_{TR} \frac{r}{\sigma_y^2} e^{-\frac{r^2}{2\sigma_y^2}} + 2\pi\alpha r \frac{P_{TR}}{(1-c) P_{TR} + c} \left[\lambda_x + \lambda_z (1-y) e^{-x}\right] \tag{3.171}$$

and the costate differential equations become

$$\begin{aligned} \dot{\lambda}_x(r) = {} & \lambda_z 2\pi\alpha r \frac{P_{TR}(r)}{(1-c) P_{TR}(r) + c} \left[1 - y(r)\right] e^{-x(r)} \\ & - P_{TR}(r) \frac{r}{\sigma_y^2} e^{-\frac{r^2}{2\sigma_y^2}} e^{-x(r)} \end{aligned} \tag{3.172}$$

$$\dot{\lambda}_y(r) = \lambda_z 2\pi\alpha r \frac{P_{TR}(r)}{(1-c) P_{TR}(r) + c} e^{-x(r)} \tag{3.173}$$

$$\dot{\lambda}_z(r) = 0 \tag{3.174}$$

Taking the partial derivative of H with respect to the decision variable P_{TR} gives

$$\frac{\partial H}{\partial P_{TR}} = \left(\lambda_y - e^{-x}\right) \frac{r}{\sigma_y^2} e^{-\frac{r^2}{2\sigma_y^2}} + \frac{\left[\lambda_x + \lambda_z \left(1-y\right) e^{-x}\right] 2\pi\alpha r c}{\left[\left(1-c\right) P_{TR} + c\right]^2} \tag{3.175}$$

Solving $\frac{\partial H}{\partial P_{TR}} = 0$, the optimal control is

$$P_{TR}^{*}\left(r\right) = \frac{c \pm \sqrt{\frac{\left\{\lambda_x(r) + \lambda_z[1-y(r)]e^{-x(r)}\right\} 2\pi\alpha c\sigma_y^2 e^{\frac{r^2}{2\sigma_y^2}}}{\left[e^{-x(r)} - \lambda_y(r)\right]}}}{c-1}. \tag{3.176}$$

Only the "minus" root is of interest, since the "plus" root puts P_{TR} outside of $[0,1]$. While taking the derivative of Eq. (3.176) with respect to r is possible, there are too many terms involved to discern any trends. Nonetheless, Eq. (3.176) shows the form of the optimal control.

3.5.2 Sensor Craft Problem. The sensor craft problem does not condition $P\left(n \geq \hat{n}\right)$ on the number of previous attacks. For Scenario 7,

$$P\left(n=1\right) = \int_0^R P_{TR}\left(r\right) \frac{r}{\sigma_y^2} e^{-\frac{r^2}{2\sigma_y^2}} dr. \tag{3.177}$$

Theorem 9 (Scenario 7 with $k = \infty$ and no constraint on $P\left(m \geq \hat{m}\right)$) *If R and α are constant, the optimal constrained solution is $P_{TR}^{*} = P_{TR_{max}}^{*} = 1$.*

Proof: With no constraint on $P\left(m \geq \hat{m}\right)$, the optimal control is clearly $P_{TR}^{*} = P_{TR_{max}}^{*} = 1$.

□

This is not a practical solution, since all false targets would be declared targets and attacked. With an infinite amount of warheads and no constraint on false target attacks, there is no reason not to attack every object encountered.

Next, the effect of adding a constraint on false target attacks is examined. The sensor craft problem does not condition $P(m \geq \hat{m})$ on the number of previous attacks.

Theorem 10 (Scenario 7 with $k = \infty$ and $P(m \geq 1) = b$) *If R and α are constant, the unbounded P_{TR}^* is monotonically decreasing.*

Proof: With a constraint on $P(m \geq \hat{m})$, the states become

$$x(r) = \int_0^r 2\pi\alpha\rho\left[1 - P_{FTR}(\rho)\right] d\rho \tag{3.178}$$

$$z(r) = 1 - \sum_{m=0}^{\hat{m}-1} \frac{[x(r)]^m}{m!} e^{-x(r)} \tag{3.179}$$

The corresponding L is

$$L = -P_{TR}(r) \frac{r}{\sigma_y^2} e^{-\frac{r^2}{2\sigma_y^2}}. \tag{3.180}$$

The derivatives of the states are

$$\dot{x}(r) = 2\pi\alpha r\left[1 - P_{FTR}(r)\right] \tag{3.181}$$

$$\dot{z}(r) = 2\pi\alpha r\left[1 - P_{FTR}(r)\right] \left\{ \frac{[x(r)]^{(\hat{m}-1)}}{(\hat{m}-1)!} \right\} e^{-x(r)} \tag{3.182}$$

After applying Eq. (2.12) for the ROC model, the Hamiltonian becomes

$$H = -P_{TR} \frac{r}{\sigma_y^2} e^{-\frac{r^2}{2\sigma_y^2}} + 2\pi\alpha r \frac{P_{TR}}{(1-c) P_{TR} + c} \left\{ \lambda_x + \lambda_z \left[\frac{x^{(\hat{m}-1)}}{(\hat{m}-1)!} \right] e^{-x} \right\} \tag{3.183}$$

and the costate differential equations become

$$\dot{\lambda}_x(r) = -\frac{\lambda_z 2\pi\alpha r P_{TR}(r)}{(1-c) P_{TR}(r) + c} \left[\frac{(\hat{m}-1)}{x(r)} - 1 \right] \left\{ \frac{[x(r)]^{(\hat{m}-1)}}{(\hat{m}-1)!} \right\} e^{-x(r)} \tag{3.184}$$

$$\dot{\lambda}_z(r) = 0 \tag{3.185}$$

Taking the partial derivative of H with respect to the decision variable P_{TR} gives

$$\frac{\partial H}{\partial P_{TR}} = -\frac{r}{\sigma_y^2} e^{-\frac{r^2}{2\sigma_y^2}} + \frac{2\pi\alpha rc\left\{\lambda_x + \lambda_z\left[\frac{x^{(\hat{m}-1)}}{(\hat{m}-1)!}\right]e^{-x}\right\}}{\left[(1-c)P_{TR}+c\right]^2} \tag{3.186}$$

Solving $\frac{\partial H}{\partial P_{TR}} = 0$, the optimal control is

$$P_{TR}^*(r) = \frac{c \pm \sqrt{2\pi\alpha c\sigma_y^2\left\{\lambda_x(r) + \lambda_z\left[\frac{[x(r)]^{(\hat{m}-1)}}{(\hat{m}-1)!}\right]e^{-x(r)}\right\}e^{\frac{r^2}{2\sigma_y^2}}}}{c-1}. \tag{3.187}$$

Only the "minus" root is of interest, since the "plus" root puts P_{TR} outside of $[0,1]$. Taking the derivative of Eq. (3.187) with respect to r gives

$$\begin{aligned}\dot{P}_{TR}^*(r) = \frac{-1}{2(c-1)}\sqrt{\frac{2\pi\alpha c\sigma_y^2}{\left\{\lambda_x(r) + \lambda_z\left[\frac{[x(r)]^{(\hat{m}-1)}}{(\hat{m}-1)!}\right]e^{-x(r)}\right\}e^{\frac{r^2}{2\sigma_y^2}}}} \times \\ \left\{\dot{\lambda}_x(r)e^{\frac{r^2}{2\sigma_y^2}} + \lambda_z\dot{x}(r)\left[\frac{(\hat{m}-1)}{x(r)} - 1\right]\left\{\frac{[x(r)]^{(\hat{m}-1)}}{(\hat{m}-1)!}\right\}e^{-x(r)}e^{\frac{r^2}{2\sigma_y^2}}\right. \\ \left. + \left[\lambda_x(r) + \lambda_z\left(\frac{[x(r)]^{(\hat{m}-1)}}{(\hat{m}-1)!}\right)e^{-x(r)}\right]e^{\frac{r^2}{2\sigma_y^2}}\frac{r}{\sigma_y^2}\right\}\end{aligned} \tag{3.188}$$

Using Eq. (3.181) for $\dot{x}(r)$ with Eq. (2.12) for the ROC model and Eq. (3.184) for $\dot{\lambda_x}(r)$ yields

$$\dot{P}_{TR}^*(r) = \frac{r}{2\sigma_y^2}\left[P_{TR}^*(r) - \frac{c}{c-1}\right] < 0. \tag{3.189}$$

□

As radius increases, the amount of expected false target encounters in an annulus *increases*, and the probability of encountering the target in an annulus *decreases*. With infinite warheads, the focus becomes meeting the constraint on false target attacks. Since the amount of expected false target encounters in an annulus *increases* with radius, it makes intuitive sense to tighten the operating point on the ROC curve. That is, decrease P_{TR} as radius increases.

IV. Applications

In this chapter, sample applications of the techniques and equations provided in this dissertation are given. First, the simplest form of the problem where all variables are fixed is examined. Second, the effects of varying P_{TR} along a single ROC curve over time is examined. Finally, varying both P_{TR} and Q over time is examined. Matlab's® fmincon routine, which is a discrete-time, gradient-based solver is used. Analytic conclusions from Chapter III are used to verify the numerical results.

Effectiveness measures are the probability of at least one target attack, $P(n \geq 1)$, and the probability of at least one false target attack, $P(m \geq 1)$. The following constrained optimization problem is solved:

$$\begin{aligned} \text{Max:} \quad & P(n \geq 1) \\ \text{Subj to:} \quad & P(m \geq 1) \leq b \end{aligned}$$

Having $\hat{n} = \hat{m} = 1$ allows one to compare of the munition, UCAV, and sensor craft problems. Thus, the sensitivity of effectiveness to the number of warheads can be evaluated. By varying b, the sensitivity of effectiveness to the upper bound on false target attacks can be evaluated. Finally, by examining a variety of battle space scenarios, the effect of the target-to-false-target ratio being fixed or a function of sensor footprint location can be evaluated.

4.1 Numerical Solution Method

The numerical solution method comes from Bryson's gradient algorithm [7]. A synopsis of the algorithm is now given. First the continuous state equations are put into discrete form using Euler's method. The problem is then put into Mayer form, where the state vector is augmented by one state representing the cumulative sum of L to step i. The problem statement then becomes:

$$
\begin{aligned}
\text{Min:} \quad & \phi\left[\mathbf{s}\left(\mathrm{N}\right)\right] \\
\text{subj to:} \quad & \mathbf{s}\left(i+1\right) = \mathbf{f}\left[\mathbf{s}\left(i\right), \mathbf{u}\left(i\right), i\right],\ i = 0, \ldots, \mathrm{N}-1 \\
& \mathbf{s}\left(0\right) = \mathbf{s}_0 \\
& \psi\left[\mathbf{s}\left(\mathrm{N}\right)\right] = 0
\end{aligned}
$$

where N is the number of time or distance steps, as opposed to N, which is the number of targets. ψ represents terminal constraints and is some function of the terminal states. In this case, $\psi\left[\mathbf{s}\left(\mathrm{N}\right)\right] = z\left(\mathrm{N}\right) - b$. Mayer form is equivalent to Bolza form; however, Mayer form yields simpler expressions and is easier to code for numerical solutions. Matlab's® fmincon routine is used, so one does not have to guess step size. The values for $\mathbf{f}$, $\mathbf{f_s}$, $\mathbf{f_u}$, $\phi_{\mathbf{s}}$, and $\psi_{\mathbf{s}}$ at any time or distance step must be provided in a subroutine. The algorithm then proceeds as follows:

- Guess $\mathbf{u}\left(i\right)$ for $i = 0, \ldots, \mathrm{N}-1$
- Forward propagate the state equations from $\mathbf{s}\left(0\right)$ using $\mathbf{u}\left(i\right)$ and store $\mathbf{s}\left(i\right)$
- Evaluate ϕ and ψ and set $\lambda^{\phi}\left(\mathrm{N}\right) = \phi_{\mathbf{s}}^{\mathrm{T}}$, $\lambda^{\psi}\left(\mathrm{N}\right) = \psi_{\mathbf{s}}^{\mathrm{T}}$
- Backward propagate and store the response sequences $H_{\mathbf{u}}^{\phi}\left(i\right)$ and $H_{\mathbf{u}}^{\psi}\left(i\right)$

$$
\begin{aligned}
\lambda^{\phi}\left(i\right) &= \mathbf{f}_{\mathbf{s}}^{\mathrm{T}}\left(i\right)\lambda^{\phi}\left(i+1\right), \qquad i = \mathrm{N}-1, \ldots, 0 \\
\lambda^{\psi}\left(i\right) &= \mathbf{f}_{\mathbf{s}}^{\mathrm{T}}\left(i\right)\lambda^{\psi}\left(i+1\right) \\
\left[H_{\mathbf{u}}^{\phi}\left(i\right)\right]^{\mathrm{T}} &= \mathbf{f}_{\mathbf{u}}^{\mathrm{T}}\left(i\right)\lambda^{\phi}\left(i+1\right) \\
\left[H_{\mathbf{u}}^{\psi}\left(i\right)\right]^{\mathrm{T}} &= \mathbf{f}_{\mathbf{u}}^{\mathrm{T}}\left(i\right)\lambda^{\psi}\left(i+1\right)
\end{aligned}
$$

The process is repeated until the terminal constraint error and the gradient sequence are negligibly small. The problem becomes a parameter optimization involving $n_c \times$ N decision variables, where n_c is the number of control variables. A method for nondimensionalization was proposed in a handout by Pachter and is included in Appendix C.

4.2 Fixed Q, Fixed P_{TR}

If all parameters are fixed, the results from Decker [15] or Jacques and Pachter [26] can be used. To illustrate how the generalized equations derived in this dissertation collapse to the results in [15] and [26], consider a Scenario 3 problem and the calculation of the first elemental probability P_1. From Table 2.5,

$$P_1 = \sum_{j=n-1}^{N-1} \left\{ \binom{N-1}{j} \binom{j}{n-1} \left[\int_0^t \frac{1}{A_B} P_{TR}(\tau) Q(\tau) d\tau \right]^{n-1} \times \left[\int_0^t \frac{1}{A_B} Q(\tau) d\tau - \int_0^t \frac{1}{A_B} P_{TR}(\tau) Q(\tau) d\tau \right]^{j-(n-1)} \times \left[1 - \int_0^t \frac{1}{A_B} Q(\tau) d\tau \right]^{N-1-j} \right\} \frac{N}{A_B} P_{TR}(t) Q(t) dt \quad (4.1)$$

Assuming fixed parameters gives

$$P_1 = \sum_{j=n-1}^{N-1} \left\{ \binom{N-1}{j} \binom{j}{n-1} \left[P_{TR} \frac{A}{A_B} \right]^{n-1} \left[(1 - P_{TR}) \frac{A}{A_B} \right]^{j-(n-1)} \times \left[1 - \frac{A}{A_B} \right]^{N-1-j} \right\} \frac{N}{A_B} P_{TR} Q dt \quad (4.2)$$

Decker showed encounters could be decoupled from classifications resulting in

$$P_1 = \sum_{j=n-1}^{N-1} \left\{ \binom{N-1}{j} \left[\frac{A}{A_B} \right]^{j} \left[1 - \frac{A}{A_B} \right]^{N-1-j} \times \binom{j}{n-1} [P_{TR}]^{n-1} [(1 - P_{TR})]^{j-(n-1)} \right\} \frac{N}{A_B} P_{TR} Q dt \quad (4.3)$$

He then applied a truncated binomial conversion giving

$$P_1 = \binom{N-1}{n-1} \left[P_{TR} \frac{A}{A_B} \right]^{n-1} \left[(1 - P_{TR}) \frac{A}{A_B} \right]^{N-n} \frac{N}{A_B} P_{TR} Q dt \quad (4.4)$$

Letting $N = 1$ and $k = 1$ gives

$$P_1 = \frac{1}{A_B} P_{TR} Q dt \tag{4.5}$$

which matches the results derived by Jacques and Pachter [26].

A fixed-parameter problem has advantages. The operator simply sets P_{TR} at the beginning of the mission. No sophisticated scheduling software or hardware is needed. Finding the optimal P_{TR} can be done looking at a plot or table. For example, in Scenario 1 with $k = 1$, the effectiveness measures become

$$P\left(n \geq 1\right) = P_{TR} \frac{\left[1 - e^{-(1-P_{FTR})\alpha QT}\right]}{\left(1 - P_{FTR}\right)\alpha A_B} \tag{4.6}$$

and

$$P\left(m \geq 1\right) = 1 - P_{TR} \frac{\left[1 - e^{-(1-P_{FTR})\alpha QT}\right]}{\left(1 - P_{FTR}\right)\alpha A_B} - \left(1 - \frac{P_{TR} QT}{A_B}\right) e^{-(1-P_{FTR})\alpha QT}. \tag{4.7}$$

Equation (2.12) can be used for the ROC model with $c = 100$. Assume the munition covers A_B by time T. Thus, $QT = A_B$. One of three mutually exclusive events are possible. The munition either attacks a target, attacks a false target, or attacks nothing and self destructs. Figure 4.1 shows the outcome probabilities versus P_{TR} when $c = 100$, $\alpha Q = 50$ [1/hr], and $T = 0.5$ hr.

If the constraint on a false target attack is removed, Figure 4.1 shows the best unconstrained solution is $P^*_{TR_u} = 0.723$ with a corresponding $P\left(n \geq 1\right)^* = 0.535$ and $P\left(m \geq 1\right)^* = 0.318$. If $P\left(m \geq 1\right)$ is bounded by $b = 0.2$, the best constrained solution is $P^*_{TR} = 0.563$ with a corresponding $P\left(n \geq 1\right)^* = 0.483$. In Figure 4.1, the outcome probability functions are smooth and well-behaved. The function for $P\left(n \geq 1\right)$ has one peak. The function for $P\left(m \geq 1\right)$ is monotonically increasing, so any constrained solution will be unique. Finally, the function for the probability of no attack always starts at $(0, 1)$, then monotonically decreases. Since the three

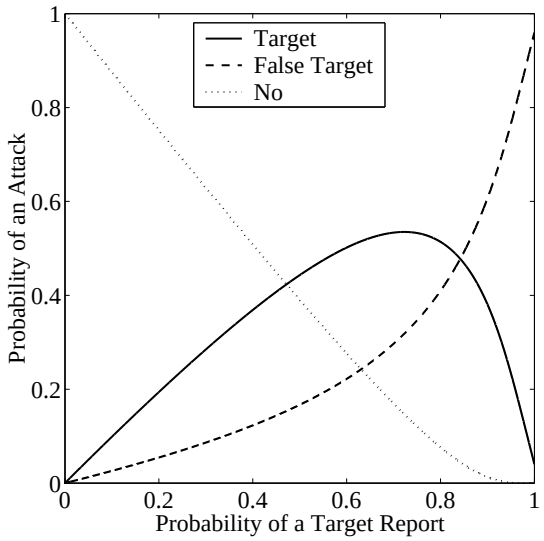

Figure 4.1 Outcome probabilities versus probability of a target report. Scenario 1 with constant parameters, $c = 100$, $\alpha Q = 50$ [1/hr], and $T = 0.5$ [hr].

outcome probabilities are mutually exclusive in a munition problem, they sum to one for each P_{TR} considered.

The problem can be solved for a number of b values and a plot of P^*_{TR} versus b can be generated. If $b \geq 0.318$, the unconstrained solution $P^*_{TR_u} = 0.723$ is used. Figure 4.2 illustrates the sensitivity of the solution to changes in b. Figure 4.2 is the plot an operator needs to set P_{TR} at the beginning of a mission, assuming b has been determined by the commander.

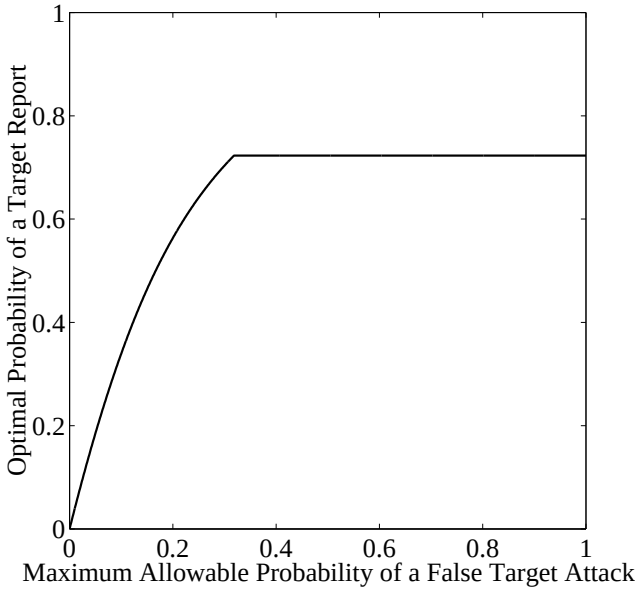

Figure 4.2 Optimal probability of a target report versus maximum allowable probability of a false target attack, b. Scenario 1 with constant parameters, $c = 100$, $\alpha Q = 50$ [1/hr], and $T = 0.5$ [hr].

Similar results are expected for Scenarios 2-4, where target-to-false-target ratios are the same regardless of sensor footprint location. For Scenarios 5-7, target-to-false-target ratios depend on the sensor footprint location. Therefore, the function for $P(m \geq 1)$ is not always monotonically increasing. Hence solutions are not unique. For example, Figure 4.3 shows the function for $P(m \geq 1)$ initially increases, then decreases, then increases again for a Scenario 7 problem with $k = 1$. For values of $P(m \geq 1)$ above the local minimum at $P(m \geq 1) = 0.385$, the unconstrained solution is used. On a plot of P^*_{TR} versus b, a discontinuous jump appears as shown in Figure 4.4.

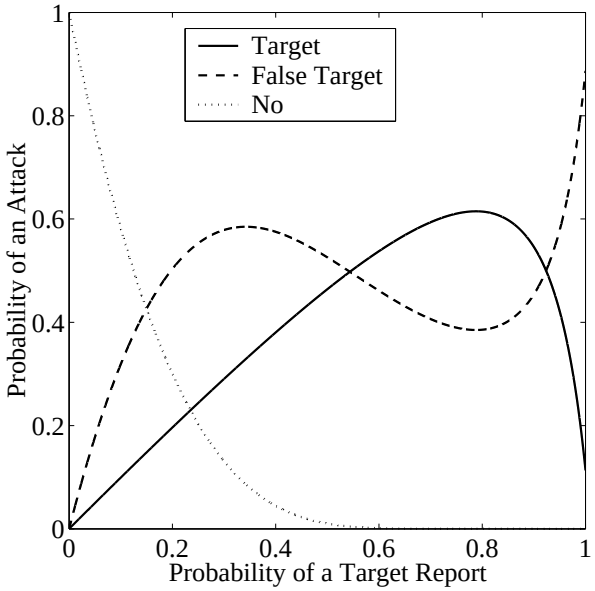

Figure 4.3 Outcome probabilities versus probability of a target report. Scenario 7 with constant parameters, $c = 100$, $\alpha = 5$ [1/km^2], $\sigma^2 = 0.25$ [km^2], and $R = 5$ [km].

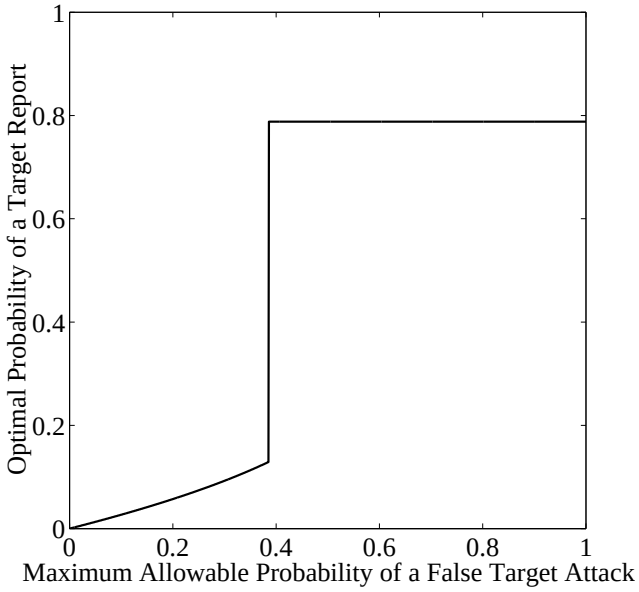

Figure 4.4 Optimal probability of a target report versus maximum allowable probability of a false target attack. Scenario 7 with constant parameters, $c = 100$, $\alpha = 5$ [1/km^2], $\sigma^2 = 0.25$ [km^2], and $R = 5$ [km].

4.3 Fixed Q, Variable P_{TR}

Fixed-parameter problems are readily solvable and simple to employ operationally. Improvement when parameters are allowed to vary is now examined. To begin, the case where P_{TR} is allowed to vary while Q remains fixed is considered. Having a fixed area coverage rate means a single ROC curve is used. Moving along a single ROC curve is done by adjusting the sensor threshold, which is tantamount to adjusting P_{TR}.

Consider Scenario 1 with $k = 1$ and Eq. (2.12) for the ROC model with $c = 100$. Assume the munition covers A_B by time T. Thus, $QT = A_B$. The optimal control problem can be solved for a number of b values. Figure 4.5 shows optimal P_{TR} schedules for three constraint values. In Chapter III, the optimal P_{TR} was shown to increase over time when the constraint on false target attacks is removed. Figure 4.5 shows the optimal P_{TR} increases over time even when a constraint on false target attacks exists. The increases diminish as constraint values are tightened (lowered).

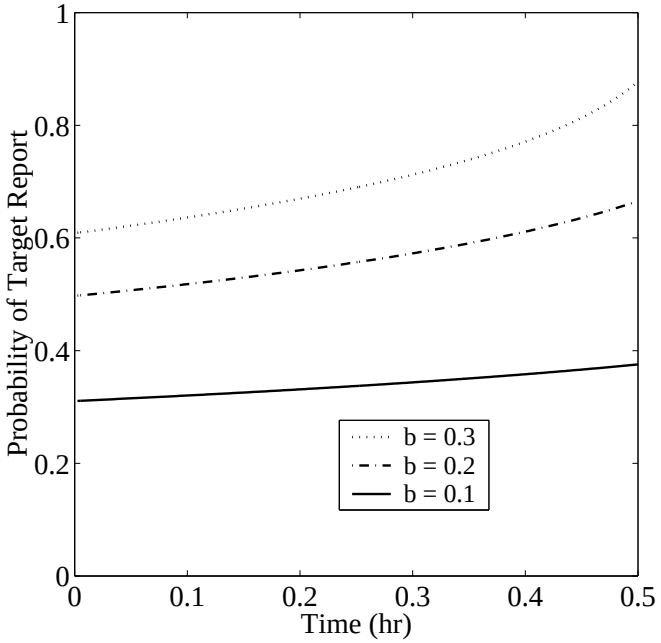

Figure 4.5 Optimal probability of a target report versus time. Scenario 1 with $k = 1$, $c = 100$, $\alpha Q = 50$ [1/hr], and $T = 0.5$ [hr].

The problem can be solved for a number of constraint values and the objective function values can be compared to those obtained using fixed parameters. In the system operating characteristic shown in Figure 4.6, there is negligible improvement for constraint values below 0.15 and marginal improvement (up to 3.4 percent) for constraint values above 0.15. Depending on the application, this improvement may or may not be worth the added complexity.

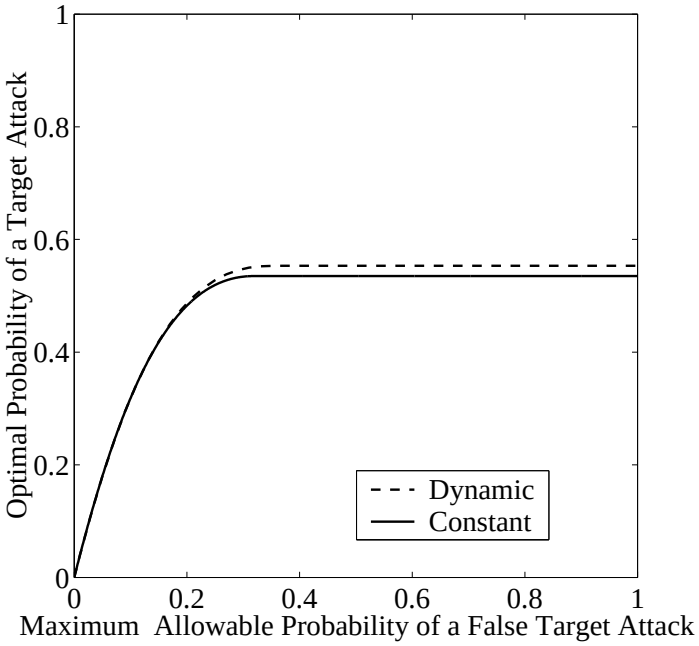

Figure 4.6 System Operating Characteristic. Dynamic versus constant P_{TR}. Scenario 1 with $k = 1$, $c = 100$, $\alpha Q = 50$ [1/hr], and $T = 0.5$ [hr].

Up to now, only the munition and sensor craft problems have been considered. It was shown in Chapter III that the optimal P_{TR} increases over time for the Scenario 1 munition problem, when the constraint on false target attacks is removed. It was also shown in Chapter III that the optimal P_{TR} is constant when $k = \infty$ and, for Scenario 1, is given by

$$P_{TR}^{*}(t) = \frac{-c \ln[1-b]}{(1-c)\ln[1-b] + \alpha Q T}. \tag{4.8}$$

Now consider the effect of multiple warheads. Figure 4.7 shows the system operating characteristic for $k = 1, 2, 6, \infty$ and $\hat{m} = \hat{n} = 1$. The results for $k = \infty$ come analytically from Eq. (4.8). The $k = 1$ results do not exactly conform to other k values which are bound by $k = \infty$. The munition problem has three mutually exclusive outcomes; whereas, the outcomes for the $k > 1$ problems are not mutually exclusive. Nonetheless, Figure 4.7 can be used by commanders to make decisions about constraint values and number of warheads. For $b < 0.20$, there is not much to be gained by adding warheads. In this single-target scenario, there are more false targets present, which means the probability of the first attack being a false target attack is relatively high. Thus it does not matter how many warheads there are. The constraint is met by the first attack. For $b < 0.20$, one can simply use the constant closed-form P_{TR} given by Eq. (4.8). In Figure 4.7, it is clear the benefits of more than 6 warheads is negligible throughout most of the range of b. These types of insights are possible using the techniques and equations provided in this dissertation.

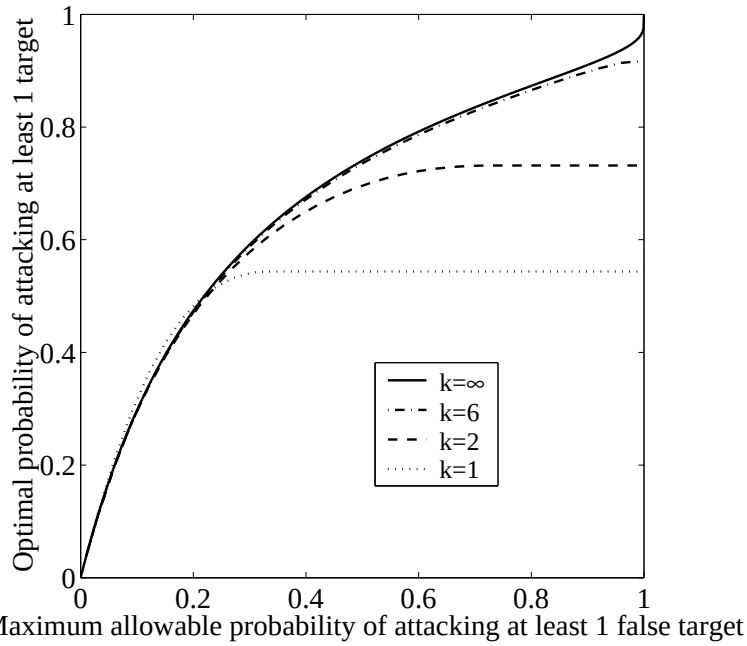

Figure 4.7 System Operating Characteristic. Dynamic P_{TR}. Scenario 1 with $c = 100$, $\alpha Q = 50$ [1/hr], and $T = 0.5$ [hr].

Consider Scenario 7 with $k = 1$ and Eq. (2.12) for the ROC model with $c = 100$. The target-to-false-target ratio depends on the sensor footprint location. Figure 4.8 shows optimal P_{TR} schedules for three constraint values. No conclusions were made for the Scenario 7 munition problem in Chapter III. Figure 4.8 shows as b tightens (decreases), the sensor is "turned off" earlier in the search.

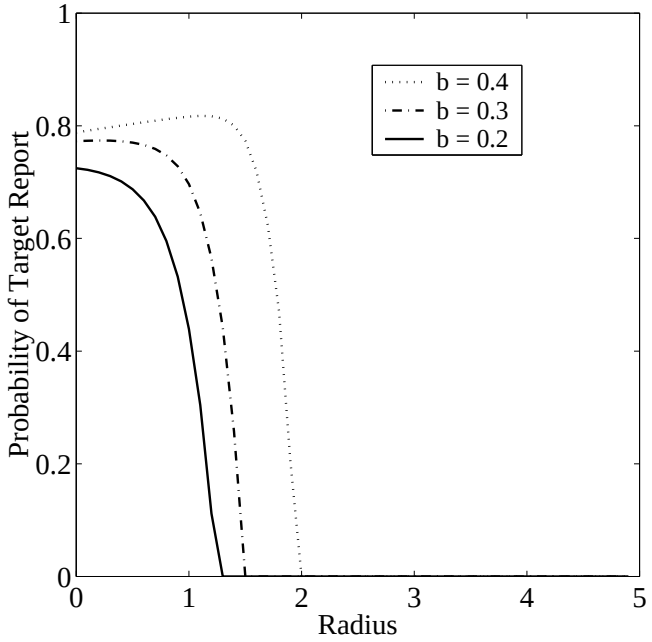

Figure 4.8 Optimal probability of a target report versus radius. Scenario 7 with $k = 1$, $c = 100$, $\alpha = 5$ [1/km^2], $\sigma^2 = 0.25$ [km^2], and $R = 5$ [km].

The objective function values of the dynamic solutions can be compared to those of the constant solutions. Figure 4.9 shows the poor performance of the constant-P_{TR} solution when $b < 0.385$. Unlike the Scenario 1 example where dynamic-P_{TR} solutions were only a few percent better than constant-P_{TR} solutions, there are substantial improvements when $b < 0.385$. Since the dynamic problem allows the sensor to be "turned off" at some point, solutions are similar to those at smaller R values. How far out in radius to search is clear. The dynamic problem "recognizes" the benefit of staying close to the origin when a target is normally distributed. The fixed-parameter problem requires an arbitrary pick for R. Thus, performance is poor

when R is chosen too large. To improve performance, one would need to make R a parameter and run a sensitivity study.

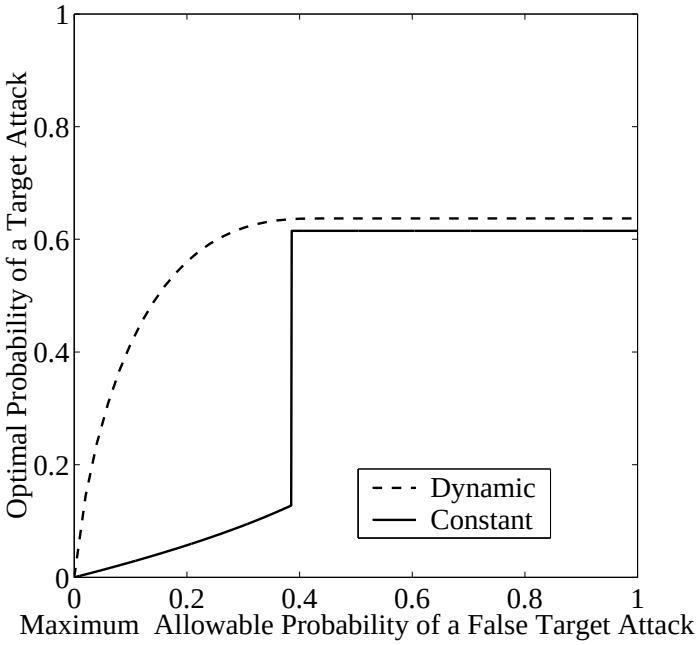

Figure 4.9 System Operating Characteristic. Dynamic versus constant P_{TR}. Scenario 7 with $k = 1$, $c = 100$, $\alpha = 5$ [1/km^2], $\sigma^2 = 0.25$ [km^2], and $R = 5$ [km].

The dynamic-P_{TR} solutions have been compared to fixed-P_{TR} solutions. The amount of improvement varies based on problem parameters and whether the target-to-false-target ratio is constant throughout the search. Next the requirement of fixed area coverage rate is relaxed.

4.4 Variable Q, Variable P_{TR}

Allowing Q to vary while keeping T fixed introduces another trade space. For a given b, larger Q means more area is covered in time T resulting in more target encounters. However, there is less chance of correctly classifying the targets. Conversely, for a given b, smaller Q means less area is covered in time T resulting in less target encounters. However, there is more chance of correctly classifying the targets. In Section 2.3, a way was presented to model sensor performance by making the ROC parameter c a function of area coverage rate Q. Specifically,

$$c\left(Q\right) = \frac{Q_n}{Q} \tag{4.9}$$

where Q_n is a scaled nominal area coverage rate.

Allowing both Q and P_{TR} to vary means the trajectory on the P_{TR} versus $(1 - P_{FTR})$ plane is bound by a region instead of a single ROC curve. The region is formed by a Q_{min} ROC curve and a Q_{max} ROC curve. Q_{min} might be tied to an air vehicle's stall speed, which is available in the air vehicle performance specification. Q_{max} might be tied to an air vehicle's maximum speed, gimbal limits, or search area. Assuming the real Q_{max} would result in $A_s > A_B$, an artificial limit needs to be invoked. Otherwise, probabilities could be greater than one. To ensure $A_s \leq A_B$, one can define Q_{max} as

$$Q_{max} \equiv \frac{A_B}{T}. \tag{4.10}$$

In Chapter III it was shown that when Q is unbounded,

$$P_{TR}^{*}\left(t\right) = \frac{Q_n}{2Q_n - Q^{*}\left(t\right)} \tag{4.11}$$

regardless of α, b, or number of warheads. Further, for $Q^{*} \in (0, Q_n)$, $P_{TR}^{*} \in \left(\frac{1}{2}, 1\right)$. In other words,

$$P_{TR}^{*}\left(t\right) > 0.5 \tag{4.12}$$

For $Q_n >> Q^*$, $P_{TR}^* \approx 0.5$ for all time. If Q is at its lower or upper bound for a particular region, then it can be considered fixed in that region. Therefore, one expects to see fixed-Q trends in regions where Q is at a bound.

To illustrate what is going on in the dynamic-Q, dynamic-P_{TR} problem, one can plot the trajectory of the operating point on the ROC plot for Scenario 1 with $k = 1$, $\alpha = 2$, $T = 0.5$, $Q_n = 1000$, $Q_{min} = 10$, and $Q_{max} = 20$. Figure 4.10 shows four trajectories for different values of b on one plot. Figure 4.11 shows the four trajectories on 4 different plots. When the constraint on false target attacks is tight (low), the air vehicle must fly at Q_{min} to get the best sensor performance, and P_{TR}^* increases with time. When $b = 0.09$, the air vehicle starts at Q_{min}, but eventually gets off the bound. As predicted, this occurs at a P_{TR} value slightly above 0.50. When $b = 0.15$, the air vehicle flies the entire mission with Q unbounded and the corresponding $P_{TR}^* \approx 0.5$. When $b = 0.25$, the air vehicle starts with an unbounded Q, but then hits the upper bound.

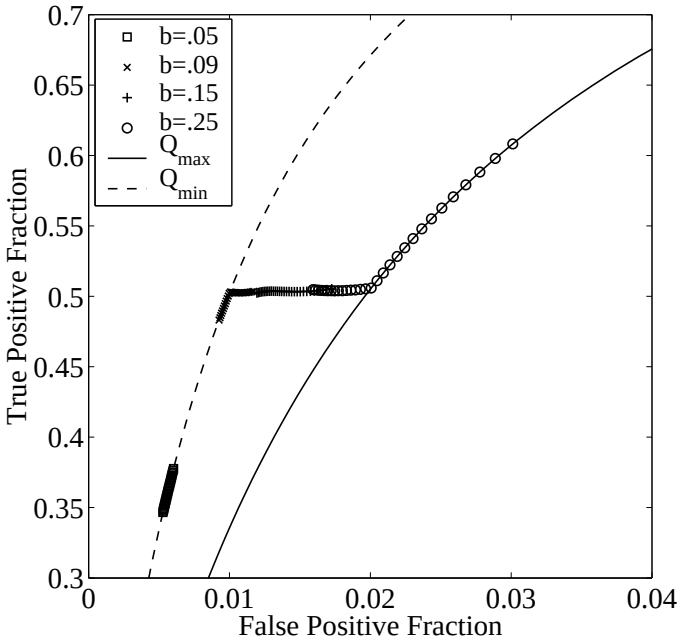

Figure 4.10 ROC plot. Scenario 1 with dynamic-Q, dynamic-P_{TR}, $k = 1$, $\alpha = 2$ [1/km^2], $Q_n = 1000$, $Q_{min} = 10$, $Q_{max} = 20$, and $T = 0.5$ [hr].

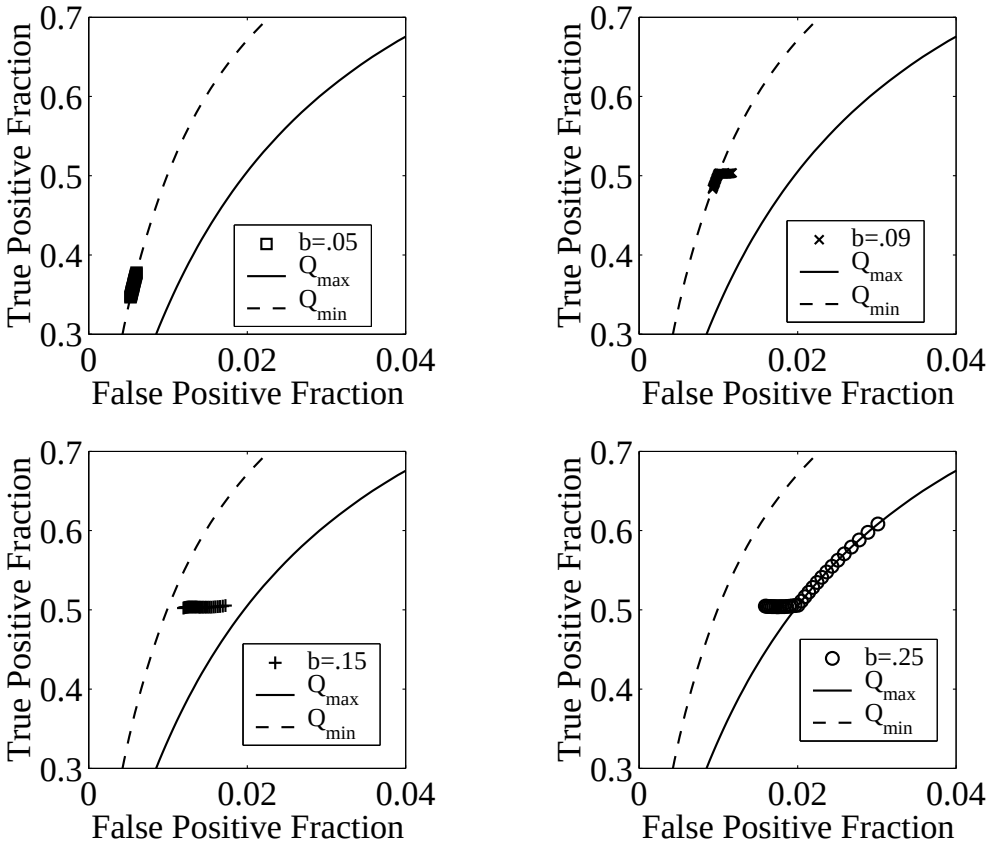

Figure 4.11 ROC plot broken out by upper bound. Scenario 1 with dynamic-Q, dynamic-P_{TR}, $k = 1$, $\alpha = 2$ [1/km^2], $Q_n = 1000$, $Q_{min} = 10$, $Q_{max} = 20$, and $T = 0.5$ [hr].

Time is implicit to the trajectories in Figures 4.10 and 4.11. If a trajectory is along the Q_{min} or Q_{max} ROC curve, time increases as the trajectory moves up and to the right. If a trajectory is in a region where Q is unbounded, time increases as the trajectory moves to the right.

Optimal schedules of the design variables Q and P_{TR} are shown in Figures 4.12(a) and 4.12(b). When Q^* is at either of its bounds, P^*_{TR} behaves similarly to the fixed-Q results shown previously. That is, P^*_{TR} is monotonically increasing with flatter curves at tighter constraint levels. When Q^* is unbounded, $P^*_{TR} \approx 0.5$ as predicted and Q^* is increasing. This represents the strategy seen before of staring conservatively, then increasing aggressiveness with time.

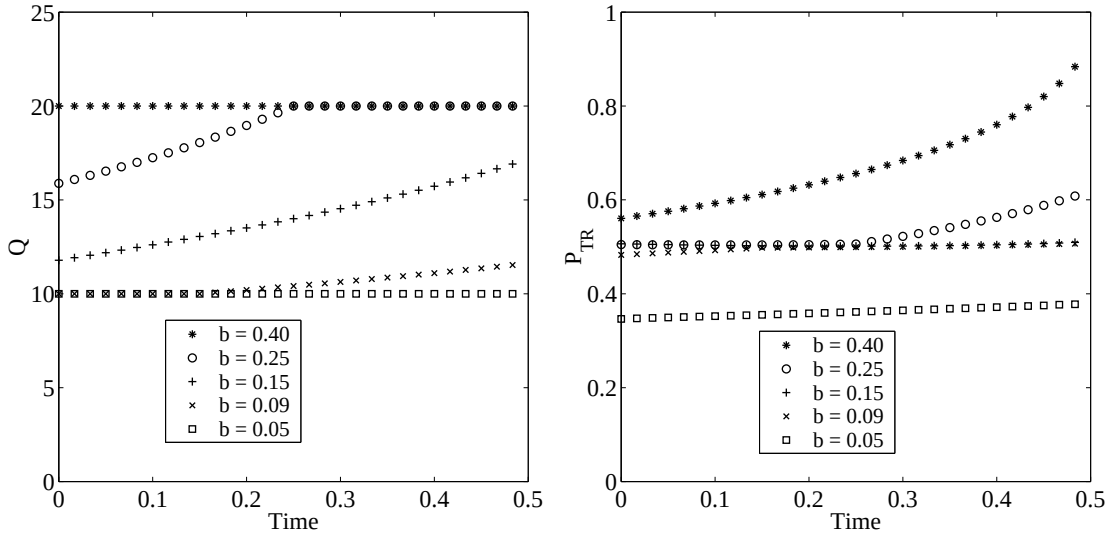

(a) Q schedule

(b) P_{TR} Schedule

Figure 4.12 Optimal Schedules for the Design Variables. Scenario 1 with dynamic-Q, dynamic-P_{TR}, $k = 1$, $\alpha = 2$ [1/km^2], $Q_n = 1000$, $Q_{min} = 10$, $Q_{max} = 20$, and $T = 0.5$ [hr].

A better indication of what is going on comes from looking at the schedule for $(1 - P_{FTR})$. Figure 4.13 shows $(1 - P_{FTR})$ is always smooth and increasing. These are the optimal functions required for meeting the constraint on false target attacks. Q and P_{TR} must combine at each time such that $(1 - P_{FTR})$ falls on one of the functions in Figure 4.13.

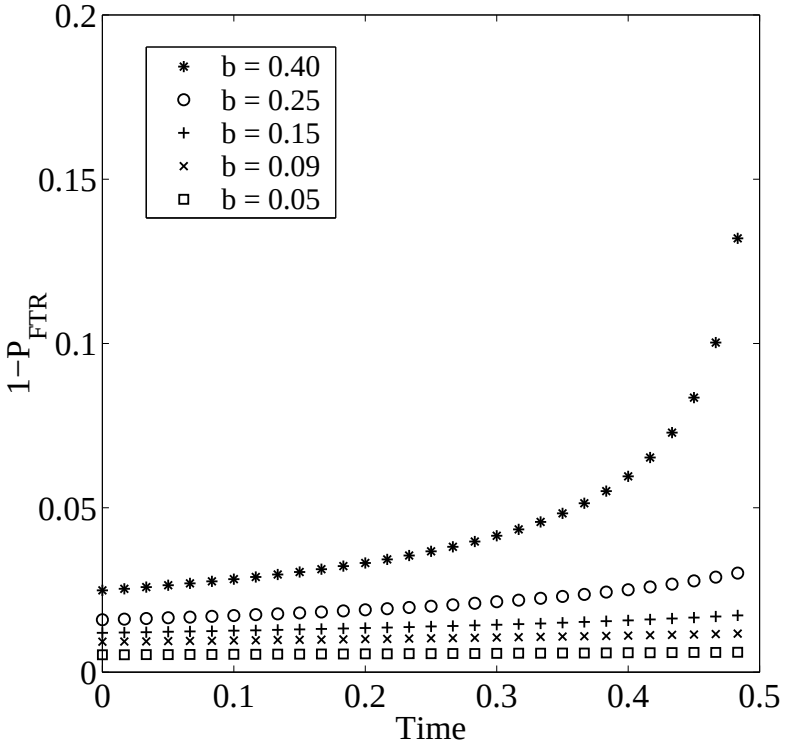

Figure 4.13 Optimal $(1 - P_{FTR})$ schedule. Scenario 1 with dynamic-Q, dynamic-P_{TR}, $k = 1$, $\alpha = 2$ [1/km^2], $Q_n = 1000$, $Q_{min} = 10$, $Q_{max} = 20$, and $T = 0.5$ [hr].

The tradeoff situation where lower Q values provide better sensor performance at the expense of less area searched was mentioned earlier. All this depends on b. Figure 4.14 shows the transition from the minimum search area to the maximum search area.

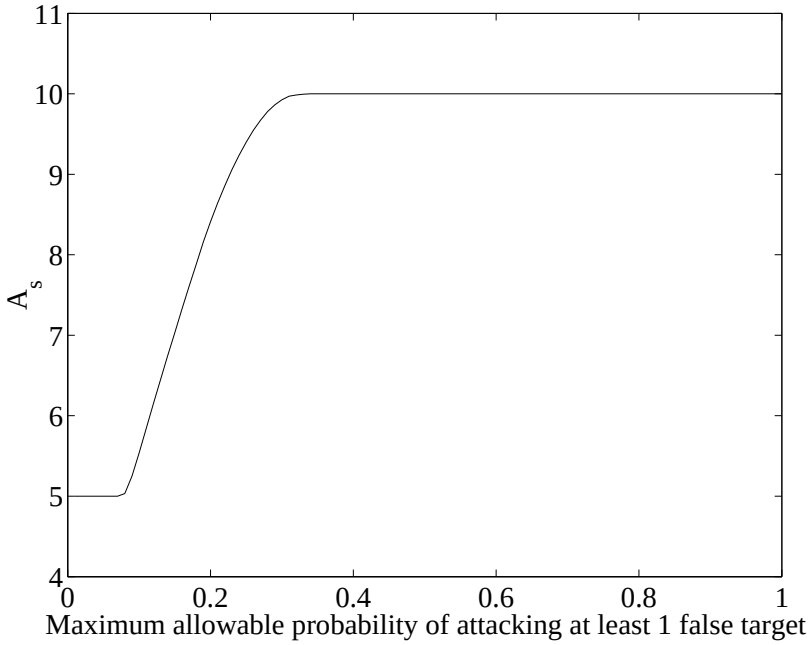

Figure 4.14 Area searched versus constraint on false target attacks. Scenario 1 with dynamic-Q, dynamic-P_{TR}, $k = 1$, $\alpha = 2$ [1/km^2], $Q_n = 1000$, $Q_{min} = 10$, $Q_{max} = 20$, and $T = 0.5$ [hr].

As with previous results, it is beneficial to compare the dynamic-parameter results to fixed-parameter results. This can be done two ways. First, one can require a fixed-parameter solution at each b value, whereby each parameter is optimized at each b value. Second, one can fix one of the parameters and allow only the other parameter to be optimized at each b value. Figure 4.15 compares dynamic and fixed solutions when each parameter is optimized at each b value. Only marginal improvement is seen for the dynamic-parameter problem.

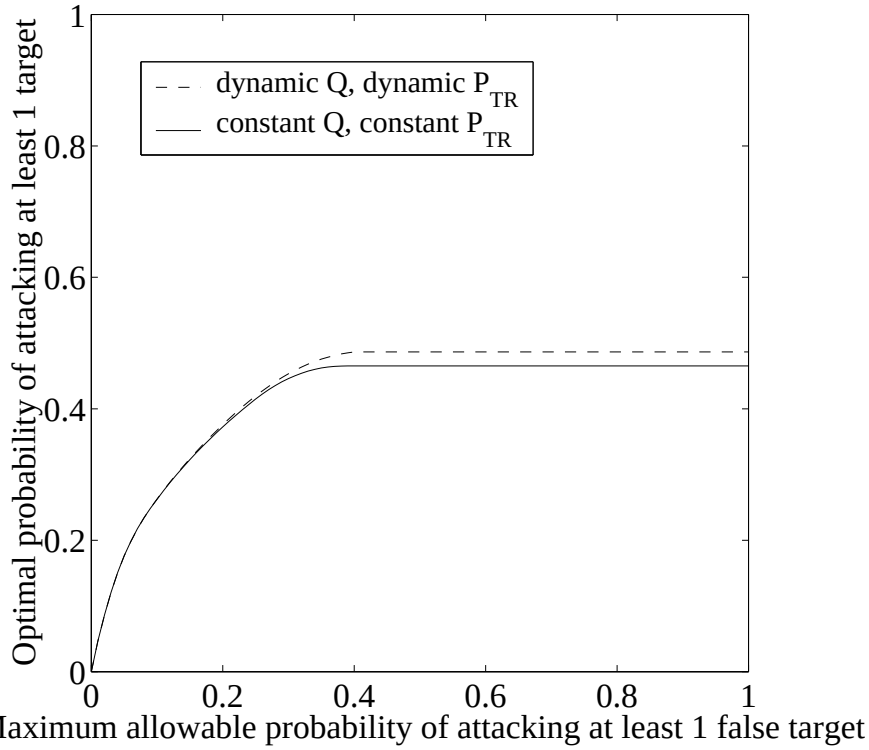

Figure 4.15 System Operating Characteristic. Dynamic versus constant solutions. Scenario 1 with $k = 1$, $\alpha = 2$ [1/km^2], $Q_n = 1000$, $Q_{min} = 10$, $Q_{max} = 20$, and $T = 0.5$ [hr]. Fixed-parameter problem had both Q and P_{TR} optimized at each b

In Figure 4.16, operating points for different b values are plotted on a ROC plot when both Q and P_{TR} are fixed but optimized at each b value. The operating points were determined using Eq. (4.6) and Eq. (4.7) with

$$(1 - P_{FTR}) = \frac{QP_{TR}}{QP_{TR} + Q_n\,(1 - P_{TR})}. \tag{4.13}$$

A grid search was used at each b value to find the optimal fixed operating point, whereby Q and P_{TR} were both varied from their minimum to maximum values. The upper bound b was incremented by 0.01 to 0.40. The trajectory is similar to the dynamic-Q, dynamic-P_{TR} trajectory in Figure 4.11. For low values of b, the air vehicle flies at Q_{min}. For high values of b, the air vehicle flies at Q_{max}. A "bridge" occurs somewhere above $P_{TR} = 0.5$. Though not dynamic, this behavior of $P^*_{TR} \approx 0.5$ when Q^* is unbounded matches the dynamic analytical predictions. This kind of insight can help designers and mission planners.

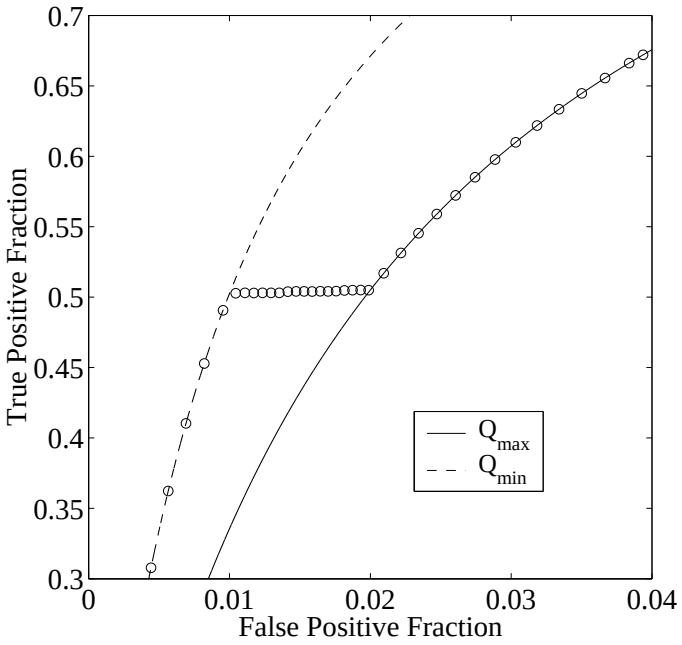

Figure 4.16 ROC plot. Scenario 1 with $k = 1$, $\alpha = 2$ [1/km^2], $Q_n = 1000$, $Q_{min} = 10$, $Q_{max} = 20$, and $T = 0.5$ [hr]. Fixed-parameter problem had both Q and P_{TR} optimized at each b

Next consider the case when one of the two design variables is fixed for all b values. Figure 4.17 shows when $Q = 15$ for all b values, the improvements for the dynamic-parameter problem are more pronounced. Hence, there are benefits to allowing both Q and P_{TR} to be optimized at each b value, even when they are required to be fixed.

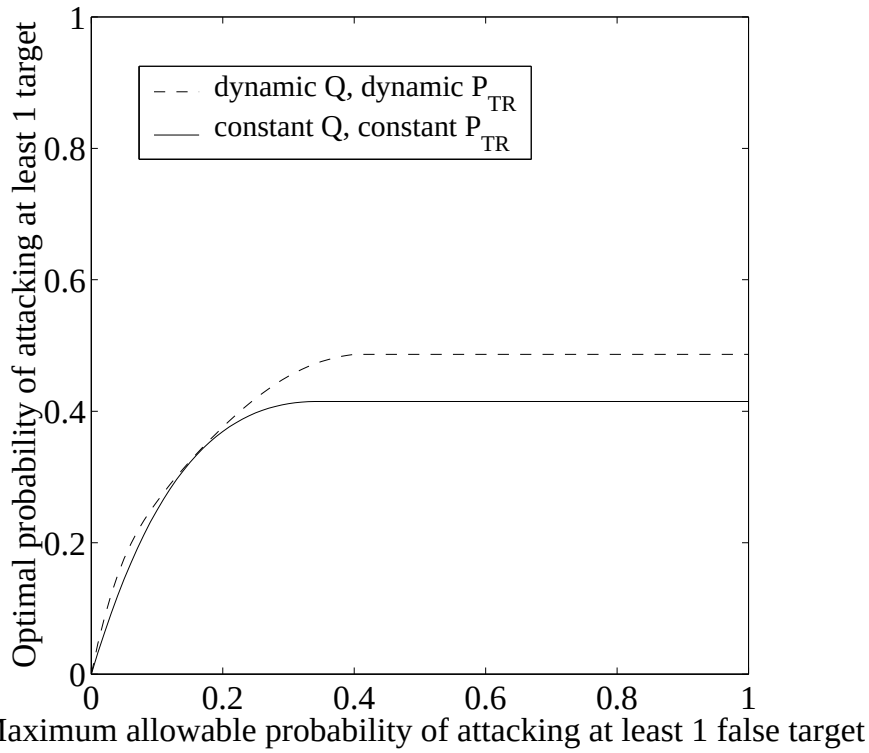

Figure 4.17 System Operating Characteristic. Dynamic versus constant solutions. Scenario 1 with $k = 1$, $\alpha = 2$ [1/km^2], $Q_n = 1000$, $Q_{min} = 10$, $Q_{max} = 20$, and $T = 0.5$ [hr]. Fixed-parameter problem had $Q = 15$ [km^2/hr] and P_{TR} optimized at each b

The effects of additional warheads remains to be examined. All the example problems thus far have been either Scenario 1 or Scenario 7. Therefore an example using Scenario 2 is in order, since analysis of Scenario 2 was also done in Chapter III. Consider Scenario 2 with $\alpha = 1$ [1/km^2], $\beta = 0.1$ [1/km^2], $Q_n = 1000$ [km^2/hr], $Q_{min} = 10$ [km^2/hr], $Q_{max} = 20$ [km^2/hr] and $T = 0.5$ [hr]. Analysis showed if $k = \infty$, $\hat{m} = 1$, and $P(m \geq 1) = b$ with T, Q, and α constant, then

$$P_{TR}^{*}(t) = \frac{-Q_n \ln(1-b)}{(Q-Q_n)\ln(1-b) + \alpha Q^2 T} \tag{4.14}$$

assuming $c = \frac{Q_n}{Q}$.

Equation (4.14) can be used to gain a rough idea of when it is better to fly at Q_{min} and when it is better to fly at Q_{max}. Figure 4.18 shows a crossover in the trade space around $b = 0.10$. At tight constraints on false target attacks, the system must be on the best ROC curve and uses Q_{min}. As the constraint loosens, the system can transition to a worse ROC curve with the idea of encountering more targets by using a larger Q. While Figure 4.18 applies to $k = \infty$ and fixed Q, the dynamic problem should approach the $k = \infty$, $Q = Q_{max}$ at high values of b.

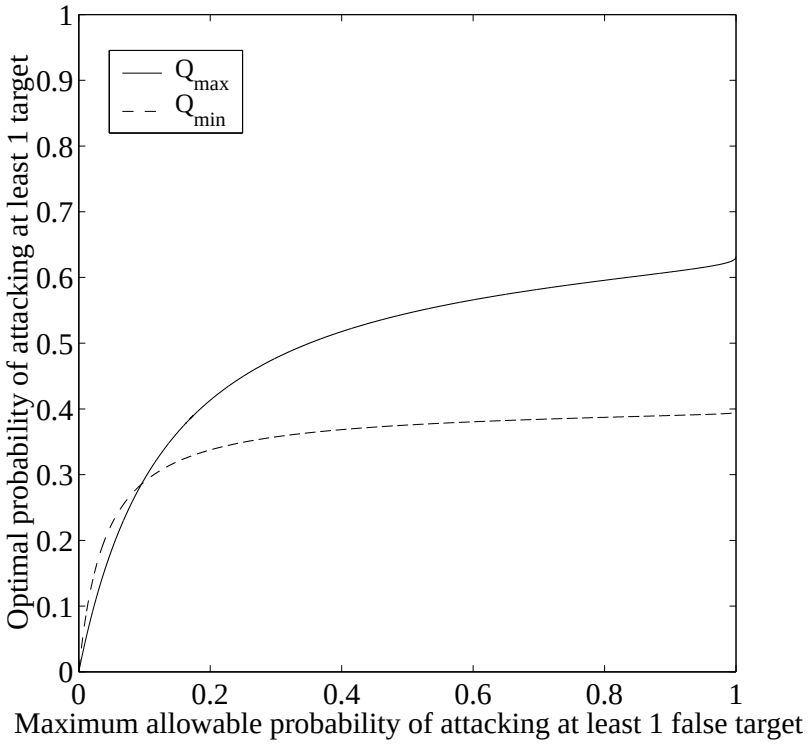

Figure 4.18 System Operating Characteristic. Scenario 2 with Q fixed at either Q_{min} or Q_{max}, $Q_n = 1000$, $k = \infty$, $\alpha = 1$ [1/km^2], $\beta = 0.1$ [1/km^2], and $T = 0.5$ [hr].

Figure 4.19 shows the trade space for the dynamic-Q, dynamic-P_{TR} problem for $k = 1, 2, 4, 6$. As seen before, increasing warheads for a tight constraint on false target attacks provides no value. As the constraint loosens, increasing warheads eventually adds value. For this problem, there is minimal benefit to adding more than 4 warheads. For the most part, the 4-warhead solution follows the asymptote generated by the $k = \infty$, $Q = Q_{max}$ solution from Eq. (4.14).

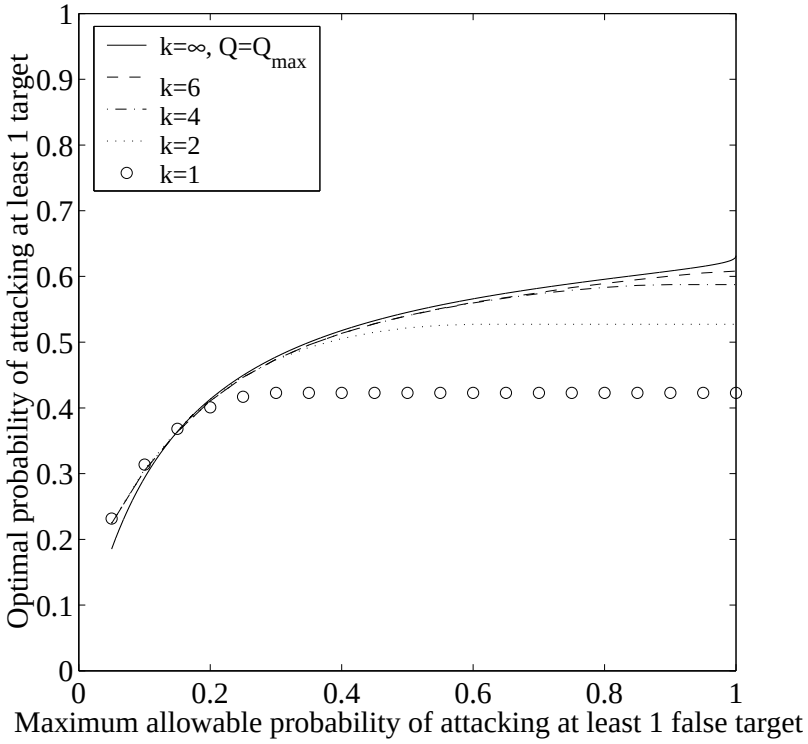

Figure 4.19 System Operating Characteristic. Scenario 2 with dynamic-Q, dynamic-P_{TR}, $\alpha = 1$ [1/km^2], $\beta = 0.1$ [1/km^2], and $T = 0.5$ [hr].

One can look to trajectories on a ROC plot to gain further insight. Figure 4.20 shows 4 trajectories for 4 different b values when $k = 1$. When the constraint on false target attacks is tight (low), the air vehicle must fly at Q_{min} to get the best sensor performance, and P^*_{TR} increases with time. When $b = 0.05$, the air vehicle starts at Q_{min}, but quickly gets off the bound. As predicted in Chapter III, this occurs at a P_{TR} value slightly above 0.50. When $b = 0.10$, the air vehicle flies the entire mission with Q unbounded and the corresponding $P^*_{TR} \approx 0.5$. When $b = 0.15$, the air vehicle starts with an unbounded Q, but then hits the upper bound. It is interesting to note that the crossover from Q_{min} to Q_{max} occurred around the same b value as the $k = \infty$, fixed-Q results in Figure 4.18. While P_{TR} varies in Figure 4.20, the variation is small.

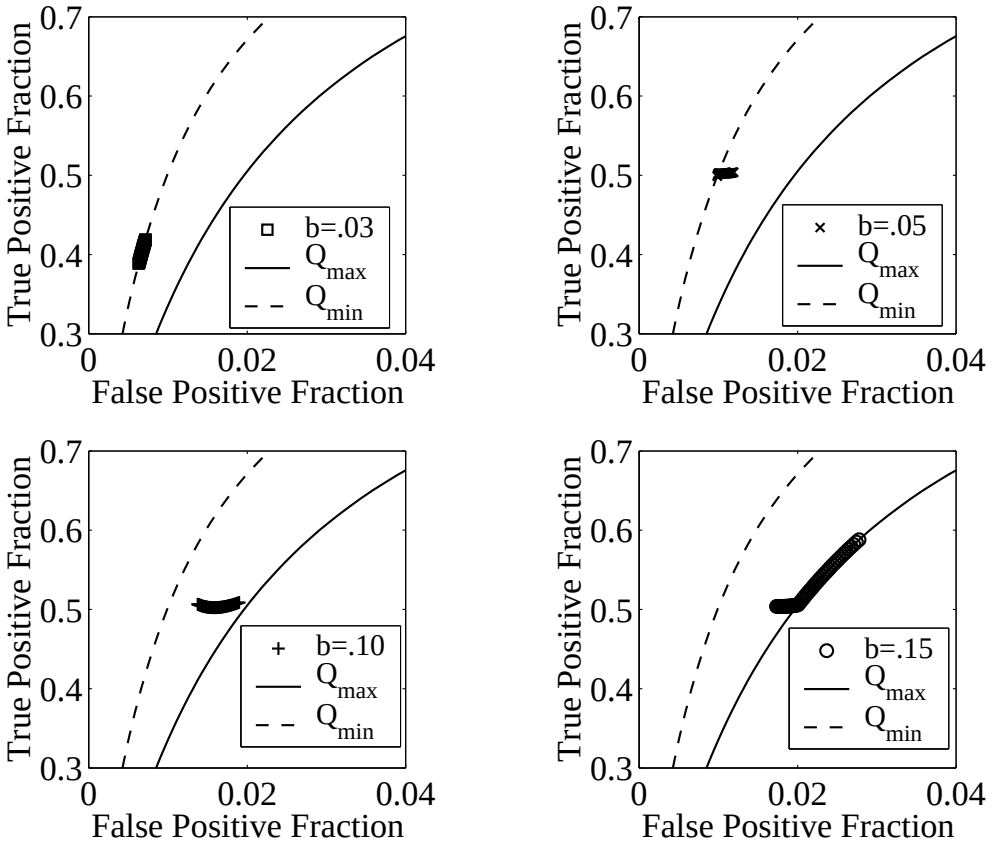

Figure 4.20 ROC plot. Scenario 2 with dynamic-Q, dynamic-P_{TR}, $\alpha = 1$ [1/km^2], $\beta = 0.1$ [1/km^2], $T = 0.5$ [hr], and $k = 1$.

Figure 4.21 shows 4 trajectories for 4 different b values when $k = 2$. The variations in P_{TR} are even smaller. In addition, at each b, the magnitudes of P_{TR} and Q are smaller than the $k = 1$ results. This makes intuitive sense as increasing warheads requires a more conservative operating point to meet the constraint on false target attacks. In fact, for the given problem, adding warheads actually degraded performance for tight constraints, albeit by very small amounts not readily visible in Figure 4.19.

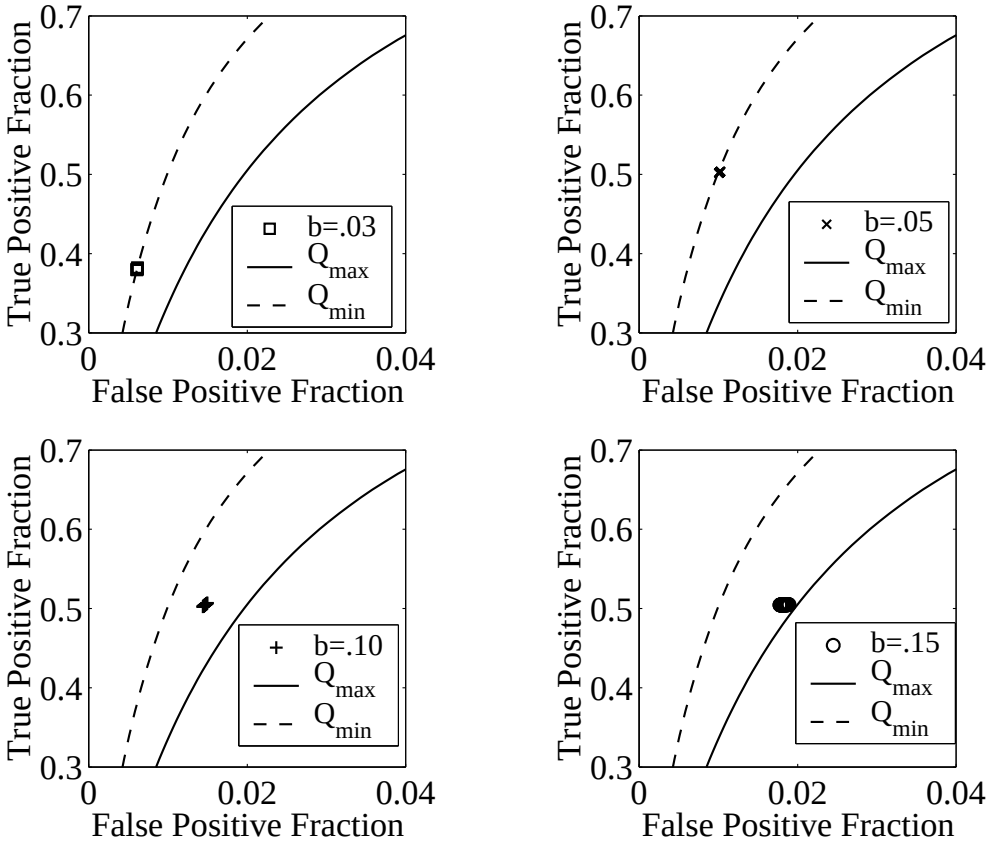

Figure 4.21 ROC plot. Scenario 2 with dynamic-Q, dynamic-P_{TR}, $\alpha = 1$ [1/km^2], $\beta = 0.1$ [1/km^2], $T = 0.5$ [hr], and $k = 2$.

V. Conclusions and Recommendations

5.1 Summary

The purpose of this research was to analytically quantify operational effectiveness of airborne systems performing search and destroy missions. The primary contribution to the field is the ability to handle time-varying parameters, which broadens the possible battle space scenarios and enables improved performance through function optimization. Prior to this research, one could only analytically solve problems where area coverage rate, sensor threshold, target density, and false target density where fixed. Now one can analytically solve problems where any or all of the above parameters vary with time.

Two types of search patterns were considered. The first type was the linear search pattern, which can be used to cover any linear-symmetric battle space. The second type involved concentric annuli emanating from the origin, which can be used to cover any circular battle space. Uniform, Poisson, and normal probability distributions were used to model target and false target encounters. Expressions needed to calculate the probability of at least $\hat{n}$ target attacks, $P(n \geq \hat{n})$, and the probability of at least $\hat{m}$ false target attacks, $P(m \geq \hat{m})$, were derived for the following seven battle space scenarios:

Scenario 1 consisted of a single target uniformly distributed in a linear-symmetric battle space among a Poisson field of false targets.

Scenario 2 consisted of a linear-symmetric battle space with a Poisson field of targets and a Poisson field of false targets.

Scenario 3 consisted of N targets uniformly distributed in a linear-symmetric battle space among a Poisson field of false targets.

Scenario 4 consisted of N targets and M false targets uniformly distributed in a linear-symmetric battle space.

Scenario 5 consisted of N targets normally distributed in a circular battle space among a Poisson field of false targets. Normally distributed referred to a circular-normal distribution centered at the origin with a target standard deviation σ_z.

Scenario 6 consisted of N targets and M false targets normally distributed in a circular battle space. Normally distributed referred to circular-normal distributions centered at the origin with a target standard deviation σ_z and a false target standard deviation σ_y.

Scenario 7 consisted of a single target normally distributed in a circular battle space among a Poisson field of false targets.

Sensor performance, in terms of a system's ability to autonomously distinguish between targets and false targets, came from a Receiver Operating Characteristic (ROC) curve. A representative ROC curve model was used; whereby, a parameter c dictated the locus of operating points. The parameter c depended inversely on the area coverage rate Q. Based on a user-supplied constant Q_n, sensor performance was completely determined by Q and the probability of a target report P_{TR}. Together, Q and P_{TR} establish the system operating characteristic.

Optimal control problems were formulated to maximize $P\left(n \geq \hat{n}\right)$ subject to $P\left(m \geq \hat{m}\right) \leq b$, where b was set by the user. The decision variables were Q and P_{TR}. Due to coupling of the state and costate equations, the two point boundary value problems were solved numerically using Bryson's gradient algorithm [7] and Matlab's® fmincon routine.

Prior to numerically solving sample problems, analytic solutions were provided for the munition and sensor craft problems for Scenarios 1, 2, and 7. Using these tractable instances, the following conclusions were made and used to verify numerical results:

1. For Scenarios 1 and 2 with $k = 1$ and no constraint on $P(m \geq \hat{m})$, if T, Q, α, and β are constant, the unbounded P_{TR}^* is monotonically increasing with time.

2. For Scenarios 1, 2, and 7 with $k = \infty$, $\hat{n} = 1$, and no constraint on $P(m \geq \hat{m})$, if T (or R), Q, α, and β are constant, the bounded $P_{TR}^* = P_{TR_{max}}^* = 1$.

3. For Scenarios 1 and 2 with $k = \infty$ and $P(m \geq \hat{m}) = b$, if T, Q, α, and β are constant, then P_{TR}^* is constant for all time.

4. For Scenarios 1 and 2 with $k = 1$ or $k = \infty$, if T, α, and β are constant and $Q(t)$ is unbounded, then the unbounded P_{TR}^* is given by

$$P_{TR}^*(t) = \frac{Q_n}{2Q_n - Q^*(t)} \tag{5.1}$$

5. For Scenario 7 with $k = \infty$ and $P(m \geq \hat{m}) = b$, if R and α are constant, then P_{TR}^* is monotonically decreasing with radius.

Variants of the problem were solved where some or all of the parameters were assumed fixed. Some problem-specific trends were noticed. Dynamic solutions were compared to constant solutions. The effects of additional warheads was also examined. The ratio of targets to false targets impacted results as well as whether the ratio depended on sensor footprint location.

5.2 Applicability

The results of this dissertation apply to search vehicles with 0, 1, or k warheads. Although the real motivation for this research came from autonomous air operations, the results can be applied to manned systems, land-based systems, and water-based systems. They can be applied in the design phase or operational phase of a system. In the design phase, the results can be used to develop system requirements, compare competing designs, or verify simulation results. Parameter sensitivity studies can be done to determine the cost effectiveness of improving sensors, warheads, or vehicle performance. The mathematical framework enables sound systems engineering. In

the operational phase, tactical decisions in the form of setting operating points and determining the number of warheads are possible using the results of this dissertation. The system operating characteristic plots of $P(n \geq \hat{n})$ versus $P(m \geq \hat{m})$ that include warhead effects give mission planners a complete picture of the trade space. They can look at one figure and see the effects of changing constraint level or changing number of warheads.

5.3 Recommendations for Further Research

1. Run more sample problems. Investigate different target and false target densities. Investigate different battle spaces.

2. Change from an airborne-based mission to a land-based or sea-based mission. Investigate any problem-specific trends.

3. Take an existing computer simulation and perform Monte Carlo runs. Compare the results with the analytic results possible from this research.

4. Develop a Matlab® toolbox with a graphical user interface that allows the user to select the scenario, the parameters allowed to vary, the number of time steps, solution tolerance, etc.

5. Examine more sophisticated ROC curve models. Include both altitude and velocity effects.

6. Develop expressions for combinations of uniform, Poisson, and normal distributions not covered by Scenarios 1-7.

7. Derive expressions to handle multiple types of targets or false targets.

8. Examine a bivariate normal distribution other than circular normal.

9. Develop scenarios for a linear-symmetric battle space where the ratio of targets to false targets depends on sensor footprint location.

10. Derive expressions for Scenarios 5-7 assuming the search starts at the outer radius and progresses inward.

11. Examine multiple warhead types.

Appendix A. Probability of Exactly j Classified Encounters Occurring up through a Specified Time or Radius

The probability of exactly j classified encounters occurring up through a specified time t or radius r is of interest. A classification occurs every time an object is encountered. Poisson, uniform, and circular normal distributions are considered. The following symbology is used:

$$
\begin{aligned}
A &\equiv \text{area covered up through time } t \text{ or radius } r \\
\mathcal{E} &\equiv \text{events involving encounters} \\
\mathcal{C} &\equiv \text{events involving classified encounters} \\
\mathcal{T} &\equiv \text{events involving target attacks} \\
\mathcal{F} &\equiv \text{events involving false target attacks} \\
\mathcal{X} &\equiv \text{random variable} \\
P_c &\equiv \text{general classification probability}
\end{aligned}
$$

P_c can be P_{TR}, P_{FTR}, $(1 - P_{TR})$, or $(1 - P_{FTR})$ depending on the application. If only encounters are needed, $P_c = 1$. For each distribution, solutions are derived assuming only one classification probability is used for all j encounters. Special cases include the probability of no target attacks and the probability of no false target attacks. For the distributions having a finite number of objects (uniform and circular normal), solutions are also derived assuming l of the j encounters are classified with one probability and the other $j - l$ encounters are classified with a second probability.

A.1 Poisson Distribution

Let $\mathcal{X}$ be a random variable on the sample space $S = \{0, 1, 2, \ldots\}$. If the probability function of $\mathcal{X}$ is

$$
P\left(\{\mathcal{X} = \eta\}\right) = e^{-\nu}\frac{\nu^{\eta}}{\eta!}, \qquad \eta = 0, 1, 2, \ldots \tag{A.1}
$$

where $\nu > 0$, then $\mathcal{X}$ is said to obey the Poisson probability law with parameter ν [39]. Equation (A.1) gives the probability of encountering exactly η objects while searching a Poisson field of objects. The Poisson field of objects is characterized by a density distribution α (or β) so that when an area A is searched, the Poisson probability law parameter is $\nu = \alpha A$. This is tantamount to assuming:

1) The probability that exactly one object will be encountered in the incremental area ΔA is approximately $\alpha \Delta A$, in the sense that it is equal to $\alpha \Delta A + R_1(\Delta A)$, and $\frac{R_1(\Delta A)}{\Delta A} \to 0$ as $\Delta A \to 0$.

2) The probability that exactly zero objects will be encountered in the incremental area ΔA is approximately $1 - \alpha \Delta A$, in the sense that it is equal to $1 - \alpha \Delta A + R_2(\Delta A)$, and $\frac{R_2(\Delta A)}{\Delta A} \to 0$ as $\Delta A \to 0$.

3) The probability that exactly two or more objects will be encountered in the incremental area ΔA is equal to $R_3(\Delta A)$, such that the quotient $\frac{R_3(\Delta A)}{\Delta A} \to 0$ as $\Delta A \to 0$.

4) If an area is subdivided into n subareas and for $i = 1, \ldots, n$, E_i denotes the event that at least one or more encounters occurred in the i^{th} subarea, then, for any integer n, $E_1, \ldots, E_n$ are independent events.

Poisson parameters are often broken down into the product of an encounter rate μ and time t. If an air vehicle has an area coverage rate Q, then $\mu = \alpha Q$. How to handle an encounter rate that varies with time is now addressed.

Let $\mu(\tau)$ be the rate of encounters at time τ. Divide the time interval $[0, t]$ into n short time periods of length $\tau_1, \ldots, \tau_n$ such that

$$\sum_{i=1}^{n} \tau_i = t \tag{A.2}$$

Let the mean rate of occurrence and mean probability of classification in the i^{th} interval be μ_i and P_{c_i} respectively. From the fourth assumption above, the probability

that exactly j_i encounters occur in the interval τ_i, $i = 1, \ldots, n$ is

$$\begin{aligned} P(j_1, \ldots, j_n) &= \prod_{i=1}^{n} e^{-\mu_i \tau_i} \frac{(\mu_i \tau_i)^{j_i}}{j_i!} \\ &= e^{-\sum_{i=1}^{n} \mu_i \tau_i} \prod_{i=1}^{n} \frac{(\mu_i \tau_i)^{j_i}}{j_i!} \end{aligned} \tag{A.3}$$

The probability of no encounters occurring (and hence no classification) during $[0, t]$ is

$$P(\mathcal{E}_{0,A}) = e^{-\sum_{i=1}^{n} \mu_i \tau_i} \tag{A.4}$$

The probability of one classified encounter in the i^{th} interval is

$$P(\mathcal{C}_{1,\Delta A_i}) = e^{-\sum_{i=1}^{n} \mu_i \tau_i} \frac{(\mu_i \tau_i)^1}{1!} P_{c_i}. \tag{A.5}$$

The probability of exactly one classified encounter occurring during $[0, t]$ requires considering all the permutations where one classified encounter could occur. That is

$$P(\mathcal{C}_{1,A}) = P(\mathcal{C}_{1,\Delta A_1}) + P(\mathcal{C}_{1,\Delta A_2}) + \cdots + P(\mathcal{C}_{1,\Delta A_n}) \tag{A.6}$$

So,

$$\begin{aligned} P(\mathcal{C}_{1,A}) &= e^{-\sum_{i=1}^{n} \mu_i \tau_i} \frac{(\mu_1 \tau_1)^1}{1!} P_{c_1} + e^{-\sum_{i=1}^{n} \mu_i \tau_i} \frac{(\mu_2 \tau_2)^1}{1!} P_{c_2} + \\ &\quad \cdots + e^{-\sum_{i=1}^{n} \mu_i \tau_i} \frac{(\mu_n \tau_n)^1}{1!} P_{c_n} \\ &= e^{-\sum_{i=1}^{n} \mu_i \tau_i} \sum_{i=1}^{n} \mu_i \tau_i P_{c_i} \end{aligned} \tag{A.7}$$

The probability of exactly two classified encounters occurring during $[0, t]$ requires considering all the permutations where two classified encounters could occur. That

is

$$\begin{aligned} P\left(\mathcal{C}_{2,A}\right) &= P\left(\mathcal{C}_{1,\Delta A_1} \cap \mathcal{C}_{1,\Delta A_2}\right) + P\left(\mathcal{C}_{1,\Delta A_1} \cap \mathcal{C}_{1,\Delta A_3}\right) + \cdots + P\left(\mathcal{C}_{1,\Delta A_1} \cap \mathcal{C}_{1,\Delta A_n}\right) + \\ & P\left(\mathcal{C}_{1,\Delta A_2} \cap \mathcal{C}_{1,\Delta A_3}\right) + P\left(\mathcal{C}_{1,\Delta A_2} \cap \mathcal{C}_{1,\Delta A_4}\right) + \cdots + P\left(\mathcal{C}_{1,\Delta A_2} \cap \mathcal{C}_{1,\Delta A_n}\right) + \\ & \vdots \\ & + P\left(\mathcal{C}_{1,\Delta A_{n-1}} \cap \mathcal{C}_{1,\Delta A_n}\right) + \\ & P\left(\mathcal{C}_{2,\Delta A_1}\right) + P\left(\mathcal{C}_{2,\Delta A_2}\right) + \cdots + P\left(\mathcal{C}_{2,\Delta A_n}\right) \end{aligned} \tag{A.8}$$

So,

$$\begin{aligned} P\left(\mathcal{C}_{2,A}\right) &= e^{-\sum_{i=1}^{n} \mu_i \tau_i} \frac{\left(\mu_1 \tau_1\right)^1}{1!} P_{c_1} \left[\frac{\left(\mu_2 \tau_2\right)^1}{1!} P_{c_2} + \cdots + \frac{\left(\mu_n \tau_n\right)^1}{1!} P_{c_n} \right] + \\ & e^{-\sum_{i=1}^{n} \mu_i \tau_i} \frac{\left(\mu_2 \tau_2\right)^1}{1!} P_{c_2} \left[\frac{\left(\mu_3 \tau_3\right)^1}{1!} P_{c_3} + \cdots + \frac{\left(\mu_n \tau_n\right)^1}{1!} P_{c_n} \right] + \\ & \vdots \\ & e^{-\sum_{i=1}^{n} \mu_i \tau_i} \frac{\left(\mu_{n-1} \tau_{n-1}\right)^1}{1!} P_{c_{n-1}} \frac{\left(\mu_n \tau_n\right)^1}{1!} P_{c_n} + \\ & e^{-\sum_{i=1}^{n} \mu_i \tau_i} \left[\frac{\left(\mu_1 \tau_1\right)^2}{2!} P_{c_1}^2 + \cdots + \frac{\left(\mu_n \tau_n\right)^2}{2!} P_{c_n}^2 \right] \\ &= \frac{1}{2} e^{-\sum_{i=1}^{n} \mu_i \tau_i} \left[2\mu_1 \tau_1 P_{c_1} \left(\mu_2 \tau_2 P_{c_2} + \cdots + \mu_n \tau_n P_{c_n} \right) + \right. \\ & 2\mu_2 \tau_2 P_{c_2} \left(\mu_3 \tau_3 P_{c_3} + \cdots + \mu_n \tau_n P_{c_n} \right) + \\ & \cdots + 2\mu_{n-1} \tau_{n-1} P_{c_{n-1}} \mu_n \tau_n P_{c_n} + \\ & \left. \left(\mu_1 \tau_1 P_{c_1}\right)^2 + \left(\mu_2 \tau_2 P_{c_2}\right)^2 + \cdots + \left(\mu_n \tau_n P_{c_n}\right)^2 \right] \\ &= e^{-\sum_{i=1}^{n} \mu_i \tau_i} \frac{\left(\sum_{i=1}^{n} \mu_i \tau_i P_{c_i}\right)^2}{2} \end{aligned} \tag{A.9}$$

In general, the probability of exactly j classified encounters occurring during $[0, t]$ is

$$P\left(\mathcal{C}_{j,A}\right) = e^{-\sum_{i=1}^{n} \mu_i \tau_i} \frac{\left(\sum_{i=1}^{n} \mu_i \tau_i P_{c_i}\right)^j}{j!} \tag{A.10}$$

Taking the limit as $\tau_i \to 0$, $i = 1, \ldots, n$, $n \to \infty$ such that $\sum_{i=1}^{n} \tau_i = t$ yields

$$P\left(\mathcal{C}_{j,A}\right) = e^{-\int_0^t \mu(\tau) d\tau} \frac{\left(\int_0^t P_c\left(\tau\right) \mu\left(\tau\right) d\tau\right)^j}{j!} \tag{A.11}$$

Equation (A.11) can be used to determine the probability of either no false target attacks or no target attacks occurring up through time t. In the case of no false target attacks, the possible mutually exclusive events are

no encounters
1 encounter correctly classified
2 encounters correctly classified
$\vdots$
∞ encounters correctly classified

Thus,

$$\begin{aligned}
P\left(\mathcal{E}_{0,A} \cap \mathcal{C}_{1,A} \cap \ldots \cap \mathcal{C}_{\infty,A}\right) &= P\left(\mathcal{E}_{0,A}\right) + P\left(\mathcal{C}_{1,A}\right) + \cdots + P\left(\mathcal{C}_{\infty,A}\right) \\
&= e^{-\int_0^t \mu(\tau) d\tau} + e^{-\int_0^t \mu(\tau) d\tau} \frac{\left(\int_0^t P_c\left(\tau\right) \mu\left(\tau\right) d\tau\right)^1}{1!} + \\
&\quad \cdots + e^{-\int_0^t \mu(\tau) d\tau} \frac{\left(\int_0^t P_c\left(\tau\right) \mu\left(\tau\right) d\tau\right)^\infty}{\infty!} \\
&= e^{-\int_0^t \mu(\tau) d\tau} \left[1 + \frac{\left(\int_0^t P_c\left(\tau\right) \mu\left(\tau\right) d\tau\right)^1}{1!} + \right. \\
&\quad \left. \cdots + \frac{\left(\int_0^t P_c\left(\tau\right) \mu\left(\tau\right) d\tau\right)^\infty}{\infty!}\right] \\
&= e^{-\int_0^t \mu(\tau) d\tau} e^{\int_0^t P_c(\tau) \mu(\tau) d\tau} \\
&= e^{-\int_0^t [1 - P_c(\tau)] \mu(\tau) d\tau}
\end{aligned} \tag{A.12}$$

To calculate the probability of no false target attacks for a straight-line search, $P_c(\tau) = P_{FTR}(\tau)$ and $\mu(\tau) = \alpha(\tau) Q(\tau)$ in Eq. (A.12) giving

$$P\left(\mathcal{F}_{0,A(t)}\right) = e^{-\int_0^t [1-P_{FTR}(\tau)]\alpha(\tau)Q(\tau)d\tau} \tag{A.13}$$

where $\alpha(\tau)$ is the false target density. The Poisson parameter for false target attacks (which is time-varying) becomes

$$\nu_{FT}(t) \equiv \int_0^t [1 - P_{FTR}(\tau)]\, \alpha(\tau)\, Q(\tau)\, d\tau \tag{A.14}$$

To calculate the probability of no target attacks for a straight-line search, $P_c(\tau) = 1 - P_{TR}(\tau)$ and $\mu(\tau) = \beta(\tau) Q(\tau)$ in Eq. (A.12) giving

$$P\left(\mathcal{T}_{0,A(t)}\right) = e^{-\int_0^t [P_{TR}(\tau)]\beta(\tau)Q(\tau)d\tau} \tag{A.15}$$

where $\beta(\tau)$ is the target density. The Poisson parameter for target attacks (which is time-varying) becomes

$$\nu_T(t) \equiv \int_0^t [P_{TR}(\tau)]\, \beta(\tau)\, Q(\tau)\, d\tau \tag{A.16}$$

Now that Poisson parameters for false target and target attacks exist, more general expressions can be given. The probability of exactly m false target attacks in $A(t)$ is

$$P\left(\mathcal{F}_{m,A(t)}\right) = e^{-\nu_{FT}(t)} \frac{\nu_{FT}(t)^m}{m!} \tag{A.17}$$

and the probability of exactly n target attacks in $A(t)$ is

$$P\left(\mathcal{T}_{n,A(t)}\right) = e^{-\nu_T(t)} \frac{\nu_T(t)^n}{n!}. \tag{A.18}$$

For a straight-line search,

$$A(t) = \int_0^t Q(\tau)\, d\tau. \tag{A.19}$$

In the case of searching a circular disc of radius R using concentric annuli emanating from the origin, it can be shown that

$$\nu_{FT}(r) \equiv \int_0^r 2\pi \left[1 - P_{FTR}(\rho)\right] \alpha(\rho) \rho d\rho \tag{A.20}$$

and

$$\nu_T(r) \equiv \int_0^r 2\pi P_{TR}(\rho) \beta(\rho) \rho d\rho \tag{A.21}$$

The probability of exactly m false target attacks in $A(r)$ is

$$P\left(\mathcal{F}_{m,A(r)}\right) = e^{-\nu_{FT}(r)} \frac{\nu_{FT}(r)^m}{m!} \tag{A.22}$$

and the probability of exactly n target attacks in $A(r)$ is

$$P\left(\mathcal{T}_{n,A(r)}\right) = e^{-\nu_T(r)} \frac{\nu_T(r)^n}{n!}. \tag{A.23}$$

For a circular search using concentric annuli emanating from the origin,

$$A(r) = \pi r^2. \tag{A.24}$$

A.2 Uniform Distribution

There are N uniformly-distributed objects in the battle space A_B. Divide the time period of length t into n short time periods of length $\tau_1, \ldots, \tau_n$ such that

$$\sum_{i=1}^{n} \tau_i = t \tag{A.25}$$

Let the mean probability of classification and area coverage rate in the i^{th} interval be P_{c_i} and Q_i respectively. The incremental area is given by

$$\Delta A_i = Q_i \tau_i \tag{A.26}$$

and the search area is given

$$A_s = \sum_i^n \Delta A_i. \tag{A.27}$$

No encounters during $[0, t]$ means the first object was not encountered, the second object was not encountered, ..., the N^{th} object was not encountered. These events are independent, thus the probability of no encounters (and hence no classification) involves multiplying the individual probabilities.

$$P\left(\mathcal{E}_{0,A}\right) = \left[1 - \frac{1}{A_B}\int_0^t Q\left(\tau\right) d\tau\right]^N \tag{A.28}$$

Let $j = 1$. In the i^{th} interval, either the first object or the second object or ... or the N^{th} object is encountered. These are mutually exclusive events. Therefore, to calculate the probability of one classified encounter in the i^{th} interval, the individual probabilities are summed. That is,

$$P\left(\mathcal{C}_{1,\Delta A_i}\right) = \underbrace{\frac{P_{c_i}\Delta A_i}{A_B} + \cdots + \frac{P_{c_i}\Delta A_i}{A_B}}_{N} = N\frac{P_{c_i}\Delta A_i}{A_B} \tag{A.29}$$

The probability of exactly one classified encounter occurring during $[0, t]$ requires considering all the permutations where one classified encounter could occur. That is

$$P\left(\mathcal{C}_{1,A}\right) = P\left(\mathcal{C}_{1,\Delta A_1}\right) + P\left(\mathcal{C}_{1,\Delta A_2}\right) + \cdots + P\left(\mathcal{C}_{1,\Delta A_n}\right) \tag{A.30}$$

So

$$\begin{aligned} P\left(\mathcal{C}_{1,A}\right) &= N\frac{P_{c_1}\Delta A_1}{A_B} + N\frac{P_{c_2}\Delta A_2}{A_B} + \cdots + N\frac{P_{c_n}\Delta A_n}{A_B} \\ &= \frac{N}{A_B}\sum_i^n P_{c_i}\Delta A_i \end{aligned} \tag{A.31}$$

The probability of exactly two classified encounters occurring during $[0, t]$ requires considering all the permutations where two classified encounters could occur. That

is

$$\begin{aligned} P\left(\mathcal{C}_{2,A}\right) &= P\left(\mathcal{C}_{1,\Delta A_1} \cap \mathcal{C}_{1,\Delta A_2}\right) + P\left(\mathcal{C}_{1,\Delta A_1} \cap \mathcal{C}_{1,\Delta A_3}\right) + \cdots + P\left(\mathcal{C}_{1,\Delta A_1} \cap \mathcal{C}_{1,\Delta A_n}\right) + \\ & P\left(\mathcal{C}_{1,\Delta A_2} \cap \mathcal{C}_{1,\Delta A_3}\right) + P\left(\mathcal{C}_{1,\Delta A_2} \cap \mathcal{C}_{1,\Delta A_4}\right) + \cdots + P\left(\mathcal{C}_{1,\Delta A_2} \cap \mathcal{C}_{1,\Delta A_n}\right) + \\ & \vdots \\ & + P\left(\mathcal{C}_{1,\Delta A_{n-1}} \cap \mathcal{C}_{1,\Delta A_n}\right) + \\ & P\left(\mathcal{C}_{2,\Delta A_1}\right) + P\left(\mathcal{C}_{2,\Delta A_2}\right) + \cdots + P\left(\mathcal{C}_{2,\Delta A_n}\right) \end{aligned} \tag{A.32}$$

Bayes' rule can be applied to the joint probabilities $P\left(\mathcal{C}_{1,\Delta A_i} \cap \mathcal{C}_{1,\Delta A_k}\right)$. That is,

$$P\left(\mathcal{C}_{1,\Delta A_i} \cap \mathcal{C}_{1,\Delta A_k}\right) = P\left(\mathcal{C}_{1,\Delta A_i} | \mathcal{C}_{1,\Delta A_k}\right) P\left(\mathcal{C}_{1,\Delta A_k}\right) \tag{A.33}$$

So,

$$\begin{aligned} P\left(\mathcal{C}_{2,A}\right) &= (N-1)\frac{P_{c_2}\Delta A_2}{A_B} N \frac{P_{c_1}\Delta A_1}{A_B} + (N-1)\frac{P_{c_3}\Delta A_3}{A_B} N \frac{P_{c_1}\Delta A_1}{A_B} + \cdots + \\ & (N-1)\frac{P_{c_n}\Delta A_n}{A_B} N \frac{P_{c_1}\Delta A_1}{A_B} + \\ & (N-1)\frac{P_{c_3}\Delta A_3}{A_B} N \frac{P_{c_2}\Delta A_2}{A_B} + (N-1)\frac{P_{c_4}\Delta A_4}{A_B} N \frac{P_{c_2}\Delta A_2}{A_B} + \cdots + \\ & (N-1)\frac{P_{c_n}\Delta A_n}{A_B} N \frac{P_{c_2}\Delta A_2}{A_B} + \\ & \vdots \\ & (N-1)\frac{P_{c_n}\Delta A_n}{A_B} N \frac{P_{c_{n-1}}\Delta A_{n-1}}{A_B} + \\ & \binom{N}{2}\frac{1}{A_B^2}\sum_{i=1}^{n}\left(P_{c_i}\Delta A_i\right)^2 \\ &= \binom{N}{2}\frac{1}{A_B^2}\sum_{i=1}^{n}\sum_{k=1}^{n} P_{c_i}\Delta A_i P_{c_k}\Delta A_k = \binom{N}{2}\left[\frac{1}{A_B}\sum_{i=1}^{n} P_{c_i}\Delta A_i\right]^2 \end{aligned} \tag{A.34}$$

The last step involved using Fubini's Theorem. In general, the probability of exactly j classified encounters occurring during $[0, t]$ is

$$P\left(\mathcal{C}_{j,A}\right) = \binom{N}{j}\left[\frac{1}{A_B}\sum_{i=1}^{n} P_{c_i}\Delta A_i\right]^j. \tag{A.35}$$

Taking the limit as $\tau_i \to 0$, $i = 1, \ldots, n$, $n \to \infty$ such that $\sum_{i=1}^{n} \tau_i = t$ yields

$$P\left(\mathcal{C}_{j,A}\right) = \binom{N}{j}\left[\frac{1}{A_B}\int_0^t P_c\left(\tau\right) Q\left(\tau\right) d\tau\right]^j \tag{A.36}$$

Equation (A.36) can be used with $P_c\left(\tau\right) = 1 - P_{TR}\left(\tau\right)$ to determine the probability of no target attacks occurring up through time t. The possible mutually exclusive events are

no target encounters

1 misclassified target encounter and $N - 1$ targets not encountered

2 misclassified target encounters and $N - 2$ targets not encountered

$\vdots$

N misclassified target encounters

Bayes' rule can be applied to calculate the joint probabilities. That is,

$$\begin{aligned} P\left(j \text{ misclassified encounters} \cap N - j \text{ objects not encountered}\right) = \\ P\left(j \text{ misclassified encounters} | N - j \text{ objects not encountered}\right) \times \\ P\left(N - j \text{ objects not encountered}\right) \end{aligned} \tag{A.37}$$

Therefore, the probability of no target attacks occurring up through time t, assuming N targets, is

$$\begin{aligned} P\left(\mathcal{T}_{0,A}\right) &= \left[1-\frac{1}{A_B}\int_0^t Q\left(\tau\right)d\tau\right]^N + \\ &\quad \sum_{j=1}^{N}\left\{\binom{N}{j}\left[\frac{1}{A_B}\int_0^t\left[1-P_{TR}\left(\tau\right)\right]Q\left(\tau\right)d\tau\right]^j \times \right. \\ &\quad \left.\left[1-\frac{1}{A_B}\int_0^t Q\left(\tau\right)d\tau\right]^{N-j}\right\} \\ &= \sum_{j=0}^{N}\left\{\binom{N}{j}\left[\frac{1}{A_B}\int_0^t\left[1-P_{TR}\left(\tau\right)\right]Q\left(\tau\right)d\tau\right]^j \times \right. \\ &\quad \left.\left[1-\frac{1}{A_B}\int_0^t Q\left(\tau\right)d\tau\right]^{N-j}\right\} \\ &= \left[1-\frac{1}{A_B}\int_0^t P_{TR}\left(\tau\right)Q\left(\tau\right)d\tau\right]^N \end{aligned} \tag{A.38}$$

The last step involved using the binomial theorem.

Similarly, the probability of no false target attacks occurring up through time t, assuming M false targets is

$$P\left(\mathcal{F}_{0,A}\right) = \left\{1-\frac{1}{A_B}\int_0^t\left[1-P_{FTR}\left(\tau\right)\right]Q\left(\tau\right)d\tau\right\}^M. \tag{A.39}$$

Equation (A.36) assumes the same classification probability is used for each encounter. If j objects are encountered, suppose l are classified with $P_{c_1}\left(\tau\right)$ and $j-l$ are classified with $P_{c_2}\left(\tau\right)$. Thus,

$$\begin{aligned} &P\left[l \text{ classified with } P_{c_1}\left(\tau\right) \cap j-l \text{ classified with } P_{c_2}\left(\tau\right) | j \text{ encounters}\right] = \\ &\qquad \binom{j}{l}\left[\frac{1}{A_B}\int_0^t P_{c_1}\left(\tau\right)Q\left(\tau\right)d\tau\right]^l\left[\frac{1}{A_B}\int_0^t P_{c_2}\left(\tau\right)Q\left(\tau\right)d\tau\right]^{j-l} \end{aligned} \tag{A.40}$$

A.3 Circular-Normal Distribution

There are N normally-distributed objects. Normally-distributed refers to a circular normal distribution with standard deviation σ. Thus, the search area A_s is a circular disc. Divide the disc into n concentric annuli of area $A_1, \ldots, A_n$ such that

$$\sum_{i=1}^{n} A_i = A_s \tag{A.41}$$

Each A_i is calculated using

$$A_i = 2\pi\rho_i\Delta\rho_i \tag{A.42}$$

where ρ_i is the radius of the annulus and $\Delta\rho_i$ is the thickness. The search begins at the origin of the disc and progresses outward such that $\rho_i < \rho_{i+1}$, $i = 1, \ldots, n-1$. Let the mean probability of classification in the i^{th} annulus be P_{c_i}.

No encounters during $[0, r]$ means the first object was not encountered, the second object was not encountered, ..., the N^{th} object was not encountered. These events are independent, thus the probability of no encounters (and hence no classification) involves multiplying the individual probabilities.

$$P\left(\mathcal{E}_{0,A}\right) = \left[1 - \int_0^{2\pi}\int_0^{r} \frac{1}{2\pi\sigma^2} e^{-\frac{\rho^2}{2\sigma^2}} \rho d\rho d\theta\right]^N = \left[1 - \int_0^{r} \frac{\rho}{\sigma^2} e^{-\frac{\rho^2}{2\sigma^2}} d\rho\right]^N. \tag{A.43}$$

Let $j = 1$. In the i^{th} annulus, either encounter the first object or the second object or ... or the N^{th} object is encountered. These are mutually exclusive events. Therefore, to calculate the probability of one encounter in the i^{th} annulus, the individual probabilities are summed. That is,

$$\begin{aligned} P\left(\mathcal{E}_{1,\Delta A_i}\right) &= \underbrace{2\pi\rho_i\Delta\rho_i \frac{1}{2\pi\sigma^2} e^{-\frac{\rho_i^2}{2\sigma^2}} + \cdots + 2\pi\rho_i\Delta\rho_i \frac{1}{2\pi\sigma^2} e^{-\frac{\rho_i^2}{2\sigma^2}}}_{N} \\ &= N \frac{\rho_i}{\sigma^2} e^{-\frac{\rho_i^2}{2\sigma^2}} \Delta\rho_i \end{aligned} \tag{A.44}$$

The probability of exactly one classified encounter occurring during $[0, r]$ requires considering all the permutations where one classified encounter could occur. That is

$$P\left(\mathcal{C}_{1,A}\right) = P\left(\mathcal{C}_{1,\Delta A_1}\right) + P\left(\mathcal{C}_{1,\Delta A_2}\right) + \cdots + P\left(\mathcal{C}_{1,\Delta A_n}\right) \tag{A.45}$$

So

$$\begin{aligned} P\left(\mathcal{C}_{1,A}\right) &= N\frac{\rho_1}{\sigma^2}e^{-\frac{\rho_1^2}{2\sigma^2}}\Delta\rho_1 P_{c_1} + N\frac{\rho_2}{\sigma^2}e^{-\frac{\rho_2^2}{2\sigma^2}}\Delta\rho_2 P_{c_2} + \cdots + N\frac{\rho_n}{\sigma^2}e^{-\frac{\rho_n^2}{2\sigma^2}}\Delta\rho_n P_{c_n} \\ &= N\sum_i^n \frac{\rho_i}{\sigma^2}e^{-\frac{\rho_i^2}{2\sigma^2}}\Delta\rho_i P_{c_i} \end{aligned} \tag{A.46}$$

The probability of exactly two classified encounters occurring during $[0, r]$ requires considering all the permutations where two classified encounters could occur. That is

$$\begin{aligned} P\left(\mathcal{C}_{2,A}\right) = {} & P\left(\mathcal{C}_{1,\Delta A_1} \cap \mathcal{C}_{1,\Delta A_2}\right) + P\left(\mathcal{C}_{1,\Delta A_1} \cap \mathcal{C}_{1,\Delta A_3}\right) + \cdots + P\left(\mathcal{C}_{1,\Delta A_1} \cap \mathcal{C}_{1,\Delta A_n}\right) + \\ & P\left(\mathcal{C}_{1,\Delta A_2} \cap \mathcal{C}_{1,\Delta A_3}\right) + P\left(\mathcal{C}_{1,\Delta A_2} \cap \mathcal{C}_{1,\Delta A_4}\right) + \cdots + P\left(\mathcal{C}_{1,\Delta A_2} \cap \mathcal{C}_{1,\Delta A_n}\right) + \\ & \vdots \\ & + P\left(\mathcal{C}_{1,\Delta A_{n-1}} \cap \mathcal{C}_{1,\Delta A_n}\right) + \\ & P\left(\mathcal{C}_{2,\Delta A_1}\right) + P\left(\mathcal{C}_{2,\Delta A_2}\right) + \cdots + P\left(\mathcal{C}_{2,\Delta A_n}\right) \end{aligned} \tag{A.47}$$

Bayes' rule can be applied to the joint probabilities $P\left(\mathcal{C}_{1,\Delta A_i} \cap \mathcal{C}_{1,\Delta A_k}\right)$. That is,

$$P\left(\mathcal{C}_{1,\Delta A_i} \cap \mathcal{C}_{1,\Delta A_k}\right) = P\left(\mathcal{C}_{1,\Delta A_i} | \mathcal{C}_{1,\Delta A_k}\right) P\left(\mathcal{C}_{1,\Delta A_k}\right) \tag{A.48}$$

So,

$$\begin{aligned}
P\left(\mathcal{C}_{2,A}\right) &= (N-1)\frac{\rho_2}{\sigma^2}e^{-\frac{\rho_2^2}{2\sigma^2}}\Delta\rho_2 P_{c_2} N\frac{\rho_1}{\sigma^2}e^{-\frac{\rho_1^2}{2\sigma^2}}\Delta\rho_1 P_{c_1} + \\
&\quad (N-1)\frac{\rho_3}{\sigma^2}e^{-\frac{\rho_3^2}{2\sigma^2}}\Delta\rho_3 P_{c_3} N\frac{\rho_1}{\sigma^2}e^{-\frac{\rho_1^2}{2\sigma^2}}\Delta\rho_1 P_{c_1} + \cdots + \\
&\quad (N-1)\frac{\rho_n}{\sigma^2}e^{-\frac{\rho_n^2}{2\sigma^2}}\Delta\rho_n P_{c_n} N\frac{\rho_1}{\sigma^2}e^{-\frac{\rho_1^2}{2\sigma^2}}\Delta\rho_1 P_{c_1} + \\
&\quad (N-1)\frac{\rho_3}{\sigma^2}e^{-\frac{\rho_3^2}{2\sigma^2}}\Delta\rho_3 P_{c_3} N\frac{\rho_2}{\sigma^2}e^{-\frac{\rho_2^2}{2\sigma^2}}\Delta\rho_2 P_{c_2} + \\
&\quad (N-1)\frac{\rho_4}{\sigma^2}e^{-\frac{\rho_4^2}{2\sigma^2}}\Delta\rho_4 P_{c_4} N\frac{\rho_2}{\sigma^2}e^{-\frac{\rho_2^2}{2\sigma^2}}\Delta\rho_2 P_{c_2} + \cdots + \\
&\quad (N-1)\frac{\rho_n}{\sigma^2}e^{-\frac{\rho_n^2}{2\sigma^2}}\Delta\rho_n P_{c_n} N\frac{\rho_2}{\sigma^2}e^{-\frac{\rho_2^2}{2\sigma^2}}\Delta\rho_2 P_{c_2} + \\
&\quad \vdots \\
&\quad (N-1)\frac{\rho_n}{\sigma^2}e^{-\frac{\rho_n^2}{2\sigma^2}}\Delta\rho_n P_{c_n} N\frac{\rho_{n-1}}{\sigma^2}e^{-\frac{\rho_{n-1}^2}{2\sigma^2}}\Delta\rho_{n-1} P_{c_{n-1}} + \\
&\quad \binom{N}{2}\sum_{i=1}^{n}\left(\frac{\rho_i}{\sigma^2}e^{-\frac{\rho_i^2}{2\sigma^2}}\Delta\rho_i P_{c_i}\right)^2 \\
&= \binom{N}{2}\sum_{i=1}^{n}\sum_{k=1}^{n}\frac{\rho_i}{\sigma^2}e^{-\frac{\rho_i^2}{2\sigma^2}}\Delta\rho_i P_{c_i}\frac{\rho_k}{\sigma^2}e^{-\frac{\rho_k^2}{2\sigma^2}}\Delta\rho_k P_{c_k} \\
&= \binom{N}{2}\left[\sum_{i=1}^{n}\frac{\rho_i}{\sigma^2}e^{-\frac{\rho_i^2}{2\sigma^2}}\Delta\rho_i P_{c_i}\right]^2 \qquad \text{(A.49)}
\end{aligned}$$

The last step involved using Fubini's Theorem. In general, the probability of exactly j classified encounters occurring during $[0, r]$ is

$$P\left(\mathcal{C}_{j,A}\right) = \binom{N}{j}\left[\sum_{i=1}^{n}\frac{\rho_i}{\sigma^2}e^{-\frac{\rho_i^2}{2\sigma^2}}\Delta\rho_i P_{c_i}\right]^j. \qquad \text{(A.50)}$$

Taking the limit as $\Delta\rho_i \to 0$, $i = 1, \ldots, n$, $n \to \infty$ such that $\sum_{i=1}^{n} A_i = A_s$ yields

$$P\left(\mathcal{C}_{j,A(r)}\right) = \binom{N}{j}\left[\int_0^r P_c\left(\rho\right)\frac{\rho}{\sigma^2}e^{-\frac{\rho^2}{2\sigma^2}}d\rho\right]^j. \qquad \text{(A.51)}$$

Equation (A.51) can be used with $P_c(\rho) = 1 - P_{TR}(\rho)$ to determine the probability of no target attacks occurring up through radius r. The possible mutually exclusive events are

no target encounters

1 misclassified target encounter and $N-1$ targets not encountered

2 misclassified target encounters and $N-2$ targets not encountered

$\vdots$

N misclassified target encounters

Equation (A.37) can be used to calculate the joint probabilities. The probability of no target attacks occurring up through radius r, assuming N targets, is then

$$\begin{aligned} P\left(\mathcal{T}_{0,A(r)}\right) &= \left[1 - \int_0^r \frac{\rho}{\sigma_T^2} e^{-\frac{\rho^2}{2\sigma_T^2}} d\rho\right]^N + \\ &\quad \sum_{j=1}^{N} \binom{N}{j} \left\{\int_0^r \left[1 - P_{TR}(\rho)\right] \frac{\rho}{\sigma_T^2} e^{-\frac{\rho^2}{2\sigma_T^2}} d\rho\right\}^j \left[1 - \int_0^r \frac{\rho}{\sigma_T^2} e^{-\frac{\rho^2}{2\sigma_T^2}} d\rho\right]^{N-j} \\ &= \sum_{j=0}^{N} \binom{N}{j} \left\{\int_0^r \left[1 - P_{TR}(\rho)\right] \frac{\rho}{\sigma_T^2} e^{-\frac{\rho^2}{2\sigma_T^2}} d\rho\right\}^j \left[1 - \int_0^r \frac{\rho}{\sigma_T^2} e^{-\frac{\rho^2}{2\sigma_T^2}} d\rho\right]^{N-j} \\ &= \left[1 - \int_0^r P_{TR}(\rho) \frac{\rho}{\sigma_T^2} e^{-\frac{\rho^2}{2\sigma_T^2}} d\rho\right]^N \end{aligned} \tag{A.52}$$

where σ_T is the standard deviation for targets. The last step involved using the binomial theorem.

Similarly, the probability of no false target attacks occurring up through radius r, assuming M false targets is

$$P\left(\mathcal{F}_{0,A(r)}\right) = \left\{1 - \int_0^r \left[1 - P_{FTR}(\rho)\right] \frac{\rho}{\sigma_{FT}^2} e^{-\frac{\rho^2}{2\sigma_{FT}^2}} d\rho\right\}^M \tag{A.53}$$

where σ_{FT} is the standard deviation for false targets.

Equation (A.51) assumes the same classification probability is used for each encounter. If j objects are encountered, suppose l are classified with $P_{c_1}(\rho)$ and $j-l$ are classified with $P_{c_2}(\rho)$. Thus,

$$P\left[l \text{ classified with } P_{c_1}(\rho) \cap j-l \text{ classified with } P_{c_2}(\rho) | j \text{ encounters}\right] = \binom{j}{l} \left[\int_0^r P_{c_1}(\rho) \frac{\rho}{\sigma^2} e^{-\frac{\rho^2}{2\sigma^2}} d\rho\right]^l \left[\int_0^r P_{c_2}(\rho) \frac{\rho}{\sigma^2} e^{-\frac{\rho^2}{2\sigma^2}} d\rho\right]^{j-l} \quad \text{(A.54)}$$

A.4 Discussion

Now that expressions for the probability of exactly j classified encounters occurring up through a specified time t or radius r exist, the 12 elemental probabilities for each of the scenarios can be calculated. This is done in Appendix B.

Appendix B. Derivation of Elemental Probabilities for Scenarios 1-7

The 12 elemental probabilities needed to calculate $P(m = \hat{m})$, $P(n = \hat{n})$, $P(m \geq \hat{m})$, and $P(n \geq \hat{n})$ are derived for Scenarios 1-7.

B.1 Scenario 1

This scenario is the specific case of Scenario 3 when $N = 1$. Hence, the derivation is given in Section B.3.

B.2 Scenario 2

For this scenario, there is a Poisson field of false targets with density $\alpha(t)$ and a Poisson field of targets with density $\beta(t)$. The air vehicle flies along a straight path with area coverage rate $Q(t)$. In a Poisson field, there is an infinite number of objects available. Unlike uniform and normal distributions, events in a Poisson field are independent. Therefore, there is no need to account for every object. The 12 elemental probabilities simplify to

$$
\begin{aligned}
P_1 &= P\left(\mathcal{T}_{n-1,A} \cap \mathcal{T}_{1,dA}\right) \\
P_2 &= P\left(\mathcal{F}_{m,A}\right) \\
P_3 &= P\left(\mathcal{T}_{n,A}\right) \\
P_4 &= P\left(\mathcal{F}_{m-1,A} \cap \mathcal{F}_{1,dA}\right) \\
P_5 &= P\left(\mathcal{F}_{0,A}\right) \\
P_6 &= P\left(\mathcal{T}_{0,A}\right) \\
P_7 &= P\left(\mathcal{T}_{n-1,A} \cap \mathcal{T}_{1,dA} \cap \mathcal{T}_{0,A_f}\right) \\
P_8 &= P\left(\mathcal{F}_{m,A} \cap \mathcal{F}_{0,A_f}\right) \\
P_9 &= P\left(\mathcal{T}_{n,A} \cap \mathcal{T}_{0,A_f}\right) \\
P_{10} &= P\left(\mathcal{F}_{m-1,A} \cap \mathcal{F}_{1,dA} \cap \mathcal{F}_{0,A_f}\right) \\
P_{11} &= P\left(\mathcal{F}_{0,A_s}\right) \\
P_{12} &= P\left(\mathcal{T}_{0,A_s}\right)
\end{aligned}
$$

To calculate joint probabilities, the individual probabilities are multiplied. Using Eqs. (A.17) and (A.18), along with the first assumption in Section A.1 multiplied by the corresponding classification probability gives

$$\begin{aligned}
P_1 &= e^{-y(t)} \frac{[y(t)]^{(n-1)}}{(n-1)!} P_{TR}(t) Q(t) \beta(t) dt \\
P_2 &= e^{-x(t)} \frac{[x(t)]^m}{m!} \\
P_3 &= e^{-y(t)} \frac{[y(t)]^n}{n!} \\
P_4 &= e^{-x(t)} \frac{[x(t)]^{(m-1)}}{(m-1)!} [1 - P_{FTR}(t)] Q(t) \alpha(t) dt \\
P_5 &= e^{-x(t)} \\
P_6 &= e^{-y(t)} \\
P_7 &= e^{-y(T)} \frac{[y(t)]^{(n-1)}}{(n-1)!} P_{TR}(t) Q(t) \beta(t) dt \\
P_8 &= e^{-x(T)} \frac{[x(t)]^m}{m!} \\
P_9 &= e^{-y(T)} \frac{[y(t)]^n}{n!} \\
P_{10} &= e^{-x(T)} \frac{[x(t)]^{(m-1)}}{(m-1)!} [1 - P_{FTR}(t)] Q(t) \alpha(t) dt \\
P_{11} &= e^{-x(T)} \\
P_{12} &= e^{-y(T)}
\end{aligned} \tag{B.1}$$

where

$$x(t) \equiv \nu_{FT}(t) = \int_0^t [1 - P_{FTR}(\tau)] \alpha(\tau) Q(\tau) d\tau. \tag{B.2}$$

and

$$y(t) \equiv \nu_T(t) = \int_0^t P_{TR}(\tau) \beta(\tau) Q(\tau) d\tau \tag{B.3}$$

B.3 Scenario 3

For this scenario, N targets are uniformly distributed among a Poisson field of false targets with density $\alpha(t)$. The air vehicle flies along a straight path with area coverage rate $Q(t)$.

Scenario 3: First Elemental Probability. At least one target is assumed to be encountered in dA. Therefore, at most, $N-1$ target encounters can occur in A. Let j be the number of target encounters in A. For $n-1$ target attacks, $j \geq n-1$. Applying Bayes' rule to the equation for P_1 gives

$$\begin{aligned} P_1 &= P\left(\mathcal{T}_{n-1,A} \cap \overline{\mathcal{T}}_{j-(n-1),A} \cap \mathcal{N}_{N-1-j,A_f} \cap \mathcal{T}_{1,dA}\right) = \\ &\quad P\left(\mathcal{T}_{n-1,A} \cap \overline{\mathcal{T}}_{j-(n-1),A} | \mathcal{N}_{N-1-j,A_f} \cap \mathcal{T}_{1,dA}\right) P\left(\mathcal{N}_{N-1-j,A_f} \cap \mathcal{T}_{1,dA}\right) = \\ &\quad P\left(\mathcal{T}_{n-1,A} \cap \overline{\mathcal{T}}_{j-(n-1),A} | \mathcal{N}_{N-1-j,A_f} \cap \mathcal{T}_{1,dA}\right) P\left(\mathcal{N}_{N-1-j,A_f} | \mathcal{T}_{1,dA}\right) P\left(\mathcal{T}_{1,dA}\right) \end{aligned} \quad \text{(B.4)}$$

For a given j,

$$P\left(\mathcal{T}_{1,dA}\right) = N \frac{1}{A_B} P_{TR}(t)\, Q(t)\, dt \quad \text{(B.5)}$$

using Eq. (A.29),

$$\begin{aligned} P\left(\mathcal{N}_{N-1-j,A_f} | \mathcal{T}_{1,dA}\right) &= \binom{N-1}{N-1-j} \left[\frac{1}{A_B} \int_t^T Q(\tau)\, d\tau\right]^{N-1-j} = \binom{N-1}{j} \times \\ &\quad \left[\frac{1}{A_B} \int_t^T Q(\tau)\, d\tau + \frac{1}{A_B} \int_0^t Q(\tau)\, d\tau - \frac{1}{A_B} \int_0^t Q(\tau)\, d\tau\right]^{N-1-j} = \\ &\quad \binom{N-1}{j} \left[1 - \frac{1}{A_B} \int_0^t Q(\tau)\, d\tau\right]^{N-1-j} \end{aligned} \quad \text{(B.6)}$$

using Eq. (A.36), and

$$P\left(\mathcal{T}_{n-1,A} \cap \overline{\mathcal{T}}_{j-(n-1),A} | \mathcal{N}_{N-1-j,A_f} \cap \mathcal{T}_{1,dA}\right) = \binom{j}{n-1} \left[\frac{1}{A_B}\int_0^t P_{TR}(\tau)\, Q(\tau)\, d\tau\right]^{n-1} \times \left[\frac{1}{A_B}\int_0^t Q(\tau)\, d\tau - \frac{1}{A_B}\int_0^t P_{TR}(\tau)\, Q(\tau)\, d\tau\right]^{j-(n-1)} \quad \text{(B.7)}$$

using Eq. (A.40). Define one new state, $q(t)$, representing the probability of encountering a specific target.

$$q(t) \equiv \frac{1}{A_B}\int_0^t Q(\tau)\, d\tau \quad \text{(B.8)}$$

The state $y(t)$ is defined as

$$y(t) \equiv \frac{1}{A_B}\int_0^t P_{TR}(\tau)\, Q(\tau)\, d\tau \quad \text{(B.9)}$$

Substituting these definitions and accounting for all possible values of j gives

$$P_1 = \sum_{j=n-1}^{N-1} \left\{ \binom{N-1}{j} \binom{j}{n-1} [y(t)]^{n-1} [q(t) - y(t)]^{j-(n-1)} [1 - q(t)]^{N-1-j} \right\} \times N\frac{1}{A_B} P_{TR}(t)\, Q(t)\, dt \quad \text{(B.10)}$$

Scenario 3: Second Elemental Probability. Using Eq. (B.1),

$$P_2 = e^{-x(t)} \frac{[x(t)]^m}{m!}. \quad \text{(B.11)}$$

Scenario 3: Third Elemental Probability. Let j be the number of target encounters in A. For n target attacks, $j \geq n$. Applying Bayes' rule gives

$$P_3 = P\left(\mathcal{T}_{n,A} \cap \overline{\mathcal{T}}_{j-n} \cap \mathcal{N}_{N-j,A_f}\right) = P\left(\mathcal{T}_{n,A} \cap \overline{\mathcal{T}}_{j-n} | \mathcal{N}_{N-j,A_f}\right) P\left(\mathcal{N}_{N-j,A_f}\right) \quad \text{(B.12)}$$

For a given j,

$$P\left(\mathcal{T}_{n,A} \cap \overline{\mathcal{T}}_{j-n} | \mathcal{N}_{N-j,A_f}\right) = \binom{j}{n} \left[y\left(t\right)\right]^n \left[q\left(t\right) - y\left(t\right)\right]^{j-n} \tag{B.13}$$

using Eq. (A.40), and

$$P\left(\mathcal{N}_{N-j,A_f}\right) = \binom{N}{j} \left[1 - q\left(t\right)\right]^{N-j} \tag{B.14}$$

using Eq. (A.36) where $q\left(t\right)$ is defined in Eq. (B.8) and $y\left(t\right)$ is defined in Eq. (B.9). Accounting for all possible values of j gives

$$P_3 = \sum_{j=n}^{N} \left\{ \binom{N}{j} \binom{j}{n} \left[y\left(t\right)\right]^n \left[q\left(t\right) - y\left(t\right)\right]^{j-n} \left[1 - q\left(t\right)\right]^{N-j} \right\} \tag{B.15}$$

Scenario 3: Fourth Elemental Probability. Using Eq. (B.1),

$$P_4 = e^{-x(t)} \frac{\left[x\left(t\right)\right]^{(m-1)}}{(m-1)!} \left[1 - P_{FTR}\left(t\right)\right] Q\left(t\right) \alpha\left(t\right) dt. \tag{B.16}$$

Scenario 3: Fifth Elemental Probability. Using Eq. (B.1),

$$P_5 = e^{-x(t)}. \tag{B.17}$$

Scenario 3: Sixth Elemental Probability. To calculate P_6, Eq. (B.15) is used with $n = 0$ giving

$$P_6 = \sum_{j=0}^{N} \left\{ \binom{N}{j} \left[q\left(t\right) - y\left(t\right)\right]^j \left[1 - q\left(t\right)\right]^{N-j} \right\}. \tag{B.18}$$

Applying the binomial theorem gives

$$P_6 = \left[1 - y\left(t\right)\right]^N. \tag{B.19}$$

Scenario 3: Seventh Elemental Probability. Applying Bayes' rule gives

$$P_7 = P\left(\mathcal{T}_{n-1,A} \cap \overline{\mathcal{T}}_{j-(n-1),A} \cap \overline{\mathcal{T}}_{N-1-j,A_f} \cap \mathcal{T}_{1,dA}\right) =$$
$$P\left(\mathcal{T}_{n-1,A} \cap \overline{\mathcal{T}}_{j-(n-1),A} | \overline{\mathcal{T}}_{N-1-j,A_f} \cap \mathcal{T}_{1,dA}\right) P\left(\overline{\mathcal{T}}_{N-1-j,A_f} \cap \mathcal{T}_{1,dA}\right) =$$
$$P\left(\mathcal{T}_{n-1,A} \cap \overline{\mathcal{T}}_{j-(n-1),A} | \overline{\mathcal{T}}_{N-1-j,A_f} \cap \mathcal{T}_{1,dA}\right) P\left(\overline{\mathcal{T}}_{N-1-j,A_f} | \mathcal{T}_{1,dA}\right) P\left(\mathcal{T}_{1,dA}\right). \quad \text{(B.20)}$$

For a given j,

$$P\left(\mathcal{T}_{1,dA}\right) = N\frac{1}{A_B} P_{TR}\left(t\right) Q\left(t\right) dt \quad \text{(B.21)}$$

using Eq. (A.29),

$$P\left(\overline{\mathcal{T}}_{N-1-j,A_f} | \mathcal{T}_{1,dA}\right) = \binom{N-1}{N-1-j} \left\{\frac{1}{A_B}\int_t^T \left[1 - P_{TR}\left(\tau\right)\right] Q\left(\tau\right) d\tau\right\}^{N-1-j}$$
$$= \binom{N-1}{j} \left[\frac{1}{A_B}\int_t^T Q\left(\tau\right) d\tau - \frac{1}{A_B}\int_t^T P_{TR}\left(\tau\right) Q\left(\tau\right) d\tau\right.$$
$$+ \frac{1}{A_B}\int_0^t Q\left(\tau\right) d\tau - \frac{1}{A_B}\int_0^t P_{TR}\left(\tau\right) Q\left(\tau\right) d\tau$$
$$\left. -\frac{1}{A_B}\int_0^t Q\left(\tau\right) d\tau + \frac{1}{A_B}\int_0^t P_{TR}\left(\tau\right) Q\left(\tau\right) d\tau\right]^{N-1-j}$$
$$= \binom{N-1}{j} \left[1 - q\left(t\right) - y\left(T\right) + y\left(t\right)\right]^{N-1-j} \quad \text{(B.22)}$$

using Eq. (A.36), and

$$P\left(\mathcal{T}_{n-1,A} \cap \overline{\mathcal{T}}_{j-(n-1),A} | \overline{\mathcal{T}}_{N-1-j,A_f} \cap \mathcal{T}_{1,dA}\right) = \binom{j}{n-1} \left[y\left(t\right)\right]^{n-1} \left[q\left(t\right) - y\left(t\right)\right]^{j-(n-1)} \quad \text{(B.23)}$$

using Eq. (A.40) where $q\left(t\right)$ is defined in Eq. (B.8) and $y\left(t\right)$ is defined in Eq. (B.9). Accounting for all possible values of j yields

$$P_7 = \sum_{j=n-1}^{N-1} \left\{\binom{N-1}{j}\binom{j}{n-1} \left[y\left(t\right)\right]^{n-1} \left[q\left(t\right) - y\left(t\right)\right]^{j-(n-1)}\right.$$
$$\left. \left[1 - q\left(t\right) - y\left(T\right) + y\left(t\right)\right]^{N-1-j}\right\} N\frac{1}{A_B} P_{TR}\left(t\right) Q\left(t\right) dt \quad \text{(B.24)}$$

Scenario 3: Eighth Elemental Probability. Using Eq. (B.1),

$$P_8 = e^{-x(T)} \frac{[x(t)]^m}{m!} \tag{B.25}$$

Scenario 3: Ninth Elemental Probability. Applying Bayes' rule gives

$$P_9 = P\left(\mathcal{T}_{n,A} \cap \overline{\mathcal{T}}_{j-n} \cap \overline{\mathcal{T}}_{N-j,A_f}\right) = P\left(\mathcal{T}_{n,A} \cap \overline{\mathcal{T}}_{j-n} | \overline{\mathcal{T}}_{N-j,A_f}\right) P\left(\overline{\mathcal{T}}_{N-j,A_f}\right). \tag{B.26}$$

For a given j,

$$\begin{aligned} P\left(\overline{\mathcal{T}}_{N-j,A_f}\right) &= \binom{N}{N-j} \left\{ \frac{1}{A_B} \int_t^T \left[1 - P_{TR}(\tau)\right] Q(\tau)\, d\tau \right\}^{N-j} \\ &= \binom{N}{j} \left[\frac{1}{A_B} \int_t^T Q(\tau)\, d\tau - \frac{1}{A_B} \int_t^T P_{TR}(\tau)\, Q(\tau)\, d\tau \right. \\ &\quad + \frac{1}{A_B} \int_0^t Q(\tau)\, d\tau - \frac{1}{A_B} \int_0^t P_{TR}(\tau)\, Q(\tau)\, d\tau \\ &\quad \left. - \frac{1}{A_B} \int_0^t Q(\tau)\, d\tau + \frac{1}{A_B} \int_0^t P_{TR}(\tau)\, Q(\tau)\, d\tau \right]^{N-j} \\ &= \binom{N}{j} \left[1 - q(t) - y(T) + y(t)\right]^{N-j} \end{aligned} \tag{B.27}$$

using Eq. (A.36), and

$$P\left(\mathcal{T}_{n,A} \cap \overline{\mathcal{T}}_{j-n} | \overline{\mathcal{T}}_{N-j,A_f}\right) = \binom{j}{n} [y(t)]^n [q(t) - y(t)]^{j-n} \tag{B.28}$$

using Eq. (A.40) where $q(t)$ is defined in Eq. (B.8) and $y(t)$ is defined in Eq. (B.9). Accounting for all possible values of j yields

$$P_9 = \sum_{j=n}^{N} \left\{ \binom{N}{j} \binom{j}{n} [y(t)]^n [q(t) - y(t)]^{j-n} \left[1 - q(t) - y(T) + y(t)\right]^{N-j} \right\} \tag{B.29}$$

Scenario 3: Tenth Elemental Probability. Using Eq. (B.1),

$$P_{10} = e^{-x(T)} \frac{[x(t)]^{(m-1)}}{(m-1)!} [1 - P_{FTR}(t)] Q(t) \alpha(t) dt. \tag{B.30}$$

Scenario 3: Eleventh Elemental Probability. Using Eq. (B.1),

$$P_{11} = e^{-x(T)}. \tag{B.31}$$

Scenario 3: Twelfth Elemental Probability. To calculate P_{12}, Eq. (B.29) is used with $n = 0$ giving

$$P_{12} = \sum_{j=0}^{N} \left\{ \binom{N}{j} [q(t) - y(t)]^j [1 - q(t) - y(T) + y(t)]^{N-j} \right\}. \tag{B.32}$$

Applying the binomial theorem gives

$$P_{12} = [1 - y(T)]^N. \tag{B.33}$$

B.4 Scenario 4

For this scenario, N targets and M false targets are uniformly distributed in A_B. The air vehicle flies along a straight path with area coverage rate $Q(t)$. The elemental probabilities for N uniformly-distributed targets (P_1, P_3, P_6, P_7, P_9, and P_{12}) were derived in Section B.3. The elemental probabilities for M uniformly-distributed false targets (P_2, P_4, P_5, P_8, P_{10}, and P_{11}) can be derived in the same manner replacing j, n, N, $P_{TR}(t)$, and $y(t)$ with i, m, M, $[1 - P_{FTR}(t)]$, and $x(t)$ respectively, where $x(t)$ is defined as

$$x(t) \equiv \frac{1}{A_B} \int_0^t [1 - P_{FTR}(\tau)] Q(\tau) d\tau. \tag{B.34}$$

The states $q(t)$ and $y(t)$ are the Scenario 3 states defined in Eqs. (B.8) and (B.9) respectively. The 12 elemental probabilities become

$$P_1 = \sum_{j=n-1}^{N-1} \left\{ \binom{N-1}{j} \binom{j}{n-1} [y(t)]^{n-1} [q(t) - y(t)]^{j-(n-1)} [1 - q(t)]^{N-1-j} \right\} \times \frac{N}{A_B} P_{TR}(t) Q(t) dt \quad \text{(B.35)}$$

$$P_2 = \sum_{i=m}^{M} \left\{ \binom{M}{i} \binom{i}{m} [x(t)]^{m} [q(t) - x(t)]^{i-m} [1 - q(t)]^{M-i} \right\} \quad \text{(B.36)}$$

$$P_3 = \sum_{j=n}^{N} \left\{ \binom{N}{j} \binom{j}{n} [y(t)]^{n} [q(t) - y(t)]^{j-n} [1 - q(t)]^{N-j} \right\} \quad \text{(B.37)}$$

$$P_4 = \sum_{i=m-1}^{M-1} \left\{ \binom{M-1}{i} \binom{i}{m-1} [x(t)]^{m-1} [q(t) - x(t)]^{i-(m-1)} [1 - q(t)]^{M-1-i} \right\} \times \frac{M}{A_B} [1 - P_{FTR}(t)] Q(t) dt \quad \text{(B.38)}$$

$$P_5 = [1 - x(t)]^{M}. \quad \text{(B.39)}$$

$$P_6 = [1 - y(t)]^{N}. \quad \text{(B.40)}$$

$$P_7 = \sum_{j=n-1}^{N-1} \left\{ \binom{N-1}{j} \binom{j}{n-1} [y(t)]^{n-1} [q(t) - y(t)]^{j-(n-1)} [1 - q(t) - y(T) + y(t)]^{N-1-j} \right\} N \frac{1}{A_B} P_{TR}(t) Q(t) dt \quad \text{(B.41)}$$

$$P_8 = \sum_{i=m}^{M} \left\{ \binom{M}{i} \binom{i}{m} [x(t)]^{m} [q(t) - x(t)]^{i-m} [1 - q(t) - x(T) + x(t)]^{M-i} \right\} \quad \text{(B.42)}$$

$$P_9 = \sum_{j=n}^{N} \left\{ \binom{N}{j} \binom{j}{n} [y(t)]^{n} [q(t) - y(t)]^{j-n} [1 - q(t) - y(T) + y(t)]^{N-j} \right\} \quad \text{(B.43)}$$

$$P_{10} = \sum_{i=m-1}^{M-1} \left\{ \binom{M-1}{i} \binom{i}{m-1} [x(t)]^{m-1} [q(t) - x(t)]^{i-(m-1)} \right.$$
$$\left. [1 - q(t) - x(T) + x(t)]^{M-1-i} \right\} \frac{M}{A_B} [1 - P_{FTR}(t)] Q(t) \, dt \quad \text{(B.44)}$$

$$P_{11} = [1 - x(T)]^M . \quad \text{(B.45)}$$

$$P_{12} = [1 - y(T)]^N . \quad \text{(B.46)}$$

B.5 Scenario 5

For this scenario, N targets are normally distributed among a Poisson field of false targets with density $\alpha(\rho)$. Each target has a circular normal distribution with standard deviation σ_y. The search area A_s is a circular disc of radius R. The air vehicle searches the disc using concentric annuli of radius r and thickness dr. The search begins at the origin of the disc and progresses outward. The 12 elemental probabilities have the same form as those calculated in Section B.3 for Scenario 3, but the states are defined as

$$q_y(r) \equiv \int_0^r \frac{\rho}{\sigma_y^2} e^{-\frac{\rho^2}{2\sigma_y^2}} d\rho \quad \text{(B.47)}$$

$$x(r) \equiv \int_0^r [1 - P_{FTR}(\rho)] 2\pi\rho d\rho \quad \text{(B.48)}$$

$$y(r) \equiv \int_0^r P_{TR}(\rho) \frac{\rho}{\sigma_y^2} e^{-\frac{\rho^2}{2\sigma_y^2}} d\rho. \quad \text{(B.49)}$$

Also, the probabilities of one attack in dA are

$$P(\mathcal{T}_{1,dA}) = N P_{TR}(r) \frac{r}{\sigma_y^2} e^{-\frac{r^2}{2\sigma_y^2}} dr \quad \text{(B.50)}$$

and

$$P(\mathcal{F}_{1,dA}) = [1 - P_{FTR}(r)] 2\pi r \alpha(r) \, dr. \quad \text{(B.51)}$$

With these substitutions,

$$P_1 = \sum_{j=n-1}^{N-1} \left\{ \binom{N-1}{j} \binom{j}{n-1} \left[y\left(r\right)\right]^{n-1} \left[q_y\left(r\right) - y\left(r\right)\right]^{j-(n-1)} \left[1 - q_y\left(r\right)\right]^{N-1-j} \right\} \times$$
$$N P_{TR}\left(r\right) \frac{r}{\sigma_y^2} e^{-\frac{r^2}{2\sigma_y^2}} dr \quad \text{(B.52)}$$

$$P_2 = e^{-x(r)} \frac{\left[x\left(r\right)\right]^m}{m!} \quad \text{(B.53)}$$

$$P_3 = \sum_{j=n}^{N} \left\{ \binom{N}{j} \binom{j}{n} \left[y\left(r\right)\right]^n \left[q_y\left(r\right) - y\left(r\right)\right]^{j-n} \left[1 - q_y\left(r\right)\right]^{N-j} \right\} \quad \text{(B.54)}$$

$$P_4 = e^{-x(r)} \frac{\left[x\left(r\right)\right]^{(m-1)}}{(m-1)!} \left[1 - P_{FTR}\left(r\right)\right] 2\pi r \alpha\left(r\right) dr \quad \text{(B.55)}$$

$$P_5 = e^{-x(r)} \quad \text{(B.56)}$$

$$P_6 = \left[1 - y\left(r\right)\right]^N \quad \text{(B.57)}$$

$$P_7 = \sum_{j=n-1}^{N-1} \left\{ \binom{N-1}{j} \binom{j}{n-1} \left[y\left(r\right)\right]^{n-1} \left[q_y\left(r\right) - y\left(r\right)\right]^{j-(n-1)} \right.$$
$$\left. \left[1 - q_y\left(r\right) - y\left(R\right) + y\left(r\right)\right]^{N-1-j} \right\} N P_{TR}\left(r\right) \frac{r}{\sigma_y^2} e^{-\frac{r^2}{2\sigma_y^2}} dr \quad \text{(B.58)}$$

$$P_8 = e^{-x(R)} \frac{\left[x\left(r\right)\right]^m}{m!} \quad \text{(B.59)}$$

$$P_9 = \sum_{j=n}^{N} \left\{ \binom{N}{j} \binom{j}{n} \left[y\left(r\right)\right]^n \left[q_y\left(r\right) - y\left(r\right)\right]^{j-n} \left[1 - q_y\left(r\right) - y\left(R\right) + y\left(r\right)\right]^{N-j} \right\} \quad \text{(B.60)}$$

$$P_{10} = e^{-x(R)} \frac{\left[x\left(r\right)\right]^{(m-1)}}{(m-1)!} \left[1 - P_{FTR}\left(r\right)\right] 2\pi r \alpha\left(r\right) dr \quad \text{(B.61)}$$

$$P_{11} = e^{-x(R)} \quad \text{(B.62)}$$

$$P_{12} = \left[1 - y\left(R\right)\right]^N . \quad \text{(B.63)}$$

B.6 Scenario 6

For this scenario, N targets and M false targets are normally distributed in A_B. Each false target has a circular normal distribution with standard deviation σ_x, and each target has a circular normal distribution with standard deviation σ_y. The search area A_s is a circular disc of radius R. The air vehicle searches the disc using concentric annuli of radius r and thickness dr. The search begins at the origin of the disc and progresses outward. The elemental probabilities for N normally-distributed targets (P_1, P_3, P_6, P_7, P_9, and P_{12}) were derived in Section B.5. The elemental probabilities for M normally-distributed false targets (P_2, P_4, P_5, P_8, P_{10}, and P_{11}) can be derived in the same manner replacing j, n, N, $P_{TR}(r)$, $q_y(r)$, and $y(r)$ with i, m, M, $[1 - P_{FTR}(r)]$, $q_x(r)$, and $x(r)$ respectively, where

$$q_x(r) \equiv \int_0^r \frac{\rho}{\sigma_x^2} e^{-\frac{\rho^2}{2\sigma_x^2}} d\rho \tag{B.64}$$

and

$$x(r) \equiv \int_0^r [1 - P_{FTR}(\rho)] \frac{\rho}{\sigma_x^2} e^{-\frac{\rho^2}{2\sigma_x^2}} d\rho. \tag{B.65}$$

The states $q_y(r)$ and $y(r)$ are the Scenario 5 states defined in Eqs. (B.47) and (B.49) respectively. The 12 elemental probabilities become

$$P_1 = \sum_{j=n-1}^{N-1} \left\{ \binom{N-1}{j} \binom{j}{n-1} [y(r)]^{n-1} [q_y(r) - y(r)]^{j-(n-1)} [1 - q_y(r)]^{N-1-j} \right\} \times N P_{TR}(r) \frac{r}{\sigma_y^2} e^{-\frac{r^2}{2\sigma_y^2}} dr \tag{B.66}$$

$$P_2 = \sum_{i=m}^{M} \left\{ \binom{M}{i} \binom{i}{m} [x(r)]^m [q_x(r) - x(r)]^{i-m} [1 - q_x(r)]^{M-i} \right\} \tag{B.67}$$

$$P_3 = \sum_{j=n}^{N} \left\{ \binom{N}{j} \binom{j}{n} [y(r)]^n [q_y(r) - y(r)]^{j-n} [1 - q_y(r)]^{N-j} \right\} \tag{B.68}$$

$$P_4 = \sum_{i=m-1}^{M-1} \left\{ \binom{M-1}{i} \binom{i}{m-1} [x(r)]^{m-1} [q_x(r) - x(r)]^{i-(m-1)} [1 - q_x(r)]^{M-1-y} \right\} \times$$
$$M [1 - P_{FTR}(r)] \frac{r}{\sigma_x^2} e^{-\frac{r^2}{2\sigma_x^2}} dr \quad \text{(B.69)}$$

$$P_5 = [1 - x(r)]^M \quad \text{(B.70)}$$

$$P_6 = [1 - y(r)]^N \quad \text{(B.71)}$$

$$P_7 = \sum_{j=n-1}^{N-1} \left\{ \binom{N-1}{j} \binom{j}{n-1} [y(r)]^{n-1} [q_y(r) - y(r)]^{j-(n-1)} \right.$$
$$\left. [1 - q_y(r) - y(R) + y(r)]^{N-1-j} \right\} N P_{TR}(r) \frac{r}{\sigma_y^2} e^{-\frac{r^2}{2\sigma_y^2}} dr \quad \text{(B.72)}$$

$$P_8 = \sum_{i=m}^{M} \left\{ \binom{M}{i} \binom{i}{m} [x(r)]^m [q_x(r) - x(r)]^{i-m} [1 - q_x(r) - x(R) + x(r)]^{M-i} \right\} \quad \text{(B.73)}$$

$$P_9 = \sum_{j=n}^{N} \left\{ \binom{N}{j} \binom{j}{n} [y(r)]^n [q_y(r) - y(r)]^{j-n} [1 - q_y(r) - y(R) + y(r)]^{N-j} \right\} \quad \text{(B.74)}$$

$$P_{10} = \sum_{i=m-1}^{M-1} \left\{ \binom{M-1}{i} \binom{i}{m-1} [x(r)]^{m-1} [q_x(r) - x(r)]^{i-(m-1)} \right.$$
$$\left. [1 - q_x(r) - x(R) + x(r)]^{M-1-i} \right\} M [1 - P_{FTR}(r)] \frac{r}{\sigma_x^2} e^{-\frac{r^2}{2\sigma_x^2}} dr \quad \text{(B.75)}$$

$$P_{11} = [1 - x(R)]^M \quad \text{(B.76)}$$

$$P_{12} = [1 - y(R)]^N . \quad \text{(B.77)}$$

B.7 Scenario 7

This scenario is the specific case of Scenario 5 when $N = 1$. Hence, the derivation is given in Section B.5.

Appendix C. Nondimensionalization

Consider the two control variables. Probability of a target report, P_{TR}, has no dimensions and is between 0 and 1. Area coverage rate, Q, has dimensions of area per time and is between Q_{min} and Q_{max}. For numerical conditioning, it can be beneficial to have all control variables with no dimensions and roughly the same order of magnitude.

One possible way to nondimensionalize area coverage rate is to divide it by the scaled nominal area coverage rate, Q_n. Thus, a new control variable, $\tilde{Q}$, is introduced such that

$$\tilde{Q} \equiv \frac{Q}{Q_n}. \tag{C.1}$$

Since $Q < Q_n$, $\tilde{Q}$ will be between 0 and 1. The new control variable must be inserted into the ROC model. Recall the ROC parameter c was defined as

$$c \equiv \frac{Q_n}{Q}. \tag{C.2}$$

Thus,

$$c \equiv \frac{1}{\tilde{Q}}, \tag{C.3}$$

and

$$[1 - P_{FTR}(t)] = \frac{\tilde{Q}(t) P_{TR}(t)}{\tilde{Q}(t) P_{TR}(t) + [1 - P_{TR}(t)]}. \tag{C.4}$$

The problem parameters can also be nondimensionalized. If the false target density, α, is assumed constant, one can define the nondimensional parameter,

$$\nu_n \equiv \alpha Q_n T \tag{C.5}$$

which represents a nominal number of false target encounters. Finally, one can define the nondimensional parameter

$$\kappa \equiv \frac{Q_n T}{A_B}. \tag{C.6}$$

which represents a nominal area ratio.

Consider Scenario 1. Table C.1 lists how the the 12 elemental probabilities and corresponding state definitions would be impacted. The other six scenarios could be modified in a similar fashion. The final result is an optimal control problem with nondimensional problem parameters ν_n and κ, nondimensional control variables P_{TR} and $\tilde{Q}$, and final time T.

Table C.1 Scenario 1 Elemental Probabilities and State Definitions with $\tilde{Q}$

P_1	$=$	$\frac{\kappa}{T} P_{TR}(t)\, \tilde{Q}(t)\, dt$
P_2	$=$	$e^{-x(t)} \frac{[x(t)]^m}{m!}$
P_3	$=$	$[1 - y(t)]$
P_4	$=$	$e^{-x(t)} \frac{[x(t)]^{(m-1)}}{(m-1)!} \frac{\nu_n}{T} \frac{\left[\tilde{Q}(t)\right]^2 P_{TR}(t)}{\tilde{Q}(t) P_{TR}(t) + [1 - P_{TR}(t)]} dt$
P_5	$=$	$e^{-x(t)}$
P_6	$=$	$[1 - y(t)]$
P_7	$=$	$\frac{\kappa}{T} P_{TR}(t)\, \tilde{Q}(t)\, dt$
P_8	$=$	$e^{-x(T)} \frac{[x(t)]^m}{m!}$
P_9	$=$	$[1 - y(T)]$
P_{10}	$=$	$e^{-x(T)} \frac{[x(t)]^{(m-1)}}{(m-1)!} \frac{\nu_n}{T} \frac{\left[\tilde{Q}(t)\right]^2 P_{TR}(t)}{\tilde{Q}(t) P_{TR}(t) + [1 - P_{TR}(t)]} dt$
P_{11}	$=$	$e^{-x(T)}$
P_{12}	$=$	$[1 - y(T)]$
$x(t)$	$\equiv$	$\int_0^t \frac{\nu_n}{T} \frac{\left[\tilde{Q}(\tau)\right]^2 P_{TR}(\tau)}{\tilde{Q}(\tau) P_{TR}(\tau) + [1 - P_{TR}(\tau)]} d\tau$
$y(t)$	$\equiv$	$\int_0^t \frac{\kappa}{T} P_{TR}(\tau)\, \tilde{Q}(\tau)\, d\tau$

Appendix D. Further Analysis of Scenario 1

It was shown in Chapter III that the optimal unconstrained solution was increasing with time until it saturated at $P_{TR_{max}} = 1$ sometime prior to the final time T. This strategy of starting conservative then gradually increasing aggressiveness until the end, where an all out effort is tried, is common in game theory. Without a constraint on false target attacks, the system has nothing to lose by declaring all objects as targets near the end. The time where the optimal solution starts to saturate, t_c, is now addressed.

The optimal unconstrained solution, at any time, was shown to be

$$P^*_{TR}(t) = \frac{c - \sqrt{\lambda_x(t)\,\alpha c A_B e^{x(t)}}}{c-1}. \tag{D.1}$$

At t_c,

$$P^*_{TR}(t_c) = 1 = \frac{c - \sqrt{\lambda_x(t_c)\,\alpha c A_B e^{x(t_c)}}}{c-1}. \tag{D.2}$$

Thus,

$$\lambda_x(t_c)\,\alpha c A_B e^{x(t_c)} = 1. \tag{D.3}$$

For $t_c \le t \le T$,

$$P^*_{TR}(t) = 1. \tag{D.4}$$

The state and costate equations when $t_c \le t \le T$ are

$$\dot{x}(t) = \alpha Q, \qquad x(T) = x(T), \qquad t_c \le t \le T \tag{D.5}$$

$$\dot{\lambda}_x(t) = -\frac{Q}{A_B} e^{-x(t)}, \qquad \lambda_x(T) = 0, \qquad t_c \le t \le T \tag{D.6}$$

Integrating the state equation gives

$$x(t) = x(T) + \alpha Q t - \alpha Q T, \qquad t_c \le t \le T \tag{D.7}$$

Substituting Eq. (D.7) into the costate equation gives

$$\dot{\lambda}_x(t) = -\frac{Q}{A_B} e^{-[x(T)+\alpha Qt-\alpha QT]} = -\frac{Q}{A_B} e^{-[x(T)-\alpha QT]} e^{-\alpha Qt}, \qquad t_c \le t \le T \tag{D.8}$$

Integrating Eq. (D.8) gives

$$\lambda_x(t) = -\frac{1}{\alpha A_B} e^{-x(T)} + \frac{1}{\alpha A_B} e^{-[x(T)+\alpha Qt-\alpha QT]}, \qquad t_c \le t \le T \tag{D.9}$$

Substituting Eq. (D.7) and Eq. (D.9) into Eq. (D.3) gives

$$\left\{ -\frac{1}{\alpha A_B} e^{-x(T)} + \frac{1}{\alpha A_B} e^{-[x(T)+\alpha Qt_c-\alpha QT]} \right\} \alpha c A_B e^{[x(T)+\alpha Qt_c-\alpha QT]} = 1 \tag{D.10}$$

Solving for t_c gives

$$t_c = T + \frac{1}{\alpha Q} \ln\left(1 - \frac{1}{c}\right). \tag{D.11}$$

Bibliography

1. *Air Force Manual 1-1, Basic Aerospace Doctrine of the United States Air Force*. 2004.
2. Bar-Shalom, Y., et al. "From Receiver Operating Characteristic to System Operating Characteristic: Evaluation of a Track Formation System," *IEEE Transactions on Automatic Control*, *35*:172–179 (1990).
3. Bar-Shalom, Y. and T.E. Fortmann. *Tracking and Data Association*. Academic Press, Inc., 1988.
4. Benkoski, S.J., et al. "A Survey of the Search Theory Literature," *Naval Research Logistics*, *38*:469–494 (1991).
5. Brown, S.S. "Optimal Search for a Moving Target in Discrete Time and Space," *Operations Research*, *28*(No. 6):1275–1289 (1980).
6. Brunet, C., et al. "A Multi-Agent Architecture for a Driver Model for Autonomous Road Vehicles." *1995 Canadian Conference on Electrical and Computer Engineering*. 772–775. 1995.
7. Bryson, A.E. *Dynamic Optimization*. Addison-Wesley, 1999.
8. Bryson, A.E. and Y. Ho. *Applied Optimal Control*. Ginn and Company, 1969.
9. C., Chong and M. Liggins II. "Fusion Technologies for Drug Interdiction." *Proceedings of the 1994 IEEE International Conference on Multisensor Fusion and Integration for Intelligent Systems*. 435–441. 1994.
10. Clausewitz, C. V. *On War*. Viking Press, 1982.
11. Cone, M. and S. Musick. "Scheduling and Sensor Management Using Genetic Algorithms." *Proceedings of the IEEE 1996 National Aerospace and Electronics Conference1*. 150–156. 1996.
12. Cozzolino, J.M. "Sequential Search for an Unknown Number Objects of Nonuniform Size," *Operations Research*, *20*:293–308 (1963).
13. Daley, D.J. and D. Vere-Jones. *An Introduction to the Thoery of Point Process*. Springer-Verlag, 1988.
14. Dambreville, F. and J. Le Cadre. "Search Game for a Moving Target with Dynamically Generated Information," *Fusion 2002*, 243–250 (2002).
15. Decker, D. *Decision Factors for Cooperative Multiple Warhead UAV Target Classification and Attack*. PhD Dissertation, Air Force Institute of Technology, 2004.

16. Dobie, J.M. "Search Theory: A Sequential Approach," *Naval Research Logistics Quarterly*, *10*:323–334 (1963).

17. Dobie, J.M. "Some Problems with False Contacts," *Operations Research*, *21*:907–925 (1973).

18. Dorigo, M., et al. "Ant System: Optimization by a Colony of Cooperative Agents." *IEEE Transactions on Systems, Man and Cybernetics*. 29–41. 1996.

19. Dunbar, W.B. and R.M. Murray. "Model Predictive Control of Coordinated Multi-Vehicle Formations." *Proceedings of the 41st IEEE Conference on Decision and Control4*. 4631–4636. 2002.

20. Goodman, I.R., et al. *Mathematics of Data Fusion*. Kluwer Academic Publishers, 1997.

21. Grocholsky, B. *Information-Theoretic Control of Multiple Sensor Platforms*. PhD Dissertation, University of Sydney, 2002.

22. Hoai, X.V. and C.T. Leondes. "The Optimal Distribution of Search Effort: Existence, Uniqueness, and the Minimax Solution." *IEEE Transactions on Aerospace and Electronic Systems*. 359–366. 1994.

23. Iida, K., et al. "An Optimal Distribution of Searching Effort Relaxing the Assumption of Local Effectiveness," *Journal of Operations Research Society of Japan*, *45*(No. 1):13–26 (2002).

24. Jacques, D.R. "Modelling Considerations for Wide Area Search Munition Effectiveness Analysis." *Proceedings of the Winter Simulation Conference*. 2002.

25. Jacques, D.R. "Search Classification and Attack Decisions." *Cooperative Control: Models, Applications and Algorithms1*. Kluwer Academic Publishers, 2003.

26. Jacques, D.R. and M. Pachter. "A Theoretical Foundation for Cooperative Search, Classification, and Target Attack." *Cooperative Control: Models, Applications and Algorithms2*. Kluwer Academic Publishers, 2004.

27. Jeffcoat, D.E. "Coupled Detection Rates: An Introduction." *Proceedings of the 4th Annual Conference on Cooperative Control and Optimization in Sandestin, Florida*. 2003.

28. Kalman, R.E. "A New Approach to Linear Filtering and Prediction Problems," *Transactions of the ASME, Journal of Basic Engineering*, 34–45 (1960).

29. Kim, H. Jin, et al. "A Hierarchical Approach to Probabilistic Pursuit-Evasion Games with Unmanned Ground and Aerial Vehicles." *40th IEEE Conference on Decision and Control*. 634–639. 2001.

30. Koopman, B.O. *Search and Screening*. Pergamon Press, Inc., 1980.

31. Mahler, R.P. "Random Set Theory for Target Tracking and Identification." *Handbook of Multisensor Data Fusion*, edited by D.L. Hall and J. Llinas. 14–1 to 14–133. CRC Press, 2002.

32. Mahler, R.P. "Approximate Multisensor-Multitarget Joint Detection, Tracking and Identification Using 1st Order Multitarget Moment Statistics," *IEEE Aerospace and Electronic Systems Magazine* (2003).

33. Mahler, R.P. "Statistics 101 for Multisensor, Multitarget Data Fusion," *IEEE Aerospace and Electronic Systems Magazine* (2003).

34. Maybeck, P.S. *Stochastic Models, Estimation and Control Volume 1*. Navtech Book and Software Store, 1994.

35. McIntyre, G.A. *A Comprehensive Approach to Sensor Management and Scheduling*. PhD Dissertation, George Mason University, 1998.

36. Moses, L.E., et al. "Combining Independent Studies of a Diagnostic Test into a Summary ROC Curve: Data-analytic Approaches and Some Additional Considerations." *Statistics in Medicine*. 1993.

37. Richardson, H.R. "Search Theory," *Report to the Center for Naval Analysis (ADA177493)* (1986).

38. Slater, G.L. "Cooperation Between UAVs in a Search and Destroy Mission." *AIAA Guidance, Navigation, and Control Conference and Exhibit*. AIAA, 2003.

39. Spiegel, M.R. *Schaum's Outline of Theory and Problems of Probability and Statistics*. McGraw-Hill, Inc., 1992.

40. Stone, L.D. *Theory of Optimal Search* (Second Edition). Operations Research Society of America, 1989.

41. Stone, L.D. "What's Happened in Search Theory Since the 1975 Lanchester Prize?," *Operations Research*, *37*(No. 3):501–506 (1989).

42. Stone, L.D., et al. *Bayesian Multiple Target Tracking*. Artech House, Inc., 1999.

43. Stone, L.D., et al. "Optimal Search in the Presense of Poisson-Distributed False Targets," *SIAM Journal of Applied Mathematics*, *23*(No. 1):6–27 (1972).

44. Stone, L.D. and J.A. Stanshine. "Optimal Search Using Uninterupted Contact Investigation," *SIAM Journal of Applied Mathematics*, *20*(No. 2):241–263 (1971).

45. Stone, L.D. and A.R. Washburn. "Introduction on Special Issue on Search Theory," *Naval Research Logistics*, *38*:465–468 (1991).

46. Stopp, A. and T. Riethmuller. "Fast Reactive Path Planning by 2D and 3D Multi-Layer Spatial Grids for Mobile Robot Navigation." *Proceedings of the 1995 IEEE International Symposium on Intelligent Contol*. 545–550. 1995.

47. Stoyan, D., et al. *Stochastic Geometry and Its Applications* (Second Edition). John Wiley and Sons, 1995.

48. Vo, B., et al. "Random Finite Sets and Sequential Monte Carlo Methods in Multi-target Tracking," *Proceedings from Radar Conference in Adelaide, Australia* (2003).

49. Washburn, A.R. *Search and Detection*. Operations Research Society of America, 1981.

50. Washburn, A.R. "Search for a Moving Target: the FAB Algorithm," *Operations Research*, *31*(No. 4):739–751 (1983).

51. Washburn, A.R. *Two-Person Zero-Sum Games*. Operations Research Society of America, 1991.

52. www.globalsecurity.org/military/world/iraq/maps baghdad.htm. 2005.

Vita

Maj Brian Kish graduated as valedictorian from Sandwich High School, Sandwich, IL in 1987. He then went to Illinois Institute of Technology where he obtained a Bachelor's Degree in Aerospace Engineering in 1991. After being commissioned through AFROTC in 1991, Brian was assigned to the Ballistic Missile Organization, Norton, AFB, CA where he worked on various missile acquisition programs. In 1993 he was selected to pursue a Master's Degree in Aeronautical Engineering from the Air Force Institute of Technology. He finished in December 1994 as a distinguished graduate and was assigned to Wright Laboratory's Flight Dynamics Division, Wright-Patterson AFB, OH. In 1996, he was selected to attend Test Pilot School, Edwards AFB, CA as a Flight Test Engineer. Following graduation in July 1997, Brian was assigned to the 445th Flight Test Squadron at Edwards AFB where he tested F-15s, T-38s, and an experimental aircraft for the U.S. Coast Guard. In January 2000, he became a Division Chief for the Joint STARS Test Force in Melbourne, FL. In September 2003, he started pursuing his PhD at the Air Force Institute of Technology under the direction of Dr. David R. Jacques.

REPORT DOCUMENTATION PAGE

Form Approved
OMB No. 0704-0188

PLEASE DO NOT RETURN YOUR FORM TO THE ABOVE ADDRESS.

1. REPORT DATE *(DD-MM-YYYY)*	2. REPORT TYPE	3. DATES COVERED *(From - To)*
Sep 2005	Doctoral Dissertation	Sep 2002 - Sep 2005

4. TITLE AND SUBTITLE

Establishment of a System Operating Characteristic for Autonomous Wide Area Search Vehicles

5a. CONTRACT NUMBER

5b. GRANT NUMBER

5c. PROGRAM ELEMENT NUMBER

6. AUTHOR(S)

Brian A. Kish, Maj, USAF

5d. PROJECT NUMBER

5e. TASK NUMBER

5f. WORK UNIT NUMBER

7. PERFORMING ORGANIZATION NAME(S) AND ADDRESS(ES)

Air Force Institute of Technology
Graduate School of Engineering and Management (AFIT/EN)
2950 Hobson Way
WPAFB OH 45433-7765

8. PERFORMING ORGANIZATION REPORT NUMBER

AFIT/DS/ENY/05-05

9. SPONSORING/MONITORING AGENCY NAME(S) AND ADDRESS(ES)

AFRL/MNGN
Attn: Dr. Robert A. Murphey
101 W. Eglin Blvd
Eglin AFB, FL 32542-6810

10. SPONSOR/MONITOR'S ACRONYM(S)

11. SPONSOR/MONITOR'S REPORT NUMBER(S)

12. DISTRIBUTION/AVAILABILITY STATEMENT

Approved for public release; distribution is unlimited

13. SUPPLEMENTARY NOTES

14. ABSTRACT

Analytic system effectiveness measures are derived using applied probability theory. The effectiveness measures handle time-varying parameters which characterize the battle space environment and the performance of the system. This allows the formulation and solution of optimization problems that maximize the probability of target attacks while at the same time constraining the probability of false target attacks.

15. SUBJECT TERMS

UAV effectiveness, optimal control, system operating characteristic

16. SECURITY CLASSIFICATION OF:			17. LIMITATION OF ABSTRACT	18. NUMBER OF PAGES	19a. NAME OF RESPONSIBLE PERSON
a. REPORT	b. ABSTRACT	c. THIS PAGE			David R. Jacques, PhD (ENY)
U	U	U	UU	161	19b. TELEPHONE NUMBER *(Include area code)* (937) 255-3555 x3329

Reset

Standard Form 298 (Rev. 8/98)
Prescribed by ANSI Std. Z39.18